# THE ROLE OF CARBONIC ANHYDRASE IX IN THE DEVELOPMENT OF THE GLYCOLYTIC PHENOTYPE OF BREAST CANCER CELLS

By

YING LI

A DISSERTATION PRESENTED TO THE GRADUATE SCHOOL
OF THE UNIVERSITY OF FLORIDA IN PARTIAL FULFILLMENT
OF THE REQUIREMENTS FOR THE DEGREE OF
DOCTOR OF PHILOSOPHY

UNIVERSITY OF FLORIDA

2010

To my husband, Yongsheng, and son, Muzi for all of their support, patience, and encouragement

ACKNOWLEDGMENTS

I would first like to thank Dr. Susan Frost for her support and guidance thoughout my graduate education. She has been an excellent advisor and mentor for many years. I would also like to thank the members of my committee, Dr. Brian Cain, Dr. Lucia Notterpack, Dr. Kathleen Shiverick, and Dr. David Silverman for the guidnance and direction. Each member of my committee unselfishly offered and shared his/her expertise so I could accomplish the degree. I would also like to acknowledge the assistance given to me by Dr. Hai Wang and Dr. Patricia Moussatche. My discussions with them have been invaluable in overcoming obstacles that ariose during this thesis. I also thank Dr. Chingkuang Tu and Xiaowei Gu for their continuous technique assistance. Finally, I am extremely grateful for my husband Yongsheng and son Muzi for their unending support and encouragement during this period of immense personal and professional growth.

TABLE OF CONTENTS

LIST OF TABLES

LIST OF FIGURES

LIST OF ABBREVIATIONS

| | |
|---|---|
| AZA | Acetazolamide |
| CZA | Chlorzolamide |
| Cpd5c | Compound 5c |
| EZA | Ethoxzolamide |
| N3500 | PEGlated aminobenzolamide |
| DFO | Desferoxamine mesylate |
| DSP | Dithiobis (succinimidyl propionate) |
| DIDs | 4, 4'-diisothiocyanostilbene-2, 2'-disulfonic acid |
| DNDs | 4, 4'-dinitrostilbene-2, 2'-disulfonfonic acid |
| SITs | 4-acetamido-4'-isothiocyanostilbene-2, 2’-disulfonic acid |
| pHi | intracellular pH |
| pHe | extracellular pH |

Abstract of Dissertation presented to the Graduate School
of the University of Florida in partial fulfillment of the
Requirements for the degree of Doctor of Philosophy

# THE ROLE OF CARBONIC ANHYDRASE IX IN THE DEVELOPMENT OF THE GLYCOLYTIC PHENOTYPE OF BREAST CANCER CELLS

By

Ying Li

Dec 2010

Chair: Susan Frost
Major: Medical Science

One of the hallmarks of malignant tumors is the switch from aerobic to anaerobic glucose metabolism, where the glycolytic pathway provides the energy required for cell survival and growth. The expression of carbonic anhydrase IX (CAIX), a marker for hypoxic tumors, is significantly associated with tumor grade, reduced survival, and poor prognosis in breast cancer.

In the studies that follow, the role of CAIX in metabolic function was assessed in breast cancer cells. We first demonstrated that MDA-MB-231 cells, which is an aggressive, "triple-negative," basal B line, have high rates of glycolysis compared with a luminal cell line (T47D) and an immortalized normal epithelial cell line, MCF10A. MDA-MB-231 cells expressed exclusively CAIX, while T47D cells expressed carbonic anhydrase XII (CAXII). CAIX expression in MDA-MB-231 was both density and hypoxia-dependent. We provided evidence that CAIX contributes to metabolic dysfunction through studies on pH, lactic acid production, glucose uptake, and CAIX inhibition. We showed that an impermeant CA inhibitor, N3500, prevented the acidification of the medium, but only under hypoxic conditions. However, among the several CA inhibitors investigated, only chlorzolamide significantly reduced cell viability, migration, and invasion. Together, these studies suggest that CAIX expression and activity are

associated with metabolic dysfunction in MDA-MB-231 cells**.** In the course of these studies we discovered that the commercially available CAIX antibody from Novus Biologicals, NB-100, recognizes a beta-tubulin by using 2-dimensional gel electrophoresis and mass spectrometry. This observation was significant because recent publications suggest that this antibody was being considered in the clinical diagnosis of CAIX expression in breast patient patients, which could lead to false positive, based on our results.

The biochemical properties of CAIX were also investigated. CAIX primarily exists as a dimer (90%) with only 10% appearing as monomers in hypoxic MDA-MB-231 cells. CAIX migrates as a doublet and both forms are glycosylated, each containing high mannose structures. Additional studied focused on CAIX association with lipid rafts which are microdomains in plasma membranes involved in signal transduction. While there is some evidence that the dimeric form of CAIX resides specifically in lipid rafts in renal carcinoma cells, we found little evidence to support this hypothesis in MDA-MB-231 cells. In hypoxic cells, only 1% of the CAIX pool is localized to lipid raft. While EGF treatment stimulated a 5-fold increase in CAIX translocation to lipid rafts, EGF did not tyrosine phosphorylate CAIX under normoxic or hypoxic conditions, although EGFR and down-stream signaling pathways were activated by EGF. Hypoxia also activated Akt independent of EGF action. Together, these data demonstrate that the active form of CAIX in the MDA-MB-231 breast cancer cell line is dimeric and that neither lipid raft localization nor its phosphorylation status are likely required for its dimerization or activity.

A technique called membrane inlet mass spectrometry (MIMS) was utilized to directly measure native CAIX activity in membrane ghosts and intact MDA-MB-231 cells. Hypoxic cells showed substantially higher exofacial CA activity than normoxic cells and was associated

with elevated levels of CAIX. This activity could be blocked by impermeant CA inhibitors. Data from membrane ghosts showed that the kinetic constants of CAIX in the membrane environment were very similar to those measured for purified, recombinant, truncated forms. Hence, activity of CAIX is not affected by the proteoglycan extension or membrane environment. Zinc did not activate CAIX activity in the membrane although previous data suggested that zinc activated soluble forms of CAIX. In addition, the catalytic activity of CAIX in the interconversion of $CO_2$ and bicarbonate increases as pH was decreased from pH 9 reaching a maximum at approximately pH 6.5. Importantly, these data indicate that CAIX may contribute to both the development and maintenance of the new pH set-point of cancer cells in response to the proton load from intracellular metabolism. In this manner, CAIX contributes to the survival fitness of tumor cells.

Physical and functional interaction of CAIX and the AE anion exchangers was assessed through co-precipitation assays and MIMS. Although AE2 was expressed in MDA-MB-231 cells, interaction of CAIX and AE2 was not observed. While activity studies with inhibitors of the AE transporters were initially encouraging, we later demonstrated that these inhibitors directly blocked purified CAII activity and very likely CAIX activity in MDA-MB-231 cells.

In conclusion, we have shown CAIX expression and activity are well correlated and associated with metabolic dysfunction in an aggressive breast cancer cells MDA-MB-231 cells. Characterization of CAIX in MDA-MB-231 cells confirms that CAIX is an N-linked glycoprotein containing high mannose structures. Lipid raft localization is not required by CAIX dimerization and activity. Further, catalysis and inhibition studies on CAIX in membrane ghost and intact MDA-MB-231 cells by MIMS suggest CAIX contributes to both the development and

maintenance of the new pH set-point of cancer cells in response to the proton load from intracellular metabolism, indicating CAIX may offer a new target for therapeutic intervention.

CHAPTER 1
OVERVIEW

## Introduction

Cancer is one of the most dangerous threats to human health causing about 13% of all human deaths. According to the American Cancer Society, 7.6 million people died, world-wide, from cancer during 2007. Breast cancer, particularly, represents a major public heath problem with more than one million new cases reported yearly around the world. A U.S. study conducted in 2005 by the Society for Women's Health Research indicates that breast cancer remains one of the most feared diseases. Among women in the U.S., breast cancer is the second-most common cause of cancer death (after lung cancer). Women in the U.S. have a 1 in 8 lifetime chance of developing invasive breast cancer and a 1 in 33 chance of breast cancer causing their death. In 2009, 193,370 new cases of breast cancer were predicted causing about 40,170 deaths (*American Cancer Society 2009)* which equates to about one death every 13 minutes. Breast cancer can metastasize to the lungs, liver, brain, and most commonly to the bones by transport of metastatic cells via blood vessels or the lymphatic system.

One of most striking features of cancer cells is their high glycolytic rate and acidification of the extracellular milieu which together is known as the glycolytic phenotype of cancer cells, discussed in the following section.

## Glycolytic Phenotype of Cancer Cells

Cancer is a class of diseases in which a group of cells display uncontrolled growth, invasion, and sometimes metastasis. Development of cancers is a multi-stage, multi-step process of genetic and epigenetic changes which promote the emergence of an increasingly aggressive phenotype (*1*). Malignant tumors invariably switch from oxidative metabolism to anerobic glycolysis for producing the necessary energy for their survival and growth (*2*). This switch is

attributed to the abnormal vascular system in these tumors (*3*). The vascular system develops in an organism to deliver and distribute oxygen and nutrients to normal tissues. However, solid tumors arise without an existing vascular system but stimulate the formation of new blood vessels that are invariably inadequate and dysfunctional which results in hypoxia in most tumor beds (*4*). Hypoxic regions in tumors undergo, on average, 1-20 cycles of fluctuation in oxygenation per hour. This means that oxygen delivery to the tumors is extremely unreliable. The tumor hypoxic microenvironment selects cells in which anaerobic glucose metabolism is constitutively unregulated, which appears to assure their survival. Therefore the key adaptation to hypoxia by cancer cells is the switch from oxidative phosphorylation to anaerobic glycolysis. Ultimately cancer cells become insensitive to oxygen. Thus, even in the presence of $O_2$, cancer cells favor the glycolytic pathway for energy production as discovered by Warburg over 80 years ago (*5*). This phenomenon is actually termed "aerobic glycolysis". Thus, on one hand, the glycolytic phenotype is selected early in *in situ* cancers because they are faced with intermittent hypoxia. On the other hand, aerobic glycolysis is also necessary for cancer progression, because glucose metabolism generates several important by-products, including ATP, NADH, NADPH, lactate and other metabolic acids any of which may contribute to increased cancer progression and metastasis (*6*). Indeed, preventing the Warburg effect by inhibition of lactate dehydrogenase attenuates tumor growth, suggesting that aerobic glycolysis might be essential for cancer progression (*7;8*). Overall, cancer cells undergo a metabolic transition which allows them to survive and grow in the hostile environment created by the decreased blood flow associated with disordered vascularization of tumor (*9;10*).

The most striking feature of tumor cells is the production of excessive amount of lactic acid due to the increased glycolysis. Upregulation of glycolysis in cancer cells is regulated by

the transcription factor hypoxia inducible factor 1 (HIF-1) which is a heterodimer consisting of an inducible subunit (HIF-1α) and a constitutively expressed subunit (HIF-1β) (*11*). Under normoxic conditions, HIF-1α is hydroxylated at P402 or P564 by a set of HIF prolylhydroxylases, followed by polyubiquination, and eventually degradation in proteosomes. Under hypoxic conditions, the lack of hydroxylation prevents HIF1α degradation. This allows interaction with the β subunit, translocation into nucleus, and activation of its 40 or so target genes (*12*). GLUT1 is one of the key target genes of HIF-1, and mediates the transport of glucose into the cells. Upregulation of GLUT1 allows cancer cells to take up glucose more efficiently (*13*). Lactate dehydrogenase (LDH5) is also a target of HIF1. Upregulation of LDH allows enhanced conversion of pyruvate to lactate (*13;14;15*). Increased production of lactic acid creates the potential for low intracellular pH (pHi). However, NMR technology revealed that the range of pHi in the cytoplasmic compartment in tumor cells is between 7.1-7.4 which is similar to normal cells. However, extracellular pH (pHe) is reduced to 6.8-7 (*16*).

Multiple membrane transport mechanisms have been proposed to explain the extrusion of protons from the cytoplasm into the extracellular environment in order to maintain a pHi of around 7.2. First, the $Na^+$-$H^+$ exchanger (NHE) is required for intracellular alkalization of cancer cells and is an essential component of the glycolytic phenotype of cancer cells (*17*). The monocarboxylate transporter (MCT), which co-transports lactate and a proton, is a target of HIF1α and upregulated in cancer cells (*18*). Vacuolar ATPase (vATPase) has also been shown to be upregulated and targeted to the plasma membrane in cancer cells, where it plays a major role in pumping protons (*19*). Each of these mechanisms stabilizes the pHi and reduces pHe. Increased extracellular acidity is not permissive to normal cell growth and leads to apoptosis (*20*). Cancer cells appear to establish a new "set-point" which allows them to tolerate an

interstitial pH of around 6.8 (*21*). Work by Gatenby and Gillies suggest that this change in set point is critical to tumor biology because acid will flow along concentration gradients from the tumor to adjacent normal tissue causing normal cell death, disruption of the extracellular matrix, promotion of angiogenesis, and loss of immune response to tumor antigens, and resistance to therapeutic drugs (*1;22*). Tumor cells are readily able to colonize this adjacent damaged normal tissue providing a mechanism for continued invasion and growth. Therefore, low pHe appears to give selective advantage for tumor growth and development. The coincidence of high lactic acid out put and low pHe has led to a popular belief that lactic acid is the source of the acidosis in the tumor microenvironment. This concept has been challenged by experiments performed on tumors with impaired glycolytic ability. In these experiments, Chinese hamster overy cells with reduced lactate dehydrogenase (LDH) activity showed considerably lower glucose utilization and lactic acid output, but still produced an acidic extracellular microenvironment when transplanted into mice (*7*). Also, glycolysis deficient Chineses hamster lung fibroblasts (lacking phosphoglucose isomerase activity), when transfected into mice, produced an acidic extracellular milieu of pH 6.7 despite negligible *in vitro* lactic acid production (*23*). These findings suggest that the acid responsible for the low pHe could be volatile. In healthy tissue at rest, the majority of cellular acid is extruded as $CO_2$. Recent work has also suggested a dominance of $CO_2$ over lactic acid as an acid generator in tumors (*24;25*) and studies in spheroids have shown that lactic acid efflux does not contribute greatly toward establishing an acidic pHe (*26*). It is therefore hypothesized that the majority of anaerobically produced protons exits cells as $CO_2$. If $CO_2$ is a significant source of acidity in tumors, this implies a contribution by the carbonic anhydrase (CA) family which catalyzes the reversible conversion of $CO_2$ to bicarbonate and a proton in the development of glycolytic phenotype of cancers.

## Carbonic Anhydrase Family

Carbonic anhydrase (CA) is a family of zinc metalloenzymes that catalyze the hydration of $CO_2$ and the dehydration of $HCO_3^-$: $CO_2 + H_2O \leftrightarrow HCO_3^- + H^+$. This reaction is involved in many physiological and pathological processes, including respiration and transport of $CO_2$ and bicarbonate between metabolizing tissues and lungs; pH and $CO_2$ homeostasis; electrolyte secretion in various tissues and organs; biosynthetic reactions (such as gluconeogenesis, lipogenesis, and ureagenesis); bone resorption, and calcification (*27;28*). The active site of most CAs contains a zinc ion, which is essential for catalysis.

There are at least four distinct CA families from human to plants to bacteria: the α-CAs (present in vertebrates, bacteria, algae and cytoplasm of green plants); the β-CAs (predominantly in bacteria, algae and plant chloroplast), the γ-CAs (mainly in archaea and some bacteria); and the δ-CA (present in some marine diatoms). To date, 16 α-CA isoforms have been identified in mammals of which three are not catalytically active, including CAVIII, X, and XI (*29*). The 13 catalytically active isoforms are further divided into 4 groups based on tissue distribution and subcellular localization. CAI, II, III, VII, and XIII are expressed in cytosol. CAV is expressed in mitochondria, but has two homologs, CAVA and CAVB that show unique tissue distribution. CAVI is the only secreted CA and found in salivary gland of a number of mammalian species. There are five membrane-associated CA isoforms, three of which (CAIX, CA XII and CA XIV) are transmembrane proteins. CAIV and the closely related CAXV are attached to the outer leaflet of the plasma membrane through a GPI anchor. CAXV is not founds in humans. Kinetic properties for these CAs are different. Among them, cytosolic CAII has the highest catalytic efficiency displaying a Kcat/Km of $1.5 \times 10^8$ $M^{-1}s^{-1}$. CAIII exhibits the lowest hydratase activity (Kcat/Km = $3 \times 10^5$ $M^{-1}s^{-1}$) of the CA isoforms. CAI, CAIV and CAVI have Kcat/Km values of $5.0 \times 10^7$ $M^{-1}s^{-1}$. Kcat/Km of CAXII, CAXIV and CAXV are lower than other isoforms, at about

$3.5 \times 10^7\ M^{-1}s^{-1}$. The catalytic domain of CAIX (CA) was first cloned into bacteria and analyzed for its kinetic properties by the Silverman group, establishing a Kcat/Km of $5.5 \times 10^7\ M^{-1}s^{-1}$ (*30*). Subsequently, the catalytic and catalytic domain with thePG extension (PG + CA form ) were cloned into *E. coli* and an insect expression system and measured for $CO_2$ hydration activity (*31*). The catalytic domain, regardless of expression system, was determined to have similar catalytic efficiency as that originally reported for CAIX. However, the addition of the PG domain appeared to contribute to an increase in the $CO_2$ hydration activity of CA domain. Together, these data suggest that CAIX belongs to the highly active human α-CAs and that its catalytic properties for the $CO_2$ hydration reaction are comparable to those of CAII, the most active CA isoform.

**Carbonic Anhydrase IX Expression and pH Regulation in Cancer**

Among the CA isoforms, two CA isoforms (CAIX and CAXII) are associated with, and overexpressed in, many solid tumors and cancer cell lines (*32;33*). CAIX, originally named MN protein, was identified using the M75 monoclonal antibody in HeLa cells by Pastorekova *et al*. (*34*). Subsequently, analysis of the encoded cDNA revealed its sequence and domain positioning (*35*). Mature MN/CAIX is a transmembrane *N*-linked glycoprotein that contains 422 amino acids (aa) and four distinct domains: a 59 aa N-terminal proteoglycan-like domain (PG domain), a highly conserved extracellular catalytic domain (CA domain) consisting of 259 aa, a 20 aa transmembrane region, and an 25 aa intracellular C-terminal, cytoplasmic domain (Figure 1-1). The extracellular N-terminal PG domain appears to play a role in cell adhesion (*36*). The catalytic domain includes 3 zinc-binding histidine residues (His 189, His 191, and His 214) at the active site (Figure1-1). One study suggests that the cytoplasmic domain of CAIX possesses a tyrosine target for the EGF receptor kinase and may be involved in amplifying EGF receptor signaling in a unique signaling pathway in renal carcinoma cells (*37*).

CAIX is overexpressed in many types of cancer such as renal, lung, colon, brain, cervix, ovarian, esophagus, and breast carcinoma, but is absent in the corresponding normal tissues (*33;38;39*). Its expression, which is regulated by the HIF-1 transcription factor complex, is strongly induced by hypoxia and considered as a marker for hypoxia (*40*). CAIX expression is significantly associated with high tumor grade, reduced survival, and poor prognosis in breast cancer (*38;41*). Thus, in contrast to the other CA isozymes, CAIX has been implicated in playing a role in the regulation of cell proliferation, adhesion, and malignant cell invasion. Although CAIX is overexpressed in many solid tumors**,** it is expressed only in a limited number of normal tissues such as epithelial cells of the proximal gastrointestinal tract including the stomach and gall bladder (*42;43*). Normal expression of CAIX is also seen in the basolateral membranes of enterocytes in the duodenum and jejunum, with most abundant expression occurring in the crypts, the region where epithelial cells exhibit high proliferative capacity (*43*). CAIX also shows low expression in pancreatic ducts and epididymis (*28*). Notably, strong expression of CAIX in numerous tumors is predominantly found in carcinomas that are derived from tissues that do not normally express CAIX. In contrast, tumors originating from CAIX-positive tissues, such as stomach, tend to have lowered expression of CAIX (*28*).

Expression pattern of CAIX is principally determined by a strong activation of *CA9* gene transcription via a hypoxia-inducible factor (HIF1), which binds to the hypoxia response element (HRE) localized in the *CA9* promoter. As mentioned earlier, HIF-1 is a heterodimer consisting of an inducible subunit (HIF-1α) and a constitutively expressed subunit (HIF-1β). HIF-1α becomes active under conditions of hypoxia. Hypoxia usually occurs at a distance of 100-200 μm from blood vessels in tumors (*44*) and seems to be strongly associated with tumor proliferation, malignancy, and resistance to radiation and chemotherapy (*45;46*). Expression of

CAIX is highly correlated with the level of hypoxia measured in different tumors, including breast tumor, and makes it a reliable intrinsic marker of tumor hypoxia (*47*). Also, it has been demonstrated that in cultured cells, CAIX expression is density-dependent and requires PI-3-kinase activity (*48*). CAIX is proposed to play a major role in regulating hydrogen ion flux, and inhibition of CAIX results in increased cell death under hypoxic conditions, indicating that its expression provides a mechanism for hypoxic adaptation (*33;49*).

Basolateral expression of CAIX suggests a role in facilitating chloride/bicarbonate exchange resulting in bicarbonate extrusion across the basolateral membrane (*42*). Thus, CAIX may promote $H^+/HCO_3^-$ transport to maintain cellular pH in gastric and duodenal epithelial cells and is involved in gastric acid secretion. The role of CAIX in promoting extracellular acidosis was first demonstrated by the Pastorekova group (*50*). In their study, MDCK epithelial cells overexpressing with CAIX were shown to acidify culture medium when exposed to periods of hypoxia, and acidification was slowed in the presence of sulfonamide inhibitors of CA. A study by Swietach *et al.* showed ectopically expressed CAIX in human bladder carcinoma RT112 cells was able to spatially coordinate pH, but only when cells were cultured as three-dimension structures (*24*). Chiche *et al.* found that CAIX expression affected pHi in isolated cells only when cells were exposed to bicarbonate-free buffer in an acidic milieu (*51*). Another very important example of CAIX-dependent pH regulation comes from the work done by Swietach and his colleagues (*26*). These investigators made CA9-expressing spheroids of human colon carcinoma cells and imaged the intracellular and extracellular pH in these spheroids using membrane-impermeant fluorescent pH-reporter dyes. With CAIX expression, spheroid core pHi was higher (pHi=6.6) than that in control spheroids (pHi=6.3) and pHe was decreased (pHe= 6.6) compared to control spheroids (pHe=6.9). These data suggested that $CO_2$ producing tumors may

express CAIX to facilitate $CO_2$ excretion. These observations support the mechanism that Harris and colleagues proposed earlier in which CAIX participates in the acidification of the tumor microenvironment. In this model, pHe is reduced through the coupled activity of CAII, CAIX and bicarbonate transporters in cancer cells (Figure 1-2) (*40*). Intracellular protons produced by glucose metabolism react with $HCO_3^-$ to form $CO_2$. The $CO_2$ diffuses to the extracellular milieu and is catalytically hydrated to bicarbonate with the production of a proton by membrane-bound CAIX. This would enable the anion exchanger (AE) to transport the newly generated $HCO_3^-$ back into the cytoplasm to provide a buffer for pHi. This proposal illustrates only one aspect of CAIX regulation of pH. We propose that CAIX could also neutralize protons ejected from the cells by catalyzing their reaction with bicarbonate to form $CO_2$ and $H_2O$. Thus, CAIX function in the regulation of pHi and pHe will likely depend on the proton and $CO_2$ concentration in the extracellular space. CAIX is a bidirectional enzyme that could accelerate both extracellular $CO_2$ hydration and the dehydration reaction depending on the concentration of the reactants. Therefore, in the extracellular space, CAIX may actually be responsible for stabilizing pHe at a value that favors cancer cell survival compared to the surrounding normal cells. At physiological pHe (or as lactic acid production is increasing in response to hypoxia), CAIX activity favors the $CO_2$ hydration and contributes to the acidification of tumor microenvironment. When pHe approaches 6.8, CAIX activity will favor dehydration of bicarbonate which consumes protons. Either way, CAIX would effectively protect the cancer cells either from over acidification of intra- or extra-cellular space, favoring cell survival and promoting the metastatic phenotype.

## CAIX Inhibitors and CAIX Target Therapy

Given that CAIX expression is associated with high tumor grade, tumor necrosis, and poor prognosis in breast cancer (*41;52*), it becomes a potential target for cancer therapy. There are

several reasons to consider CAIX as a suitable target molecule for cancer therapy. First, CAIX is expressed in commonly occurring carcinomas, which are relatively resistant to conventional therapy. Second, its normal expression is restricted to the luminal epithelia of the alimentary tract, with limited accessibility to immune cells, antibodies, and many drugs.

CA isoforms are inhibited by several classes of inhibitors: inorganic anions, sulfonamides, and phenols (*53*). The best investigated CA inhibitors are the sulfonamides. Some sulfonamide CA inhibitors are already in use in the clinical setting such as acetazolamide (AZA), methazolamide (MZA) and ethoxzolamide (EZA) (Figure 1-3A, B). To date, many CA inhibitors have been synthesized from these standard compounds and shown to inhibit to various degrees the growth of tumor cells expressing tumor-associated CAs (CAIX , CAXII) both *in vitro* and *in vivo* (*54;55*). Many sulfonamides possess low nanomolar Ki values against CAIX activity (Table 1-1). These sulfonamide inhibitors interact with the $Zn^{+}$ ion directly and participate in various interactions with amino acids in the active site to block the activity of CA (*56*). This implies that CAIX represents a new pharmacologic target for hypoxic tumors that are non-responsive to classical chemo- and radio-therapy.

Recently, several membrane impermeable and specific CAIX inhibitors have been shown to work at μmolar/nanomolar levels with therapeutic implications (*50;55*). Among these, the PEGylated inhibitor (F3500), a pyridinium derivative, and Compound 5c (Cpd 5c) are among the most interesting. F3500 is a compound that was synthesized by Conroy *et al*. (*57*). It was designed to be impermeant through covalent attachment to polyethylene glycol bisacetic acid. These investigators also showed that this compound was soluble, non-toxic, and selectively blocked cell surface CAIV activity in the kidney. The F3500 polymer inhibits CAIX activity with a binding constant of 3 μM (Ki = 3 μM). The PEGpAMBS inhibitor (N3500) is also a

PEGylated compound displaying similar inhibitory activity (Ki = 3.4 μM against CAII) (*58*) (Figure 1-3D). Like F3500, N3500 is impermeant as demonstrated in red blood cells (*58*). The pyridinium derivative is a strong CAIX inhibitor (Ki = 14 nM) which belongs to a class of positively charged sulfonamides and possesses *in vivo* selectivity for membrane-bound (CAIV) versus the cytosolic isoform (CAII) (*59*). Cpd 5c is a fluorescent sulfonamide investigated by Svastova *et al*. in which the sulfonamide is linked to fluorescein (Figure 1-3C). This inhibitor has high affinity for CAIX (Ki = 9 nM) so has high potential for use as a fluorescent probe for CAIX expression. Several studies have suggested that this inhibitor binds to CAIX only under conditions of hypoxia *in vitro* and *in vivo* (*50;60;61*). The impermeable feature of all of these inhibitors is highly attractive for targeting CAIX at it active site and separates that inhibition from CAII. In this study, I utilize a variety of sulfonamide inhibitors such as AZA, EZA, N3500 and Cpd 5c to characterize CAIX activity in breast cancer cells.

**Metabolon Theory: Interaction of CAs with Bicarbonate Transporter**

While under intensive study, the mechanism of CAIX regulation of tumor pH is still undetermined. One hypothesis is the bicarbonate transport metabolon theory. A metabolon is a complex of proteins that physically interact to enhance the channeling of substrates between enzymes involved in a pathway to improve metabolic rate. A bicarbonate transport metabolon refers to the complex of carbonic anhydrase(s) with a bicarbonate transporter to coordinate pH regulation (*62*). In the bicarbonate transport metabolon, CAs may physically and functionally interact with anion exchangers (AE) to facilitate proton extrusion. The AE group of bicarbonate transporters facilitates the movement of $HCO_3^-$ across biological membranes. In mammals, about 13 different genes encode the bicarbonate transporters, which functions through a range of mechanisms, including $Cl^-/HCO_3^-$ exchange, $Na^+/HCO_3^-$ co-transport, and $Na^+$-dependent $Cl^-$

/$HCO_3^-$ exchange (*63-65*). These bicarbonate transporters cluster into 3 separate branches upon phylogenetic analysis: $Cl^-/HCO_3^-$ exchangers of the AE family, $Na^+/HCO_3^-$ co-transporter of the NBC family, and members of the SLC 26 (solute carrier subfamily 26) family. $Cl^-/HCO_3^-$ exchangers include three isoforms (AE1, AE2 and AE3) that differ in their tissue distribution (*65*). AE1 is restricted to erythrocytes, intercalated cells of renal collecting duct, heart and colon, whereas AE2 is widely distributed in basolateral membranes in most epithelial cells. AE3 is expressed in brain, retina, heart and smooth muscle, epithelial cells of the kidney and GI tract. Many studies have been performed to investigate the interaction of CAs with AEs. These studies have shown that many CA isoforms are associated with AEs. For example, CAII binds to the C-terminus of human AE1. The binding site of CAII in AE1 had been identified as the acidic LDADD motif (amino acids 886-890). Sequence alignment of the C-termini of AEs indicate that a similar CAII binding site exists in the C-terminus of AE2 (LDANE) and AE3 (LDSED) (*66*). Truncation and mutagenesis of the basic N-terminus region of CAII showed that the AE1-binding site in CAII is a histidine-rich region (MSHHWGYGKHNGPEHWHK) (*67*). The binding of CAII and AEs accelerates the respective transport rates of bicarbonate transporters. The GPI-linked enzyme CAIV also binds AE1, AE2, and AE3 specifically within the fourth extracellular loop of AEs. Co-expression of CAIV and AEs restores the reduction of bicarbonate transport rate by the mutant of CAII in HEK 293 cells. Acetazolamide inhibited the effect of CAIV co-transfection on bicarbonate transport rate demonstrating that CAIV activity is required for increased bicarbonate transport (*68*). Recently, Morgan *et al*. have shown that CAIX binds to each of the AE isoforms and the catalytic domain of CAIX mediates the interaction with AE2 in HEK 293 cells (*69*). These interactions increased bicarbonate transport mediated by AEs. The co-localization of AE2 and CAIX in the parietal cells of stomach suggested that CAIX and AE

interaction may play a fundamental role in the gastric acid secretion (*69*). Localization CAIV or CAIX with CAII and a bicarbonate transporter at the membrane may maximize the rate of bicarbonate transport by enhancing the transmembrane gradient local to the bicarbonate transporter. The interaction between CAs and bicarbonate transporter may be critical to the bicarbonate flux in differentiated cells. Assembly and activation of such a metabolon would be especially meaningful in the low oxygen environment in cancer cells. Hypoxia may stimulate the assembly of this metabolon to enhance bicarbonate flux. As CAIX is induced by hypoxia in many types of tumor, CAIX might work as an extracellular component of the metabolon to regulate pH of tumor microenviroment. Harris and colleagues have suggested this mechanism for reducing extracellular pH (*32;40;70*), although it is still not clear that the interaction between CAIX, CAII and the bicarbonate transporter is merely functional or requires a physical union between CAs and bicarbonate transporter in cancer cells. Therefore, the study of a functional and physical interaction of AE with CAIX, and CA II in cancer cells under hypoxic conditions will be important in understanding extracellular acidification and the role of CAIX in the development of the glycolytic phenotype of breast cancer cells.

**Model System: Human Breast Cancer Cells (HBCs)**

In the present study, I utilize breast cancer cells (HBCs) as models to study the role of CAIX in the development of glycolytic phenotype of breast cancer. Breast cancer cell lines have been the most widely used models to investigate the events leading to breast cancer progression because most features of breast cancer are preserved in the breast cancer cell lines from which they derive (*71*). Recent studies divide breast cancer cells into two branches based on transcriptional activity (*71;72*). These two branches are known as the luminal group which is estrogen receptor (ER)- and ERBB3-positive and the basal-like group which is estrogen receptor-negative and caveolin-positive. Basal-like cells further are separated into two groups, Basal A

and Basal B. Luminal cells are related to a more differentiated and non-invasive phenotype. Basal B cells are associated with a more metastatic phenotype and represent "triple negative" tumors [estrogen receptor-negative ($ER^-$), progesterone receptor-negative ($PR^-$), and HER2 negative]. The number of available breast cancer cell lines is relative small and only a few of them have been extensively studied. Among these, the MCF-7, T47D and MDA-MB-231 account for more than two-thirds of all of the published studies, and they are likely to reflect the features of cancer cells from which they are derived (*72*). The T47D cell line is derived from a ductal carcinoma and is an estrogen receptor-positive cell line (*73*). Analysis of transcriptional activity reveals that these cells align with luminal markers (*72*). When injected into nude mice; these cells form a solid tumor but do not metastasize (*71*). The MDA-MB-231 line is derived from an adenocarcinoma and is an $ER^-$, $PR^-$, HER2 negative, but EGF receptor-positive cell line (*73*). When injected into nude mice, these cells form tumors and aggressively metastasize. MDA-MB-231 cells belong to the Basal B branch and are representative of triple negative tumors (*72*). MCF10A line is derived from fibrotic tissue and is frequently used as a control for breast cancer cells. These cells are ER-negative, EGF receptor-negative, and HER2 negative but E-cadheren positive. This is an immortal but non-transformed cell line, so MCF10A cells do not form tumors *in vivo*. MDA-MB-231 cells and MCF10A cells have similar transcriptional profiles, ones that define the Basal B group, despite their very different *in vivo* behaviors (*72*).

The goal of this study is to determine if CAIX expression and activity contribute to the development of the glycolytic phenotype of breast cancer cells. We discovered, among the cell lines tested, that the membrane-associated CA family members are differentially expressed. However, high expression of CAIX in the aggressive breast cancer MDA-MB-231 cells, along with that of cytoplasmic CAII, shows strong correlation with the ability to acidify the medium.

We demonstrate that CAIX expression and activity is associated with metabolic dysfunction in MDA-MB-231 cells concluding that CAIX contributes to the development of glycolytic phenotype of these breast cancer cells. This predicts that the most aggressive breast cancer cells will express CAIX, which is consistent with studies demonstrating increased mortality of breast cancer patients with tumors that express CAIX. We also show that CAIX is the only membrane CA expressed in MDA-MB-231 cells, which provide advantage for characterize CAIX activity. Using $^{18}O$ exchange technique, we show that CAIX activity is increased by hypoxic treatment. We also show that low pH, adjusted to mimic the tumor microinviroment, increases CAIX activity in the direction of $CO_2$ production. Further, we demonstrate that CAIX activity is further enhanced by the anoxic condition. Finally, we show that CAIX activity can be blocked by sulfonamide inhibitors including the impermeant inhibitor N3500 and fluorescent inhibitor Cpd 5c in MDA-MB-231 cells. Together, these data indicates that CAIX expression and activity are involved in the development of glycolytic phenotype of breast cancer cells. Inhibition of CAIX activity by sulfonamide may be a potential therapeutic tool for invasive breast cancers.

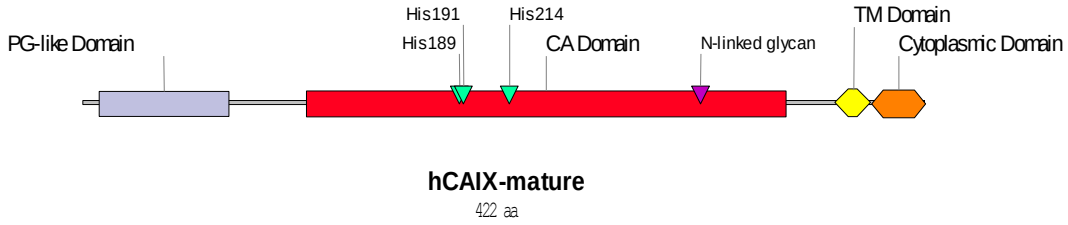


Figure 1-1. Secondary structure of carbonic anhydrase IX (CAIX). The mature form of CAIX consists of four domains: PG-like domain (proteoglycan-like domain), CA domain (carbonic anhydrase domain), TM domain (transmembrane domain), and the cytoplasmic domain.

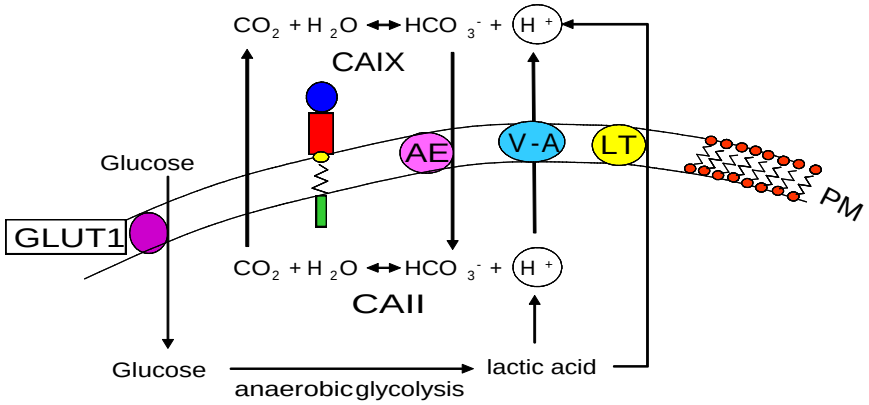


Figure 1-2. Potential mechanism of proton extrusion and the role of CAIX in the regulation of pH. GLUT1: glucose transporter, LT: lactate transporter, VA: vacuolar ATPase (vATPase): AE: anion exchanger, CAIX and CA II collaborate to extrude proton. See text for details.

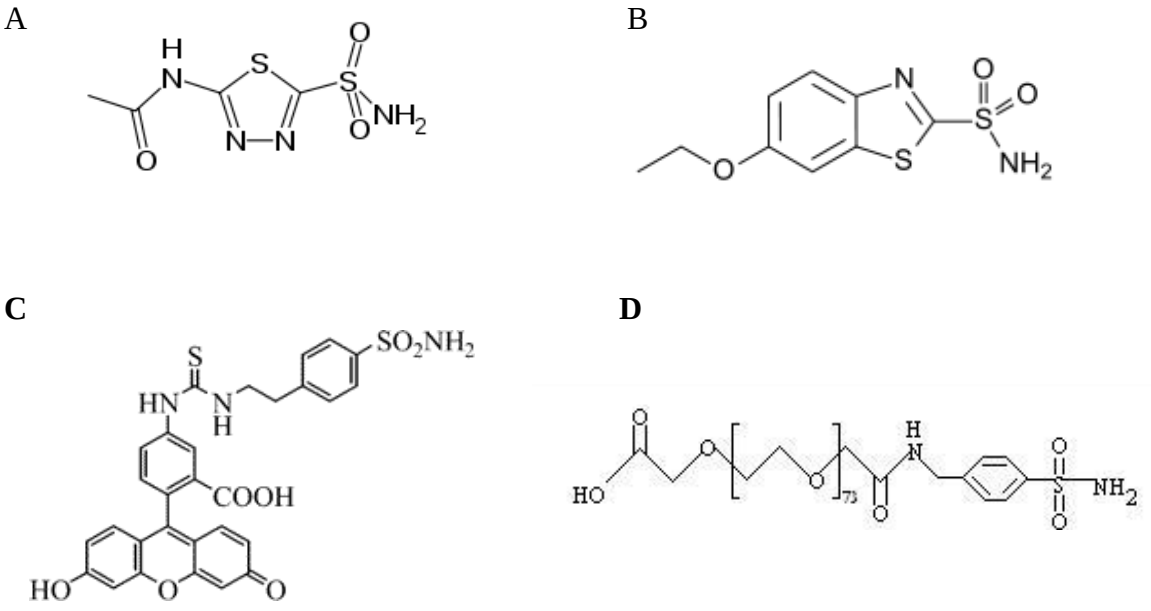


Figure 1-3. Structure of acetazolamide, ethoxzolamide, cpd 5c and N3500. A) Acetazolamide: semi-diffusible sulfonamide. B) Ethoxzolamide: rapidly diffuses across cell membranes. C) Cpd 5c: small molecular weight sulfonamide linked to fluorescein. D) N3500: impermeant CA inhibitor in which aminobenzolamine is attached to polyethylene glycol bisacetic acid.

Table 1-1. Ki values of CA inhibitors for CAIX

| CA inhibitor | Ki for CAIX |
|---|---|
| AZA | 3.0 nM |
| CZA | 1.0 nM |
| EZA | <1 nM |
| F3500 | 3.4 μM |
| N3500 | 4.0 μM |
| Cpd 5c | 9.0 nM |

# CHAPTER 2
# MATERIALS AND METHODS

## Materials

Dulbecco' Modified Eagle Medium (DMEM) powder was obtained from Invitrogen (#12100-61). Fetal bovine serum (FBS) was obtained from Atlanta Biologicals (s11450). McCoy's medium was purchased from Gibco (#16600), bovine insulin was purchase from Elanco (#4020), and Mammary Epithelial Basal Medium (MEBM) was purchased from Cambrex Bioscience, (#CC3151). Cholera toxin was purchased from Calbiochem, (#227035). The MDA-MB-231 (MDA-MB-231) cell line was provided by Dr. Kevin Brown (University of Florida). The T47D line was provided by Dr. Keith Robertson (Medical College of Georgia). The MCF 10A (MCF) line was purchased from ATCC.

In this study, I have used 4 antibodies against carbonic ahydrase IX (CAIX). NB-100 was generated in rabbits against a C-terminal peptide (Novus Biologicals). M75 is a monoclonal antibody originally developed by Pastorekova (*34*) and is considered the "gold standard" for CAIX. This reagent was provided by Dr. Egbert Osterwijk from University Hospital Nijmegen in the Netherlands. AF2188 is a goat polyclonal antibody made against a peptide including amino acids 59-419 from the CAIX sequence (R&D system). sc-25599 (Santa Cruz) is a rabbit polyclonal antibody raised against a peptide which includes amino acids 41-160 of CAIX. The caCAII antibody (NB600-919) is a polyclonal made against the entire protein (Novus Biologicals). The glucose transporter 1 (GLUT1) antibody is a rabbit polyclonal generated in our lab and previously characterized (*74*). The anion exchange 2 (AE2) antibody (N-12) was purchased from Santa Cruz Biotechnology and is a goat polyclonal antibody against a peptide mapping at the N-terminus of human AE2. Anti-rabbit IgG-conjugated horseradish peroxidase, anti-mouse IgG-conjugated horseradish peroxidase, and anti-goat IgG-conjugated horseradish

peroxidase were obtained from Sigma-Aldrich. The Enhanced Chemiluminescence kit was obtained from GE Healthcare (#RPN2106). The following antibodies were also used: EGFR (Cell Signaling Technology #2232); pEGFR (Y1173) (Santa Cruz Biotechnology #sc-101668); Akt1 (Sigma-Aldrich #p1601); pAkt (S473) (Cell Signaling Technology (#D9E); Map kinase/Erk2 (Calbiochem #442700); and pErk1/2 (Biolabs #9106).

The carbonic anhydrase (CA) inhibitors, acetezalomide and Chlorzolamide, were provided by Dr. David Silverman (University of Florida). The PEGylated CA inhibitor, N3500, was synthesized by Dr. Nicole Horenstein in the Department of Chemistry at University of Florida. Details of its synthesis are described elsewhere (*58*). The fluorescent CA inhibitor, Cpd 5c, was originally designed by Dr. Claudiu Supuran (*75*). This reagent was synthesized at UF by Dr. Rachel Witek in the laboratory of Dr. Carrie Haskell-Luevano in the Department of Pharmacodynamics. Three anion exchange (AE) inhibitors were used: 4,4'-diisothiocyanostilbene-2,2'-disulfonic acid (DIDS) was purchased from Sigma-Aldrich; 4-acetamido-4'-isothiocyanostilbene-2,2'-disulfonic acid (SITS) and 4,4'-dinitro stilbene-2,2'-disulfonate (DNDs) were provided by Dr. David Silverman (University of Florida). The iron chelator and hypoxic mimic, desferoxamine mesylate (DFO), was obtained from Sigma-Aldrich. Protein A argarose and protein A/G argarose were purchased from Invitrogen. Ampholytes for two-dimensional gel electrophoresis (pH3-10) were purchased from Sigma-Aldrich. Nitrocellulose membrane was purchased from BioRad Laboratories. Cell dissociation buffer (CBS) (# 13151-014) was purchased from Invitrogen. Proteinase inhibitor cocktail (Mini complet) was obtained from Roche Diagonostic.

2-Deoxy-D-[2, 6-$^{3}$H] glucose (45 Ci/mol) was purchased from GE Healthcare (Amersham Life Sciences). [$^{14}$C]-benzoic acid glucose (61 mCi/mol) and [$^{14}$C] 3–O-methylglucose glucose

(45 mCi/mol) were purchased from MP and Perkin Elmer, respectively. All other reagents were of analytical grade from commercial sources.

## Methods

### Human Breast Cancer Cells (HBCs) Culture and Exposure to Reduced Oxygen

MDA-MB-231 (MDA-MB-231) cells were plated in 10 cm plates at a density of 10,000 cell/mL in DMEM containing 10% FBS. T47D cells were plated at a density 20,000 cells /mL in McCoy's medium containing 10% FBS and 0.2 unit /mL bovine insulin. The MCF10A (MCF) cells were plated in Mammary Epithelia Basal Medium (MEBM) at a density of 20,000 cells/mL supplemented with 0.1 μg/mL cholera toxin. The medium overlaying MDA-MB-231 cells was changed two day after plating and then every other day. Medium overlaying the T47D and MCF 10A cells was changed three days post-plating and then every two days. All three cell lines were cultured in an humidified atmosphere at 37°C in 5% $CO_2$. Experiments were conducted when cells achieved 75% confluence (day three post-plating for MDA-MB-231 cells and day 6 post plating for MCF and T47D cells). Desferoxamine mesylate (DFO) is an iron chelator which mimics hypoxia. For DFO treatment, a 10 mM stock was prepared in sterile water and added to medium at a final concentration of 100 μM and incubated at 37°C for 16 hours. For exposure to reduced oxygen, cells were transferred to humidified Modulator Incubator Chambers (MIC-101) purchased from Billups-Rothenberg, Inc. and flushed with 1% $O_2$, 5% $CO_2$ and balanced $N_2$ for 5 min and incubated at 37°C for 1 hour. After 1 hour incubation, the chambers were re-flushed with 1% $O_2$ to purge the gases that remained trapped in the medium. Cells were then incubated at 37°C for an additional 15 hours.

**Cell Growth Assay**

The growth rate of MDA-MB-231, T47D, and MCF cells were assessed by counting cell numbers at different day after plating. The cells were cultured as described above for a specific number of days as annotated in the figure legends. Cells were washed twice with warmed PBS (120 mM NaCl, 2.7 mM KCl, 10 mM $NaH_2PO_4$, and 10 mM $NaH_2PO_4$, pH 7.4) and dissociated from plates by incubation with cell dissociation buffer for 10 min at 37°C. After triturating, an aliquot of cell solution was suspended in isotone in an Accuvet chamber. Cell number was quantitated by a Coulter Counter (Beckman). Cell number in each plate was calculated from the average of five counts.

**Glucose Transport Assay**

Glucose transport activity was measured according by previously published methods (*76*). Briefly, MCF, T47D, and MDA-MB-231 cells were plated in 35 mm plates. At 75% confluence, the cells were divided into three groups. The control group was incubated in a $CO_2$ incubator with 5% $CO_2$ at 37°C. The second group was treated with DFO at final concentration of 100 μM and maintained in 5% $CO_2$ at 37°C. The metabolic chamber was used to maintain a third group at reduced oxygen. After 16 hours, cells were washed three times with Krebs Ringer Phosphate (KRP) buffer (128 mM NaCl, 4.7 mM KCl, 1.25 mM $MgSO_4.7H_2O$, 1.25 mM $CaCl_2.2H_2O$, 5.0 mM sodium phosphate salts, pH 7.4). The plates were equilibrated in 950 μl of the same buffer for 10 minutes at 37°C. Cells were then incubated with or without 40 μM of cytochalasin B (from a stock dissolved in DMSO) for 10 min. Cytochalasin B is a mycotoxin which inhibits facilitated glucose transport. This was followed by 10 min incubation with 0.2 mM [$^3$H]-deoxyglucose. To terminate the reaction, cells were finally washed with ice-cold PBS and dried at room temperature. To quantify radioactivity, the cells were lysed in 1 ml of 0.1% SDS and an

aliquot was counted by scintillation spectrometry. The glucose transport rate was represented by the mass of [$^{3}$H]-deoxyglucose uptake per min per plate.

**Lactic Acid Assay**

MCF10A, T47D, and MDA-MB-231 cells were plated in 35 mm plates and grown to 75% confluence. Cells were fed with fresh medium and then exposed to DFO or hypoxia for 16 hours. Medium was collected from each plate at the end of the exposure and assayed for lactate concentration using a VITROS DT60 II Bioanalyzer (Ortho-Clinical Diagnostics, Rochester, NY). The fresh medium for each of the cell lines was also assayed for the lactate concentration to determine background levels. Rates of lactate production were calculated from the change in the amount of lactate during the 16 hours incubation. For samples exposed to DFO or hypoxia, medium was diluted to 1:10 or 1:15 to maintain the value of lactic acid in the linear range of the assay.

**Measurement of Extracellular pH**

MCF10A, T47D, and MDA-MB-231 cells were plated in 35mm plates. At 75% confluence, cells were exposed to hypoxia or DFO for 16 hours. Medium pH was measured immediately with a portable pH meter. In some experiments, CA inhibitors were added to the medium of MDA-MB-231 cells at a final concentration 100μM. After 24 or 48 hours, pH of the medium was assessed.

**Measurement of Intracellular pH**

**Uptake of [7-$^{14}$C] benzoic acid**

Intracellular pH was determined using the method published by L'Allemain G *et al.* (*77*). Briefly, pHi was measured based on the distribution of [7-$^{14}$C] benzoic acid in the intracellular and extracellular space. Distribution of this weak acid in the intracellular space is correlated with intracellular pH. The MDA-MB-231 cells were grown in 35 mm plate for 3 days and then

exposed to hypoxia for 16 hours. Cells were placed in the 37°C water bath and washed 2 times with warm KRP. Cells were equilibrated for 15 min in $HCO_3^-$ -free solution [130 mM NaCl, 5mM KCl, 2mM $CaCl_2$, 1 mM $MgCl_2$, 5mM glucose, and 20mM each of MES for (pH 6.6) and Hepes for (pH 7.4)] or a $HCO_3^-$ -containing solution [130 mM NaCl, 5mM KCl, 2mM 5mM $CaCl_2$, 1 mM $MgCl_2$ glucose and 25mM $HCO_3^-$]. Cells were then shifted to the same solution described above containing 1μCi/mL of [$^{14}$C] benzoic acid. After incubation at 37°C for 15 min, the plates were washed four times, very rapidly, with ice cold PBS, pH 7.4 (the four washes and aspirations lasted 6-8s). After air drying, cells were solubilized in 0.1 % SDS and radioactivity was measured by liquid scintillation spectrometry.

**Calculating intracellular water space**

The intracellular water space was calculated from the equilibrated uptake of 3-O-methyl-D-[1-$^3$H] glucose. Uptake of 3-O-methyl-D-[1-$^3$H] glucose into the cells reaches a plateau after 40-50 min and remains constant for up to at least 120 min. The cells were incubated with 5μCi/mL of this nonmetabolized hexose in glucose-free solution, pH 7.4 for 60 minutes at 37°C. The cells were then washed and assay for radioactivity as described above. Intracellular water space = cpm inside of cells/cpm in 1 μL of external medium.

**Calculation of pHi**

The intracellular pH was calculated according to the formula: pHi = pHo + log (Bi/Bo). Bo = cpm/μL of [7-$^{14}$C]benzoic acid in the external medium. Bi = cpm of [7-$^{14}$C] benzoic acid inside the cell/intracellular water space. pHo = pH of external medium.

**Isolation of Total Membrane**

A total membrane fraction was isolated based on previously published methods (*76*). Briefly, cells were washed 3 times with 5 mL KRP and incubated for 10 min. The cells were then scraped into a Tris-based buffer (TES1p) containing 20 mM Tris-HCl, 25 mM sucrose, 1

mM EDTA and protease inhibitor and homogenized by 10 stokes in a 10 mL Potter- Elvejhem flask with a Teflon pestle. Membranes were collected at 212,000 x g for 1 hour in a Beckman L8-70 ultracentrifuge. The pellet was washed once with TES1 by repeating the homogenization and centrifugation mentioned above. The final membrane pellet was then homogenized with 10 strokes using a 2 mL Potter-Elvehjem flask and resuspended in TES1p. Total membrane protein was stored at -20°C. Aliquots were assayed for protein concentration.

**Protein Determination**

All protein concentrations were determined using a modification of the Lowry procedure (*78*). This assay uses the color–generating reaction of the Folin-Ciocalteu phenol reagent with the tyrosyl and tryptophan residues of proteins in solution and compares the absorbance measurement of the sample against a standard curve. The standard curve is prepared in duplicate using a 1mg/mL stock solution of bovine serum albumin (BSA) to create a curve ranging from 0 to 100 μg. Each standard is brought to a total volume of 100 μl with $H_2O$. The buffers in which the experimental samples are suspended are added to the standards. Aliquots of the experimental samples (usually 5-10 μl) are diluted with 100 μL of $dH_2O$ so that the volume of all samples and standards is equal. One mL of a mixture of 100 parts of solution A (2.0% $Na_2CO_3$, 0.4% NaOH, 0.16% NaK tartrate, 1.0% SDS ) and 1 part of solution B ( 4% $CuSO_4$) was added to each sample, mixed well, and incubated for 10 minutes at room temperature. Diluted Folin-Ciocalteu phenol reagent was then added (0.1 ml) to each sample, mixing immediately after addition. The samples were incubated for 45 min at room temperature to develop color. A spectrophotometer was then used to measure the absorbance of the samples in the visible spectrum at a wavelength of 650 nm.

**Lipid Raft Isolation**

The isolation of lipid rafts takes advantage of the resistance to protein extraction within rafts by non-ionic detergents, such as Triton X-100 or Brij-98, at low temperatures. Lipid rafts

are also called detergent-insoluble glycolipid-enriched complexes (GEMs) or detergent-resistant membranes (DRMs). Lipid rafts were isolated as described by Kumar *et al.* with some modification (*76*). Five mg of total membrane were extracted in 1.0 mL MBS buffer (25 mM MES and 150 mM NaCl, pH 6.5) containing 1% Triton X-100 (TX-100), supplemented with protease inhibitor mix at 4°C. The samples were mixed end over end for 20 min at 4°C and then homogenized with 10 strokes in a Dounce homogenizer. The homogenizing flask was rinsed with 0.5 mL MBS/TX-100 and added to the extracted sample. The sample was mixed with 1.5 mL of 80% sucrose. The samples, now at 40% sucrose, were placed at the bottom of centrifuge tubes and overlaid with 6 mL of 30% sucrose in MBS and 3.5 mL of 5% sucrose in MBS. After centrifugation at 240,000 x g in a Beckman SW41 rotor for 18h, 13-1.0 mL fractions were collected at 4°C by upward displacement using 60% sucrose as the displacement fluid. The fractions were mixed with 500 μL of ice-cold, 30% tricholoroacetic acid (TCA). The samples were then incubated on ice for 30 minutes. The protein precipitate was collected at 16,000 x g for 15 min in a microcentrifuge. After that, protein pellets were washed 2 times in 1 mL of cold acetone to remove TCA. The precipitate was then dissolved in 65 μl of 0.1% SDS. Total membrane protein (100 μg) and proteins from 12 fractions (2-13 fractions) of sucrose gradients were resolved on a 10% SDS-PAGE gel under reducing conditions. The proteins were transferred to nitrocellulose membrane and immunoblotted for CAIX, GLUT1, raft, and non-raft markers.

**Cell Lysate Preparation**

Cells were first washed three times with cold PBS and then exposed to 1 mL per plate of lysis buffer [1% Triton X-100, 50 mM Tris-HCl (pH 7.5), 150 mM NaCl, 1 mM EDTA, 1 mM EGTA, 1 mM sodium orthovanadate, 25 mM NaF] supplemented with protease inhibitor for 15 minutes on ice. Cell lysates were then scraped from plates and clarified by centrifugation at

16,100 x g for 15 minutes at 4°C in a microcentrifuge. Clarified supernatants were collected and aliquots were stored for protein analysis. Proteins were separated by SDS-PAGE and visualized using immunoblotting.

**Endoglycosidase Digestion**

Endoglycosidase refers to a class of enzymes that catalyze the cleavage of oligosaccharide chains at specific sugar residues. These enzymes are often useful for the characterization of oligosaccharide structure on glycoprotein. *N*-Glycosidase F is an amidase that cleaves between the inner most N-acetylglucosamine (GlcNAc) and asparagine residue of high mannose, hybrid, and complex oligosaccharides of *N*-linked glycoproteins. This enzyme can be used to determine if a protein is post-translationally modified with an *N*-linked oligosaccharide. The second glycosidase, endoglycosidase H (endo H), cleaves between the two GlcNAc residues directly proximal to the asparagine residue in only high mannose type, *N*-linked oligosaccharides. High mannose glycoproteins are characteristic of proteins within the endoplasmic reticulum (ER).

To determine the extent of CAIX glycosylation, 50 µg of total membrane protein (or cell lysates) from hypoxic MDA-MB-231 or MCF10A cells were denatured in 40 mM DTT/ 0.5 % SDS in a final volume of 30 µL for 10 min at 100ºC. For *N*-glycosidase F digestion, the samples were brought to 60 µL in 50 mM sodium phosphate, pH 7.5, 1% NP-40, 1000 U *N*-glycosidase F ( Biolabs) and then incubated at 37°C for 2 hours. For endoglycosidase H digestion, denatured protein samples were brought to 60 µL in 50 mM sodium citrate, pH 5.5, 1000 U endoglycosidase (Biolabs) and then incubated at 37°C for 2 hours. Twenty µL of 4X sample dilution buffer (SDB) was added to each of the samples which were then loaded onto a 10% SDS-PAGE gel for protein separation followed by western blot analysis for CAIX expression.

CAXII glycosylation was accessed by same procedure as CAIX except total membrane was from T47D which expresses only CAXII.

**CAIX Oligomerization Analysis**

To determine the oligomerization of CAIX, MDA-MB-231 cells were exposed to hypoxia for 16 hours. Fifty µg of total membrane protein from hypoxic cells were denatured in 0.5 % SDS in a final volume of 30 µL for 10 min at 100ºC. The samples were brought to 60 µL with 50 mM sodium phosphate buffer, pH 7.5, 1% NP-40 and incubated at 37 °C for 2 hours. Proteins were mixed with an equal volume of 2X Sample dilution buffer (SDB) (20% glycerol, 120 mM Tris-HCl, pH 6.8, 4% SDS, 0.05% bromophenal blue) with or without 2% ß-mercaptoethanol. Then, proteins were separated on 10% polyacrylamide gels and transferred to nitrocellulose and probed for CAIX using the M75 monoclonal antibody.

**Gel Electrophoresis**

**One-dimensional gel electrophoresis**

One-dimensional SDS-polyacrylamide gel electrophoresis (SDS-PAGE) was performed essentially as described by Laemmli *et al*. (*79*). Protein samples were mixed with a small volume of 4 X SDB. Gels were typically run at room temperature overnight at approximately 45V using an electrophoresis unit.

**Two-dimensional gel electrophoresis**

The advantage of two-dimensional (2D) over one dimensional SDA-PAGE is that proteins are separated not just by molecular weight, but by isoelectric point as well. The isoelectric point of a protein is defined as the pH at which the protein has a net charge of zero. At this pH, the protein is immobile in an electric field. In 2D gel electrophoresis, the first dimension allows isoelectric focusing (IEF) which makes use of a stable pH gradient to focus proteins by

electrophoresis to their respective isoelectric points. This procedure was performed as previously described by Semple Rowland *et al*. (*80*).

**First dimension**: Cytosolic proteins were isolated from sub-confluent MDA-MB-231 cells and concentrated using a 30 kDa cut-off centrifugal filter (Millipore) to 400 μg in 200 μL in TES. Concentrated protein was diluted with an equal volume of IEF sample solution (6.4% NP-40, 6.5 mM DTT). Protein was mixed with a 4% acrylamide solution containing 9 M urea, 2% NP-40, and 2% carrier ampholytes (pH3-10). To initiate polymerization, 2 μL N, N, N', N'-tetramethylethylenediamine (TEMED) and 2 μL of 10% ammonium persulfate (APS) were added. Gels were cast 11 cm long in 3 mm diameter glass tubes. The anodic and cathodic buffers were 10 mM phosphoric acid and 20 mM sodium hydroxide, respectively. Gels were run at 350V for 18 hours followed by 800V for 2.5 hours. The gels were then extruded using a water-filled syringe fitted with tubing and incubated in equilibration buffer (62.5 mM Tris-HCl, pH 6.8, 5% β-mercaptoethonal, 2.3 % SDS, and 10 % glycerol) for 30 min. The pH gradient was determined by running an identical gel with 200 μL TES: IEF sample solution in place of protein, cutting it into 0.5 cm pieces, soaking each piece in 1 mL distilled water for at least 2 hours, and measuring each pH.

**Second dimension**: One SDS-PAGE gel was poured for each tube gel, which was layered onto the stacking gel using embedding agarose (1% agarose in SDS-PAGE Stacking gel buffer). Molecular weight standards were prepared by mixing 10 μL of low molecular standards (BioRad) with 300 μL 1% agarose in equilibration buffer and allowing it to solidify in a tube, which was then cut and placed beside the sample gel. The marker gel and sample gel were then overlaid with more embedding solution which contained bromophenol blue to allow the gel to be

tracked while running. The second dimension was run overnight as described above for one–dimensional gel electrophoresis.

**Electrotransfer and Immunoblotting**

For immunoblotting, or Western blot analysis, protein samples were electrotransferred from SDS-PAGE gels to a nitrocellulose membrane which had been previously soaked for 30 minutes in transfer buffer (25 mM Tris-base, 192 mM glycine, 20% methanol). The protein was transferred to nitrocellulose at 200 mA for 2 hours at 4°C. To visualize proteins after transfer, the nitrocellulose was stained with amido black [0.2% amido black (w/v) in 40% methanol, 10% acetic acid], destained (40% methanol, 10% acetic acid), and washed in distilled water. The blots were then blocked to inhibit non-specific antibody interactions in 5% Carnation non-fat dry milk dissolved in Tris-buffered saline (20 mM Tris, 137 mM NaCl, 0.1% Tween-20) (TBST) for 1 hour at room temperature with agitation on an orbital shaker. A washing step followed which consisted of 3 washes in TBST for 5 minutes each. The primary antibody was then added to fresh blotting solution (5 % non-fat dry milk or 5% BSA in some experiments) in TBST for an overnight incubation at 4 °C with agitation. After this, the blot was washed as described above. The blot was then incubated with the secondary antibody, an anti-IgG linked to horseradish peroxidase (HRP), for an hour in TBST. The blot was finally washed 3 times in TBST for 5 minutes each, to remove the non-reacted IgG-HRP. The Enhanced Chemiluminescence (ECL) detection method was used according to manufacturer's direction, followed by to exposure Amersham Hyperfilm. Band intensity was quantitated using Un-Scan-It (Silk Scientific, Inc.) in the linear range of the film.

**EGF-Dependent Phosphorylation of the EGF-Receptor, Akt, and Erk**

MDA-MB-231 cells, grown to day 3 in 10 cm culture dishes, were exposed to serum-free medium overnight under normoxic or hypoxic conditions. Recombinant epidermal growth factor

(rEGF Santa Cruz) was dissolved in 10 mM acetic acid containing 0.1% BSA at a stock concentration of 10 µg/ mL. One hundred ng /mL of rEGF (16 nM) were added to the serum-starved, control and hypoxic cells for specific times as indicated in the figure legends. Immediately after treatment, cells were placed on ice, washed with ice-cold PBS, and lysed in RIPA buffer [1% NP-40, 10mM phosphate buffer, 0.1% SDS, 150 mM NaCl, 0.5% sodium deoxycholate, 1 mM sodium orthovanadate, 0.5 mM phenylmethyl sulfonyl fluoride (PMSF) and protease inhibitor (Roche Diagnostics), pH, 7.4]. Cell lysates were clarified at 16,100 x g for 15 minutes at 4°C. Protein concentration of the clarified supernatants was determined as described above. Proteins were separated on an 8% SDS-PAGE gel and transferred to nitrocellulose membranes for Western blot analysis.

**Immunoprecipitation of CAIX**

Immunoprecipitation (IP) with a specific antibody is a widely used and effective technique for separating a target protein from a crude mixture of protein. Once an immunocomplex of protein and antibody is formed, it is captured on a matrix, commonly protein A/G Sepharose or agarose, so that it is can be removed from solution. Protein associated in a non-specific manner can then be removed by washing the protein A/G beads-immunocomplex. Finally, the immunoprecipted protein can be released by interfering with the interaction between the antibody and the matrix by a denaturing solution such as, SDS and β-mercaptoethanol.

CAIX were immunoprecipitated from total membranes in the following manner. MDA-MB-231 cells were treated with serum-free medium under normoxic or hypoxic conditions overnight as described above. Cells were then exposed to rEGF (16 nM) for 30 minutes. Total membranes were prepared from these cells. One mg of total membrane protein from each sample was adjusted to equal volume with TES1, and then lysed in RIPA buffer on ice for 15 minutes. Any insoluble material was then removed by centrifugation at 16,100 x g in a

microcentrifuge for 15 minutes at 4°C. Supernatants were then processed for immunoprecipitation. First, to eliminate non-specific protein binding, the supernatants were incubated with 50 µL of a 50% suspension of protein A/G plus-agarose (Santa Cruz) for 1 hour at 4°C. Samples were exposed to brief centrifugation in a microcentrifuge to collect the protein A/G beads. The pre-cleared supernatant was transferred to a new microcentrifuge tube. To the pre-cleared supernatants, 50 µL of a 50% solution of protein A/G plus-agarose beads and 3 µg of a goat polyclonal antibody against CAIX (R&D Systems) or a rabbit polyclonal antibody against CAIX (Santa Cruz) were added and subjected to gentle end-over-end mixing overnight at 4°C. The immune complexes were collected by centrifugation at 3000 x g for 5 minutes. The beads were washed 3 times with 1 mL RIPA buffer. The washed pellet was then incubated in 50 µl of 2 X SDS-PAGE sample dilution buffers at 100°C for 5 minutes. The beads were then collected by centrifugation and supernatants were subjected to gel electrophoresis. Proteins were then transferred to nitrocellulose membranes. Phosphorylated CAIX was detected with an antibody against phosphotyrosine (Santa Cruz Biotechnology, #sc-7020). Total CAIX was detected with the M75 monoclonal antibody.

**CA Activity Assay**

CA activity was assayed by Membrane Inlet mass spectromety (MIMS) which was developed by Dr. David Silverman (*81*). This method uses $^{18}O$ exchange between $CO_2$ and bicarbonate into water which is caused by repeated hydration /dehydration cycles, catalyzed by carbonic anhydrase. The depletion of $^{18}O$ in $CO_2$ is catalyzed by carbonic anhydrase according to Equation 2-1 below and is irreversible since $H_2{}^{18}O$ is greatly diluted in $H_2{}^{16}O$. This technique is well suited to measure extracellular and intracellular CA activity, along with the flux rate of bicarbonate into cells. It has been applied to the red blood cell system in which flux rate of $CO_2$ across the plasma membrane has been examined (*82*).

$$CO^{18}O+H_2O \leftrightarrow HCO^{18}O\ ^{16}O^- + H^+ \rightarrow COO + H_2{}^{18}O \quad (2\text{-}1)$$

In a suspension of cells, such as the red blood cells in which there is no extracellular CA activity, depletion of $^{18}O$ from $CO_2$ and bicarbonate depends on several processes 1): the flux of $CO_2$ across the cell membrane providing access of $CO^{18}O$ to catalysis by intracellular CA II, 2): the flux of $H\ C^{18}O^{18}O\ ^{16}O^-$ across the cell membrane providing access to intracellular CA II. This latter step is slow relative to $CO_2$ diffusion. In the red blood cell suspension, interconversion in solution (extracellular face of cells) between $CO_2$ and $HCO_3^-$ occurs rather slowly because red blood cells lack exofacial CA activity (Figure 2-1). However, in a suspension of hypoxic MDA-MB-231 cells in which CAIX expression is induced, the presence of extracellular CA activity speeds up the reaction in the solution (Figure 2-2). CAIX competes for the extracellular pool of $CO^{18}O$ resulting in the diverted depletion of $^{18}O$ that can be measured by MIMS. The $^{18}O$ exchange apparatus uses a membrane permeable to $CO_2$ as an inlet to the mass spectrometer, and hence provides a continuous measure of $^{18}O$ content in $CO_2$ in a reaction vessel. The rate of depletion or decrease in atom fraction of $^{18}O$ from $CO_2$ is a measure of carbonic anhydrase activity (*81*). This technique is very sensitive in measuring purified CA at concentrations in the low nanomolar range and can also be used distinguish external and internal CA activity (*58*).

**Plasma membrane isolation**

The plasma membranes were isolated by Dr. Hai Wang using a modification of the method published by Sennoune *et al*. (*83*). Briefly, control or hypoxic MDA-MB-231 cells were washed three times with Buffer A (10 mM Tris, 1 mM EDTA, 150 mM NaCl, 1 mM PMSF, pH 7.4) and then scraped into the same buffer. After centrifugation at 1000 × g for 7 minutes, the supernatant was removed and the pellet was resuspended in 3 mL of Buffer B (10 mM Tris, 1 mM EDTA, 5

mM NaCl, pH 7.4) and incubated on ice for 10 min. The cell suspension was then homogenized in a Potter Elvehjem homogenizer with 15 strokes of the Teflon pestle. Cell debris was collected by centrifugation at 500 × g for 5 minutes. The supernatant was removed and kept on ice. Two mL of Buffer B was added to the pellet which was then re-homogenized. After centrifugation at 250,000 × g for 5 min, this second supernatant was combined with the first supernatant. Five mL of Buffer C (160 mM Tris, 20mM EDTA, 2 M NaI, 5 mM $MgCl_2$, pH 7.4) was added to the combined supernatants and stirred on ice for 10 min. Twenty mL of Buffer D (10 mM Tris, 1 mM EDTA, pH 7.4) was then added to the solution. After mixing, the solution was exposed to ultracentrifugation at 105,000 × g for 45 minutes at 4 ºC. The pellet was washed 3 times with Buffer D. After resuspending the pellet with homogenizing buffer (50 mM Tris, 1 mM EGTA, 250 mM sucrose, pH 7.4), the solution was loaded onto a step gradient of 20% and 40% sucrose (20% or 40% sucrose, 10 mM Tris, 1 mM EDTA, pH 7.4) and exposed to centrifugation at 200,000 × g for 1 hour at 4ºC. The membranes at the interface between the steps (i.e., the plasma membranes) were collected and resuspended in Buffer D. After centrifugation at 100,000 × g for 30 minutes at 4ºC, the pellet was resuspended in homogenizing buffer and kept at -80ºC. Protein concentration was determined as described above.

**Preparing intact MDA-MB-231 cells**

Control or hypoxic MDA-MB-231 cells were washed 3 times with warm PBS. Cells were released from plates by exposure to Cell Release Buffer (GIBCO) at 37°C for 15 minutes. Cells were gently triturated and collected by centrifugation at 1000 × g for 5 minutes. Cell pellets were washed multiple times with warm $HCO_3^-$ free DMEM containing 10% FBS and 25 mM Hepes (pH 7.4). After washing, cells were then resupended in $HCO_3^-$ free DMEM containing 10% FBS and 25 mM Hepes (pH 7.4). Cell number was determined using a Coulter Counter. Cells ($1 \times 10^6$) were assayed for CA activity using MIMS in the presence or absence CA

inhibitors at concentrations indicated in the figure legends. In the assays to study anoxic conditions, cells were isolated in medium flushed with nitrogen. In addition, nitrogen was blown on the surface of the cell suspensions and then capped to avoid the introduction of $O_2$. Other procedures were same as decribed above.

**Membrane ghost preparation**

MDA-MB-231 cells on day 3 after plating were exposed to hypoxia for 16 hours. Cells were washed 3 times with cold PBS (2.7 mM KCl, 10 mM phosphate salts, 120 mM NaCl, pH 7.4) and then exposed to hypotonic buffer (1 mL/plate of a solution containing 2.7 mM KCl, 10 mM phosphate salts, pH 7.4) in the presence of protease inhibitor (Roche Diagnostics) for 15 minutes at 4°C. Cells were scraped from plates and collected by centrifugation at 10,000 x g for 15 minutes at 4°C in a microcentrifuge. Membrane ghosts were collected and washed 4 times with hypotonic buffer and twice with cold PBS. After washing, the ghosts were resuspended in PBS and assayed for CA activity. Membrane aliquots were stored at -20°C for protein analysis.

**$^{18}O$ depletion from $CO_2$ measured by MIMS**

The MIMS assay was performed by Dr. Chingkuang Tu in Dr. David Silverman's laboratory to assay CA activity in intact MDA-MB-231 cells, membrane ghosts, or isolated plasma membranes. To decrease inaccuracies arising from $^{12}C$-containing $CO_2$ in the cell preparations, $^{13}C$- and $^{18}O$-enriched $CO_2/HCO_3^-$ were used to measure the rate of depletion of $^{18}O$ in $^{13}C$-containing $CO_2$. Thus, the atom fraction of $^{18}O$ in $^{13}C$-containing $CO_2$ was determined by MIMS in the suspension of membrane or suspensions of cells. The atom fraction of $^{18}O$ in extracellular $^{13}C$-containing $CO_2$ was specifically measured using peak heights from the mass spectrometer: $^{18}O$ atom fraction = [(47) + (49)]/ [(45) + (47) + (49)]. Here the numbers in parentheses represent the peak heights of the corresponding masses. Mass spectra were obtained on an Extrel EXM-200 mass spectrometer using electron impact ionization (70 eV) at an

emission current of 1 mA. Source pressures were approximately 1 x $10^{-6}$ torr. The resulting mass scans were well resolved with a return of ion current (detector response) to the baseline separating each mass unit. $^{18}O$-labeled $CO_2$ and bicarbonate was prepared by dissolving $KHCO_3$ in $^{18}O$ enriched water and distilling the water off 24 hours later using a vacuum line.

Cells (ghosts or membranes) were added to a reaction vessel containing 2 mL of PBS or medium in which was dissolved $^{18}O$-enriched CO2/HCO3$^-$ at 25 mM total $CO_2$ species. The membrane inlet was immersed in the suspension in this vessel and used to detect the atom fraction of $^{18}O$ in extracellular $CO_2$. This activity was measured after addition of cells (ghosts or membranes) to solutions containing different concentrations of selected inhibitors, including N-3500, ethoxzolamide, acetazolamide and Cpd 5c. There was no pre-incubation of inhibitors with cells prior to activity measurements. In some assays, the activity was measured after addition of cells to medium at specific pH values (pH 7.9, 7.4, or 6.8). These assays were performed in DMEM containing 10% FBS and 25 mM concentration of a buffer: Hepes for pH7.9, MOPS for pH 7.4, and MES for pH 6.8. For the assay in anoxic condition, cells were isolated in the medium flushed with nitrogen and assayed for the CA activity in the medium that was flushed with helium. Zinc was pre-incubated with cells, or not, prior to activity measurements as indicated in the figure legend. Anion exchange inhibitors SITs, DIDs or DNDs were used in a fashion similar to the CA inhibitors.

**Cell Viability Analysis Using the MTT Assay**

The MTT cell Viability assay is a colorimetric assay system which measures the reduction of a tetrazolium component [MTT: 3-(4, 5-Dimethylthiazol-2-yl)-2, 5-diphenyltetrazolium bromide, a yellow tetrazole] into an insoluble formazan product by the mitochondria of viable cells. After incubation of the cells with the MTT reagent for approximately 2 to 4 hours, DMSO is added to lyse the cells and solubilize the colored crystals. The samples are read at a

wavelength of 570 nm. The amount of color produced is directly proportional to the number of viable cells. To investigate if the optical density at 570 nm is proportional to cell density, MDA-MB-231 cells were seeded in 24 well plates at a different densities (1000, 2,000, 4,000, 6,000, 8,000, or 10,000 cells per well). Cells were incubated in the 37°C for 48 hours to allow the cells to attach and initiate growth in the wells. Fifty μL of MTT (5mg/mL) was added to each well and incubated at 37°C in an environment of 5% $CO_2$ for 2 hours to allow the MTT to be metabolized. Medium was aspirated in each well and 1 mL DMSO was added to each well to dissolve formazan. Optical density was read at 570 nm. OD was also measured at 650nm for background subtraction. In order to determine the effect of CA inhibitors on cell growth, MDA-MB-231 cells were seeded in 24 well at density of 2,000 cells /per well in 24 well plates. Cells were incubated in the 37°C for 24 hours to allow the cells to attach to the wells. Then the medium were replaced with 500 μL of medium containing 100 μM of CAIX inhibitors: acetazolamide, chlorzalomide, or N3500, in each well. Cells were either incubated under normoxic (5% $CO_2$, 20% $O_2$) or hypoxic (5% $CO_2$, 1% $O_2$) conditions for 24 hours or 48 hours. Fifty μL of the MTT reagent (5mg/mL) was added to each well and incubated at 37°C in an environment of 5% $CO_2$ for 2 hours to allow the MTT to be metabolized. Each reaction was stopped with 1mL DMSO. Optical density was read at 570 nm and 650 nm.

**Cell Migration and Cell Invasion Assays**

Cell migration and invasion assays were performed using 12 μm pore size transwell polycarbonate membrane insert (Millipore) in 24 well plates. In the migration assay, confluent MDA-MB-231 cells were trypsinized and suspended in FBS-free DMEM. Cell number in the suspension was counted and adjusted to 1 x $10^6$/mL. Six hundred μL of DMEM containing 10% FBS was added to the lower chamber. A 100 μL aliquot of the cell suspension (1 x $10^5$ cells) containing 100 μM of each CAIX inhibitor (acetazolamide, chlorzolamide, or N3500) was

placed in the upper chamber. Cells were cultured at 37C° under hypoxic conditions for 24 hours. The inserts were then removed and cells on the upper side of the insert membrane were carefully removed by scraping the membrane with cotton q-tip. The cells on the underside of the membrane were incubated with MTT in medium for 2 hours at 37°C. After incubation, cells on the underside of membrane were lysed with DMSO and absorbance was read at 570 nm and 650 nm.

For the cell invasion assay, 100 µL of cold Matrigel (BD Bioscience), diluted 1:5 with cold serum-free DMEM, was placed on the 12 µm pore size membrane insert to mimic the basement membrane. Matrigel was incubated at 37°C for 4 hours to solidify. MDA-MB-231 cells were then seeded onto the Matrigel. The subsequent procedures were the same as described in the cell migration assay.

**Co-Immunoprecipitation**

Co-immunoprecipitation is a powerful tool for identifying protein-protein interactions by precipitating one protein, believed to be in a complex, with antibody specific for another protein in the complex. The complex is captured on a protein A sepharose/agarose, so that it is can be removed from solution. Additional members of the complex are captured as well and can be identified by gel electrophoresis and Western blotting. Co-immunoprecipitation of CAIX, CAII, and AE were performed based on previous published methods by our lab (*76*). First, CAIX was immunoprecipitated from total cell lysates. MDA-MB-231 cells grown in DMEM supplemented with 10% FBS were exposed to hypoxia for 16 hours to induce CAIX expression. Cells were washed with PBS and detergent-solubilized by immunoprecipitation buffer (IPB) (1% Igepal, 5 mM EDTA, 0.15 M NaCl, 0.15 % deoxycholate, 10 mM Tris, pH 7.4), supplemented with protease inhibitor cocktail. Extracted proteins were clarified by centrifugation at 16,100 x g for 15 minutes at 4°C. Protein concentration was determined as described earlier. Cell lysates

containing equal protein (1.5 mg) were incubated with Protein A agarose beads for 1 hour at 4°C to eliminate non-specific interactions. After incubation, Protein A beads and non-specific proteins were removed by centrifugation. Fifty µl of a 50% solution of Protein A-agarose beads and 5 µg of the M75 antibody were added to the pre-cleared cell lysates and incubated overnight at 4°C by end-over-end rotation. Beads were then collected and washed 3 times with buffer 1 (0.1% Igepal, 1 mM EDTA, 0.15 M NaCl, 10 mM Tris, pH 7.4), buffer 2 (2 mM EDTA, 0.05% SDS , 10 mM Tris, pH 7.4) and buffer 3 (2 mM EDTA,10 mM Tris, pH 7.4) once each. Proteins were released from the immune complex in 50 µL of a 2X SDS-PAGE sample dilution buffer. After brief centrfugation, eluted proteins were separated on SDS-PAGE gels and transferred to nitrocellulose membrane. Antibodies specific for AE2 or CAII were used in Western blotting, along with CAIX to determine if CAIX had been immunoprecipitated. Furthermore, since AE2 and CAIX are membrane proteins, CAIX was immunoprecipitated from total membrane fraction to increase enrichment in the following manner. A total membrane fraction was obtained by the methods described earlier and suspended in TES1 supplemented with protease inhibitor cocktail, and stored in -20°C. One mg total membrane protein was then extracted in IPB buffer. Any insoluble material was then removed by centrifugation in a microcentrifuge for 15 min at 4°C. Clarified extracts were used for immunoprecipitation of CAIX as described above.

AE2 was immunoprecipitated from total membranes as described above except that an AE2 antibody was used for the immunoprecipitation. Further, Protein A/G argarose beads were used to collect immune complex instead of Protein A beads. All other steps were the same as described above.

**Protein Crosslinking**

Interaction of CAIX and AE2 or CAII might be transient; therefore the interactions may be disrupted by extraction of proteins from cells by detergent. To potentially stabilize these

interactions, chemical crosslinking before immunoprecipitation was performed. The crosslinker dithiobis[succinimidylpropionate] (DSP) was used to create covalent bonds between interacting proteins. DSP is homobifunctional N-hydroxysuccimide ester. This crosslinker is thiol-cleavable, primary amine reactive, and forms covalent amide bonds between two proteins. The space arm length of this crosslinker is 12 Å. MDA-MB-231 cells were treated with hypoxia for 16 hours to induce CAIX expression. To crosslink the proteins with DSP, cells were washed 3 times with PBS (0.15 M NaCl, 0.1 M phosphates salts, pH 7.2) and incubated with 2 mM freshly made DSP in PBS at 4ºC for 30 minutes. Reactions were quenched by addition of TES1. Total membranes were isolated as described earlier and suspended in TES1 supplemented with protease inhibitor. This membrane fraction was then used for co-immunoprecipitation experiments described above.

**Statistical Analysis**

Data, where appropriate, are reported as the mean ± S.D. The statistical significance of the difference in the means throughout this study was calculated by one way ANOVA (SigmaStat 3.5) with $P < 0.05$ being regarded as statistically significant.

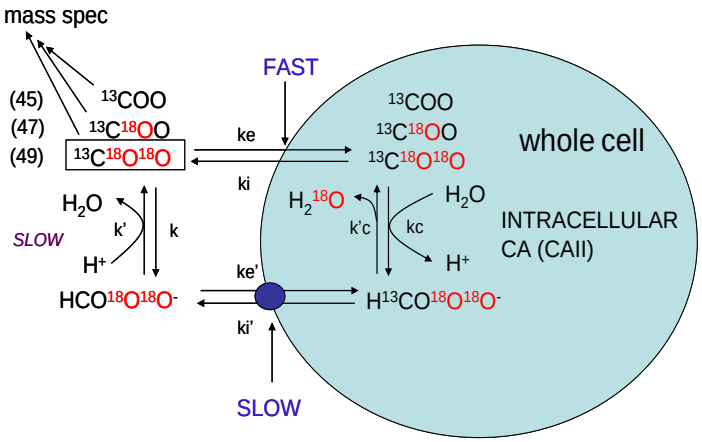


Figure 2-1. Diagram of $^{18}O$ exchange in cell suspensions without exofacial CA activity. The mass spectrometer measures $^{18}O$ atom fraction in $CO_2$ in the extracellular solution. The rate of depletion or decrease in atom fraction of $^{18}O$ from $CO_2$ is a measure of carbonic anhydrase activity. Once cells are added to the solution, dissolved $CO_2$ species rapidly cross the membrane into the intracellular space and depletion of $^{18}O$ from $CO_2$ is a measure of catalysis by the intracellular CA. Without exofacial CA, interconversion between $CO_2$ and $HCO_3^-$ in solution occurs rather slowly. The slow flux of H $C^{18}O^{18}O$ $^{16}O^-$ across the cell membrane also provides access to intracellular CAII.

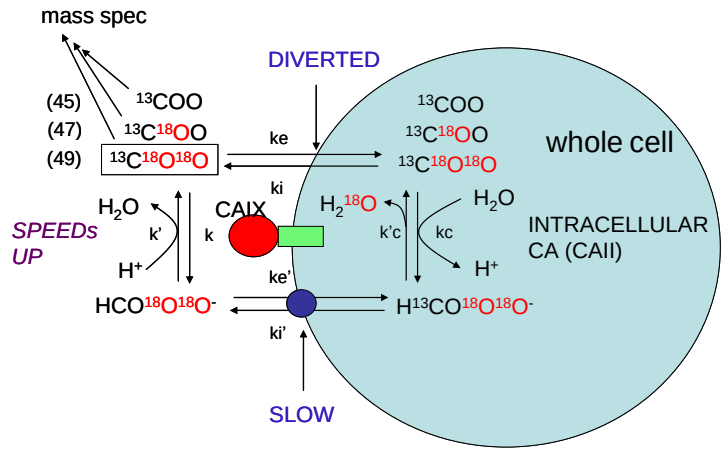


Figure 2-2.. Diagram of $^{18}O$ exchange in the cell suspensions with exofacial CA activity. When cell are added to the solution, dissolved $CO_2$ species rapidly cross the membrane into the intracellular space and catalysis by intracellular CA leads to the depletion of $^{18}O$ from $CO_2$. Extracellular CA speeds up interconversion between $CO_2$ and $HCO_3^-$ in extracellular solution and competes for the $CO_2$ in the solution, resulting in diversion of $CO_2$ from the intracellular compartment.

# CHAPTER 3
# GLYCOLYTIC PHENOTYPE OF BREAST CANCER CELLS

## Introduction

Tumor cells undergo metabolic transitions which allow them survive and grow in the hostile environment created by inadequate oxygen delivery associated with the disordered vascularization of tumors (*9;10*). One of striking features of tumor cells is the shift of their metabolism toward glycolysis, which is less efficient in energy yield compared to oxidative phosphorylation (producing only 2 mol of ATP vs. a possible 38 mol of ATP per mol of glucose). However, enhanced glycolysis is often sustained even in the presence of oxygen (aerobic glycolysis) as discovered by over 70 years ago (*84*). Even though glycolysis is a less efficient energy production process, its metabolic intermediates can be utilized for biosynthesis of certain amino acids, nucleotides, and lipids, providing selective advantage to proliferating tumor cell. Increased glycolysis is related to the overexpression of GLUT1 in human cancers (*13;85;86*) in addition to the increased expression of key glycolytic enzymes (*87*).

As a major product of glycolysis, lactic acid production is increased in tumor cells. In addition, cells generate an excess of protons and carbon dioxide through metabolic activity. Together, these catabolites make intracellular pH (pHi) more acidic, which is toxic to the cells. While it was originally thought that the pHi of tumor cells would be reduced relative to normal cells, it is the pH of the interstitial fluid that drops. In order to preserve the neutral pHi that is optimum for cell proliferation and survival, tumor cells extrude the acidic catabolites to the extracellular space. This is a result of the expression of several proteins whose function is to export protons from the cytosol to the extracellular space. As discussed earlier, these includes the lactate transporter (*18*), vacuolar ATPase (*19;83*), and $Na^+/H^+$ exchanger (*88*). Acid export leads to a reduction of extracellular pH (pHe). The combination of increased glycolysis and

acidification in the tumor microenvironment is defined as "the glycolytic (or metabolic) phenotype" of cancer cells. It appears that acidosis of tumors provides an advantage for tumor progression as cancer cells are resistant to the toxic effects of acidification (*21*). However normal cells, which lack mechanisms to adapt to extracellular acidosis, are unable to survive under such conditions. Further, acidification of the microenvironment of tumors alters the efficacy of chemo- and radiation therapy. Finally, low pH stimulates *in vitro* invasion and *in vivo* metastasis (*1;2*).

Lactic acid was previously considered the sole reason for extracellular acidification. An early study indicated that tumors generated from glycolysis-deficient cells still create acidic microenvironments which suggested that lactic acid is not the only cause of acidification *in vivo* (*23*). In that regard, metabolic profiling of glycolysis-impaired versus parental cells revealed that $CO_2$ may be a significant source of acidity in tumors as $CO_2$ concentration increases in the tumor microenvironment (*7;23*). It is believed that this is not a result of oxidative metabolism but rather a byproduct of an increase in the activity of the pentose phosphate pathway (*89*). $CO_2$ is an acidic oxide that reacts with water to form carbonic acid. *In vivo*, this reaction is catalyzed by members of the carbonic anhydrase (CA) family of enzymes that mediate the reversible hydration of $CO_2$ to bicarbonate: $CO_2 + H_2O \leftrightarrow HCO_3^- + H^+$. Therefore, CA has the potential of producing the acid oxide, $CO_2$, and protons, either of which reduced pH although the proton is more acidic than is $CO_2$.

To study the glycolytic phenotype of breast cancer, we used human breast cancer cell lines (HBCs) as our model. Breast cancer cell lines have provided an important tumor model system because most features of breast cancer are preserved in the cell line from which they derive and reflect the characteristics of cancer cells *in vivo* as discussed in Chapter 1. Two widely studied

lines, the MDA-MB-231 and T47D cell lines were chosen to represent highly invasive and non-invasive tumors, respectively. The T47D cell line is derived from a ductal carcinoma and is estrogen receptor-positive. Analysis of transcriptional activity reveals that these cells align with luminal markers. When injected into nude mice, cells form a solid tumor but do not readily metastasize. The MDA-MB-231 line is derived from an adenocarcinoma and expresses the receptor for EGF. These cells align with a group defined as basal B which represents the "triple-negative" tumors (estrogen and progesterone receptor negative, and HER2 negative). When injected into nude mice, these cells form tumors and aggressively metastasize. The MCF10A line which is derived from fibrotic tissue is used as a control for cancer cell lines. These cells are estrogen receptor negative, EGF receptor negative, HER2 negative, but E-cadheren positive cells. The goal of this section is first to examine the glycolytic rate of the three cell lines under normoxic and hypoxic conditions, and then to determine if the glycolytic rate in cultured cell lines reflects the intrinsic features of the cancer cells.

## Results

### Growth Rate of Cultured Human Breast Cancer Cells

One important feature of invasive breast tumors is increased growth rate. To compare the rate of glycolysis in different breast cell lines, it is important to conduct experiments in which cells are at similar densities. Thus, we first assessed the growth rate of the MCF10A, T47D, and MDA-MB-231 cell lines.

Aggressive cancer cells proliferate more rapidly than non-invasive and normal epithelia cells (*1*). Those data were confirmed here with cell number determination over 10 days in culture using the Coulter Counter (Figure 3-1). As might be expected, the MDA-MB-231 cells grew more rapidly than either MCF10A or T47D cells, although MDA-MB-231 cells were seeded at half the density of the other two cell lines. At day 2 after plating, the number of MDA-

MB-231 cells was equivalent to that of MCF10A and T47D at day 3 after plating. At this point in their growth curve, each cell line is 50% confluent. We refer to cells at this stage as subconfluent cells in subsequent experiments. MDA-MB-231 cells attained confluence at day 4 after plating, whereas MCF10A and T47D attained confluence at day 7. T47D cells grew at same rate as MCF 10A cells, even though they are tumor cells. These data indicate that MDA-MB-231 cells have a more robust proliferative capability compared to the other two cell lines. This feature is consistent with their more aggressive phenotype.

**Glucose Consumption and Lactate Production in Breast Cancer Cells**

Cancer cells have high glycolytic rates even in the presence of $O_2$ which is known as aerobic glycolysis. This means that cancer cells shift their energy production from oxidative phosphorylation to glycolysis which results in significant lactic acid production. This was confirmed here by measuring the loss of glucose and secretion of lactate into the culture medium under normoxic conditions. At confluence, the MDA-MB-231 and T47D cells consumed significantly more glucose and secreted significantly more lactate than did the MCF10A cells (Figure 3-2A, B). In glycolysis, metabolism of 1 mole of glucose can produce 2 moles of lactate. Thus, the lactate produced in MCF10A cells accounts for 50% of the glucose consumed. In the T47D and MDA-MB-231 cells, the lactate produced accounts for 80% and 94% of the glucose consumed, respectively. Our data provide evidence to support the Warburg effect in the breast cancer cells.

**Extracellular pH of Breast Cancer Cells**

Acidification of the tumor microenvironment is another typical feature of the glycolytic phenotype of cancers cells. Thus, extracellular acidification was investigated in the three breast cell lines. Surprisingly, the pH of the medium overlaying normoxic cells was the same for each of the three lines after 24 hours of culture (Figure 3-2C). This raised our awareness of the

buffering capacity of the different media in which the cells are grown. The content of bicarbonate and phosphate in the cell-specific medium is listed in Table 3-1. DMEM, in which MDA-MB-231 cells are cultured, has a high bicarbonate concentration, which suggests DMEM has the highest buffering ability. At lower bicarbonate, we would predict that the MDA-MB-231 cells would acidify the medium to a greater extent than we have actually observed with normal DMEM. Such would fit with our observations that both glucose metabolism and lactate production are highest in the MDA-MB-231 cells.

**Glucose Uptake in Breast Cancer Cells**

Cancer cells have increased glucose utilization and lactate production when measured by direct analysis as described above. Another characteristic of cancer cells is upregulated GLUT1 which increases glucose uptake (*86*). Thus, we sought to determine if enhanced glycolysis was in part due to increase glucose uptake. In the following experiments, we have measured the uptake of [$^3$H] deoxyglucose in the presence or absence of cytochalasin B, a specific inhibitor of facilitated glucose uptake. [$^3$H] deoxyglucose is not metabolized once transported into cells and accumulates as the 2-deoxy 6-phosphoglucose. Figure 3-3A demonstrates that the capacity of MDA-MB-231 cells to transport glucose was substantially greater than that of either MCF10A or T47D cells. These data are consistent with those previously published evidence which showed that the aggressive MDA-MB-231 cell line has much greater glucose transport activity than the non-invasive MCF7 cell line (*1*), a luminal line with properties similar to the T47D line.

**Glucose Uptake and Lactate Production in Response to DFO or hypoxia**

In the above experiments, we compared the glycolytic phenotype in the three breast cell lines under normoxic conditions. These data showed that the aggressive MDA-MB-231 cells have a high growth rate and high glycolytic rate in agreement with previously published observations. Yet, the tumor microenvironment is hypoxic. Therefore, we were also interested

in determining whether hypoxia could enhance the glycolytic phenotype of cancer cells compared to controls. In these experiments, we used cells that had achieved confluence (day 4 after plating for the MDA-MB-231 cells, and day 7 for the MCF10 and T47D cells). At this point, cell number per plate for each of the cell lines is comparable (Figure 3-1). DFO and hypoxia-induced changes in glucose transport activity is illustrated in Figure 3-3A. After exposure to DFO and hypoxia, glucose uptake increased in all three cell lines to varying degrees. In the MCF10A cells, DFO and hypoxia increased glucose uptake by 20%. In T47D, this increase was about 2-fold. While the intrinsic capacity of MDA-MB-231 cells to transport glucose is already about 3-fold higher than the MCF10A and T47D cells, DFO and hypoxia stimulated by an additional 50% the ability of MDA-MB-231 cells to increase glucose uptake.

As indicator of the glycolytic rate, lactic acid production in three cell lines in response to DFO and hypoxia were also investigated. Figure 3-3B shows that lactate production in MCF10A and T47D cells was significantly less than observed in MDA-MB-231 cells. DFO and hypoxia increased lactace production in T47D cells and MDA-MB-231 cells but the increasing was not significant. Coupled with much greater glucose uptake (Figure 3-3A), we conclude that MDA-MB-231 cells have both a higher intrinsic glycolytic phenotype (i.e., in the presence of $O_2$) and a greater capacity to respond to oxygen stress than do the MCF10A and T47D cells. Again, this is consistent with the aggressive nature of the MDA-MB-231 cell line.

**Effect of DFO and Hypoxia on Extracellular pH in Breast Cancer Cells**

To further assess metabolic changes in response to DFO and hypoxia, pHe of MCF10A, T47D, and MDA-MB-231 cells was examined in response to DFO and hypoxia. After 16 hours of exposure, DFO and hypoxia decreased pHe in all three cell lines (Figure 3-4). Particularly striking is the decrease in pHe of the MDA-MB-231 cells. The small changes in lactic acid production in these cells (Figure 3-3B) do not account for the observed acidification and suggest

lactic acid is not only cause for the acidification, thus provide evidence for a role for $CO_2$ in pH regulation.

## Conclusions

Cancer cells and normal cells show different metabolic features and respond differently to hypoxia. Gillies and Gatenby (*1*) have argued that intermittent hypoxia leads to upregulation of glycolysis in early *in situ* cancers and that this feature is further selected for because it provides some advantage to cancer progression. This glycolytic phenotype is more complex than just upregulation of the enzymes that control glycolytic rate. Rather it is a series of events (often heterogenous in nature) that lead to permanent changes in protein expression that drives both glycolysis and the upregulation of proton exporters. Enhanced glycolytic activity results in intracellular acidification while upregulation of the proton export machinery contributes to extracellular acidification avoiding intracellular proton toxicity. It is not really understood why cancer cells are able to adjust their sensitivity to low pH while normal cells surrounding cancer cells die off, but it clearly contributes to their metastatic potential (*1*). Elevated GLUT1 expression leads to increased glucose metabolism leading to an increase in lactic acid production. In the normoxic environment, MDA-MB-231 cells grow faster than T47D or MCF10A cells, which is consistent with their aggressive phenotype. In addition, MDA-MB-231 cells show greater glucose uptake and lactic acid production than the other two cell lines. However, pHe of the three cell lines are the same at 24 hours after giving fresh medium. This may be related to the enhanced buffering capacity of the DMEM which bathes the MDA-MB-231 cells. Hypoxia and DFO strongly enhanced glucose uptake in MDA-MB-231 and T47D cells, but not in MCF cells. Again, the MDA-MB-231 cells have the highest growth rate and the highest rate of lactic acid production among the cells that were tested. In terms of glycolysis, 94% of the glucose consumed was converted to lactic acid. By comparison, the MCF10A cells converted only about

50% of the glucose to lactic acid. Thus, not only was glucose uptake increased in MDA-MB-231 cells relative to MCF10A cells but there also was a shift in metabolic flux which typifies cancer cells. Metabolic activity in T47D cells was intermediate between these cell types. Hypoxia further enhanced glucose uptake and anaerobic glycolysis in MDA-MB-231 cells, but the intrinsic metabolic behavior of these cells was pre-established. Interestingly, the drop in medium pH in response to hypoxia could not be accounted for by lactic acid production alone. This lends to the possibility that the induction of $CO_2$ contributes to acidification. Although MCF10A cells and MDA-MB-231 cells belong to the same basal B group, MCF10A cells clearly did not exhibit the same intrinsic metabolic phenotype as the MDA-MB-231 cells. MDA-MB-231 cells can be readily distinguished metabolically from MCF10A cells in culture. This may be a contributing factor in their *in vivo* behavior.

Overall, results in this section demonstrate that aggressive cells, like the MDA-MB-231 cells, have high rate of glycolysis compared to non-invasive cells T47D cells and normal epithelial cells MCF10A cells. In addition, hypoxia significantly enforces the already high glycolytic rate of MDA-MB-231 cells, resulting in increased lactic acid production and acidification of extracellular pH. However, the changes in lactic acid, does not account for the observed acidification induced by hypoxia, which provides evidence for $CO_2$ in the development of glycolytic phenotype of MDA-MB-231 cells in hypoxic environment. The contribution by carbonic anhydrase IX to this phenotype will be considered in Chapter 4.

Table 3-1. Concentration of bicarbonate and phosphate salt in cell culture medium

| Cell lines | Medium | Bicarbonate | Phosphate salt |
|---|---|---|---|
| MCF10A | MEBM | 13 mM | 0.58 mM |
| T47D | McCoy | 26 mM | 4.2 mM |
| MDA-MB-231 | DMEM | 44 mM | 0.9 mM |

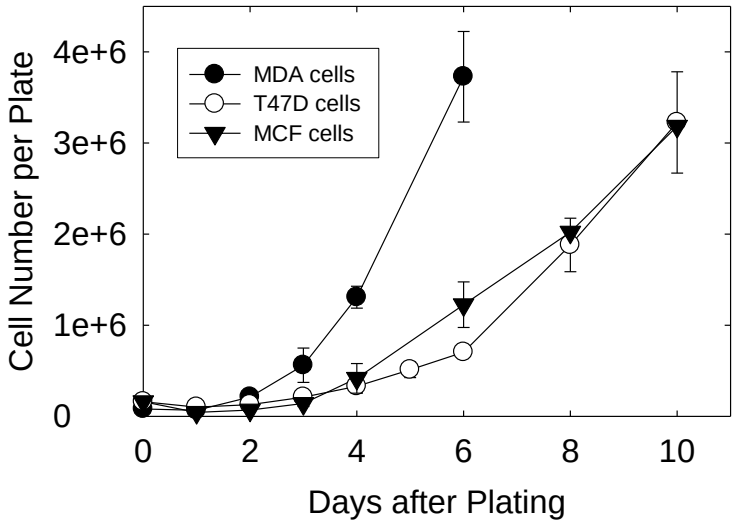


Figure 3-1. Growth curves of three human breast cell lines (HBCs). MDA-MB-231, T47D, and MCF10A cells were plated in 10 cm plates. At specific time points, cells were released from plates by cell dissociation buffer. Cell aliquots were resuspended in isotone. Cell number was determined by Coulter Counter. Data represent the mean ± S.D. of three independent experiments.

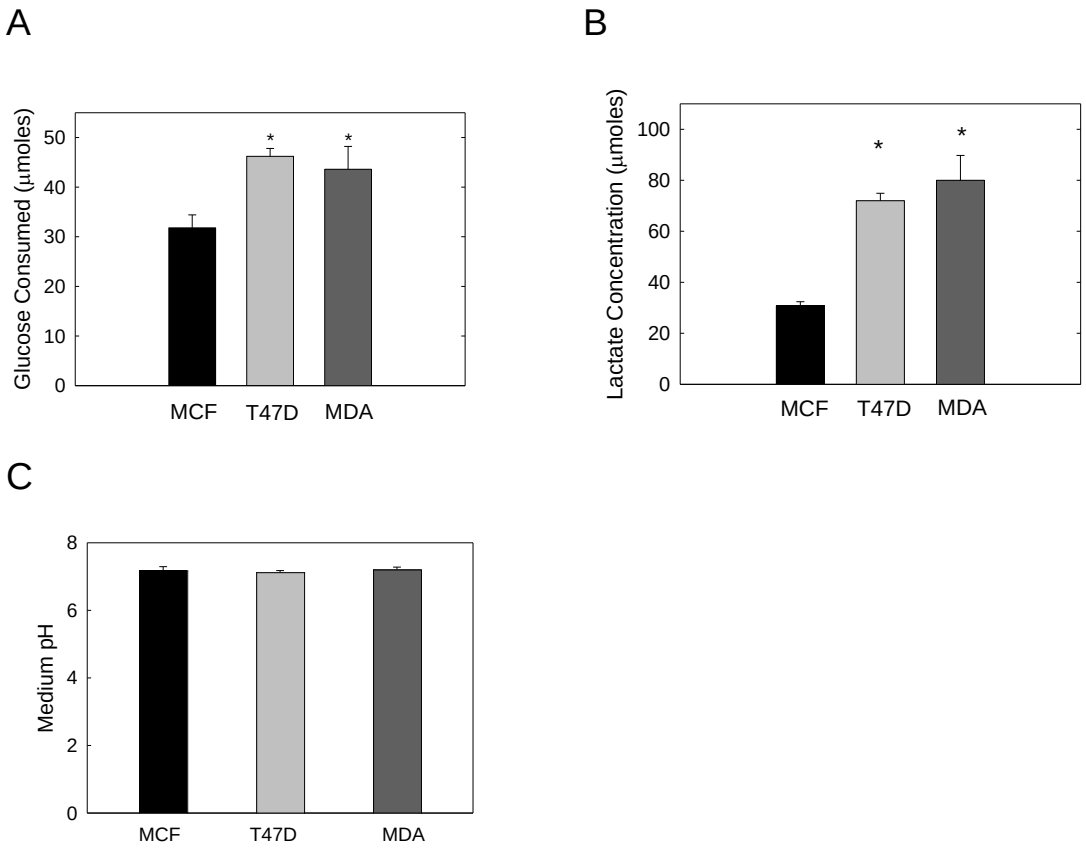


Figure 3-2. Comparision of glucose uptake, lactate production, and pH in HBCs. A) Confluent cells [MCF10A cells (day 7), T47D cells (day 7), and MDA-MB-231 cells (day 4)] were washed and given fresh DMEM containing 15 mM glucose. After 4 h, medium was collected for determining glucose concentration. Data represent the mean ± S.D. of a single experiment where n = 6. (*, $P < 0.001$ vs MCF10A cells). B) Medium collected as in panel A and used for determining lactate production. Data represent the mean ± S.D. of a single experiment where n = 6 (*, $P < 0.003$ vs MCF10A cells). C) Cells were fed with fresh medium and after 24 hours were analyzed for pH. Data represent the mean ± S.D. of two independent experiments, each of which evaluated triplicate samples.

A

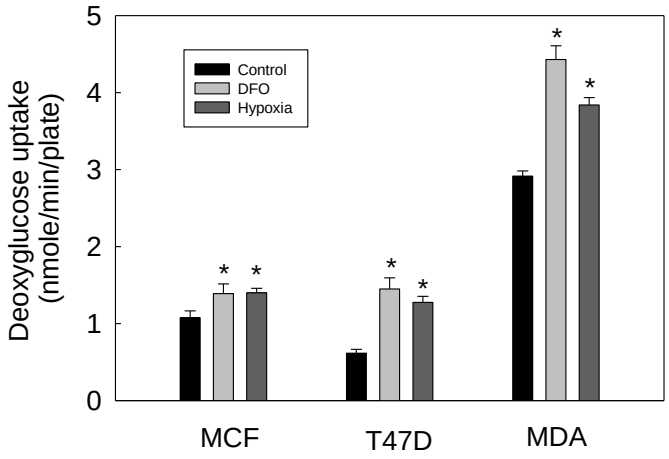


B

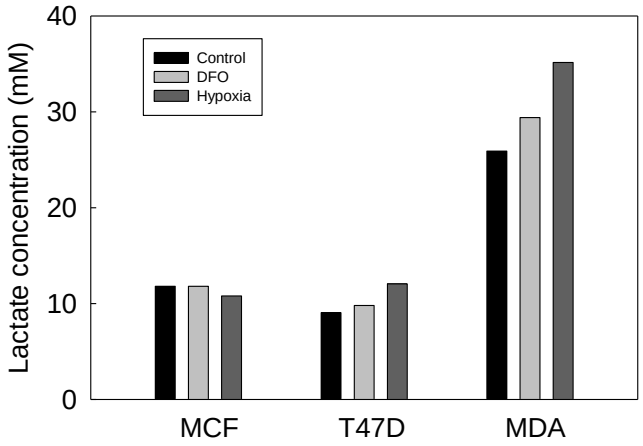


Figure 3-3. Effect of DFO or hypoxia on deoxyglucose uptake and lactate production in HBCs. A) Cells were grown in 35 mm plates and exposed to 100 μM DFO or hypoxia for 16 hours. Subsequently, cells were washed with KRP buffer and then incubated with or without 40 μM of cytochalasin B for 10 minutes. Transport of deoxyglucose was assayed for 10 min. The rates, reported as nmol/plate/min, are for duplicate assays and are the average of two independent experiments ± S.D. (*, $P < 0.05$ vs control cells). B) Cells [MCF cells (day 6), T47D cells (day 6), and MDA-MB-231 cells (day 3)] were given fresh medium and then exposed to DFO or hypoxia for 16 hours. Medium was collected and lactate concentration was measured. Data in MCF and T47D represent a single experiment, which evaluated duplicate samples. Data in MDA represent two independent experiments, each of which evaluated duplicate samples.

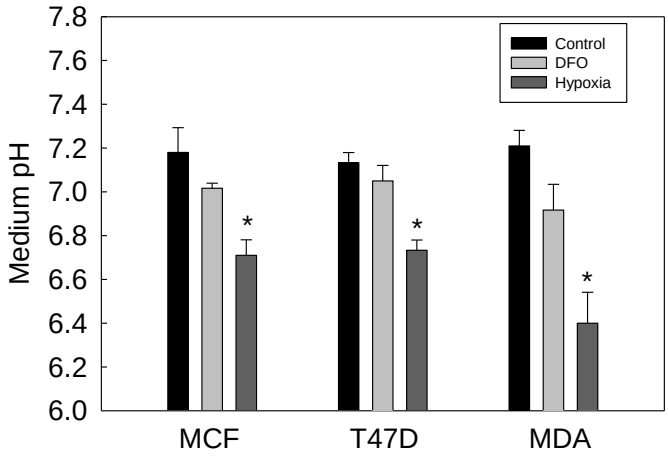


Figure 3-4. Effect of DFO or hypoxia on medium pH in HBCs. Cells [MCF cells (day 6), T47D cells (day 6), and MDA-MB-231 cells (day 3)] were given fresh mediumand then exposed to DFO or hypoxia for 16 hours. Medium pH was measured immediately with a hand-held pH meter. Data are the average of two independent experiments ± S.D, each of which evaluated duplicate samples. (* $P < 0.05$).

CHAPTER 4
CHARACTERISTICS OF CAIX IN BREAST CANCER CELLS

## Introduction

Carbonic anhydrases (CAs) are ubiquitous metalloenzymes that catalyze the hydration of $CO_2$ and the dehydration of $HCO_3^-$ : $CO_2 + H_2O \leftrightarrow HCO_3^- + H^+$. All human CAs belong to the α-class. There are 16 isoforms in this group that differ in their kinetic and inhibitory properties, cell and tissue distribution, and function *(29)*. Two of the catalytically active members of this family, CAIX and CAXII, are associated with and overexpressed in tumors *(28;42)*. CAIX is abundant in several tumors, such as renal, cervical, lung and breast carcinomas (*33;90*), but is absent or reduced in normal corresponding tissues. High expression of CAIX is also associated with poor prognosis and poor radio- and chemo-therapy in several carcinomas including breast cancer (*38;41;91*). As shown by Hussain *et al.* in 2007 *(41)*, CAIX expression is associated with poor survival in patients with invasive breast cancer. CAIX expression is also significantly associated with tumor grade and tumor necrosis in breast cancer patients *(52)*. The expression pattern of CAIX is principally determined by a strong activation of *CA9* gene transcription via a hypoxia-inducible factor (HIF1), which binds to the hypoxia response element (HRE) localized in the *CA9* promoter. CAIX is induced by hypoxia in wide range of malignant cells (*49*). Tumor hypoxia is an important phenomenon with dramatic implications for cancer development and therapy. Therefore, CAIX offers significant potential as an intrinsic hypoxic marker with prognostic/predictive value and as a promising therapeutic target (*92*). A recent study demonstrates that CAIX expression is an independent prognosticator in oligodendroglial brain tumors, and inversely correlates with cell proliferation (*93*). Therefore, CAIX function in tumors may depend on the specific tumor type in which it is expressed and needs further investigation.

In addition to the potential clinical exploitation of CAIX in cancer, there is increasing interest in resolving many basic molecular and functional aspects of the protein as its precise role in cancer cells is still not clear. CAIX is an integral plasma membrane protein that consists of the following four domains: An N-terminal proteoglycan-like domain (PG), the CA catalytic domain (CA), a transmembrane domain, and a short cytoplasmic tail. It was originally reported that CAIX is able to form disulfide-linked homotrimers *(34).* More recently, Hilvo et al. *(31)* showed that recombinant CAIX (constructed with the soluble PG + CA domains or the CA domain alone and produced in insect cells) consist of a mixture of monomeric (34%, 46%, respectively) and disulfide-linked dimeric species (60%, 54%, respectively). While the catalytic domain construct could adapt both trimeric and dimeric structures, the proteoglycan domain construct preferred the dimer configuration *(31).* This suggests that the presence of the proteoglycan domain favors dimerization. These investigators also identified two sets of specific sulfhydryl groups that participate in forming intermolecular disulfide bridges.

Lipid rafts are cholesterol- and sphingomyelin-enriched microdomains in the plasma membrane. These domains comprise a select set of proteins which reside in or transiently associate with lipid rafts. Lipid rafts are involved in signal transduction and intracellular trafficking (*94*). Evidence has shown that GLUT1 is transiently associated with rafts which affects GLUT1 activity (*76*). Dorai and coworkers have suggested that CAIX may translocate to lipid rafts and form oligomers in an EGF-dependent manner in renal carcinoma cancer cells (37). They also demonstrated that EGF stimulated CAIX phosphorylation on tyrosine 412 in the cytoplasmic domain in a renal carcinoma cell line, SKRC-01. This phosphorylation led to a direct interaction between CAIX and PI3-kinase. In a similar line that does not express CAIX, SKRC-17, the authors demonstrated that EGF action leading to phosphorylation of Akt was more

robust when CAIX was ectopically expressed. This infers that EGF stimulates CAIX phosphorylation which independently activates the EGF signaling path. The EGFR is known to reside in lipid rafts in both normal cells and cancer cells (*95;96*) and to mediate the activation of down-stream signaling pathways in cancer cells when recruited to lipid rafts (*97*). In addition, cholesterol levels change EGFR function, trafficking, and activation (*98;99*). Thus, Dorai et al. demonstrated, indirectly, that phosphorylated CAIX was present in lipid rafts which imply that EGF stimulation causes the recruitment of CAIX to lipid rafts.

In this section, expression of CA isoforms such as CAII, CAIX and CAXII are first investigated in MCF10A, T47D, and MDA-MB-231 cells, collectively called human breast cells (HBCs). CAIX is further characterized using the MDA-MB-231 cells as our model. In these studies, we sought to determine some specific characteristics of CAIX including its expression, oligomerization, glycosylation, and localization. Next, we determined if DFO exposure or hypoxic treatment of MDA-MB-231 cells enhanced the distribution of GLUT1 and CAIX to lipid raft. CAIX localization and its phosphorylation in response to EGF were also investigated. The overall goal of these studies was to correlate the characteristics of CAIX expression with the metabolic features described in Chapter 3.

## Results

### Hypoxia-dependent Expression of CA Proteins in HBCs

While CAIX is the most likely membrane-associated CA family member to contribute to the regulation of extracellular pH in tumors, the expression of other membrane isoforms (CAIV, CAXII, and CAXIV) could confound interpretation of CAIX function. Using RT-PCR, we have shown that there is no message for CAIV in MCF10A, T47D, or MDA-MB-231 cells (*100*) and thus did not pursue the identification of this isoform at the protein level. Message for CAXIV was only observed in T47D cells (*100*). We were unable to confirm its expression at the protein

level for lack of an appropriate antibody. Commercially available antibodies did allow us to initiate studies to evaluate the expression of CAIX and CAXII in HBCs in response to hypoxia. As the project proceeded, we were also able to obtain the M75 monoclonal antibody specific for CAIX. The ubiquitous cytosolic CA isoform, CAII, and HIF1α were also examined. Western blotting using the M75 antibody showed that CAIX protein was only detected in confluent MDA-MB-231 cells. CAIX migrated as a doublet of 54 kDa and 58 kDa (Figure 4-1), as observed by others (*42*). DFO and hypoxic treatment induced CAIX expression by 3-5 folds. While CAIX expression was not observed in confluent MCF10A cells, DFO and hypoxia exposure induced CAIX expression. T47D expressed no CAIX protein either constitutively or in response to DFO or hypoxia. While only MCF10A and MDA-MB-231 cells showed enhanced expression of CAIX in response to DFO and hypoxia, all three cell lines showed an increased expression of the transcription factor, HIF1α after exposure to DFO or hypoxia. These data suggest that CAIX expression is cell-type specific and its regulation may be at the post-transcriptional level in the different cell lines. Although CAIX expression was not observed in T47D cells, CAXII protein expression was robust. However, CAXII expression in T47D cells was not sensitive to DFO and hypoxia. CAXII expression was not detected in MDA-MB-231 cells. MCF10A cells expressed less CAXII than observed in T47D cells but its expression appeared elevated in response to hypoxia, although not to DFO. CAII was strongly expressed in the MDA-MB-231 cells, detectable in MCA10A cells, but not observed in T47D cells. From these studies, it became clear that the MDA-MB-231 cells exclusively express only one member of the membrane-bound forms of the CA family (CAIX) and that its expression is induced by hypoxia. This is an obvious advantage for the characterization of cell surface CA activity in response to hypoxia or in the presence of CA inhibitors as described in Chapter 5.

**Cell Density-dependent Expression of CAIX**

The following experiment was conducted by Dr. Hai Wang in our laboratory to examine the expression of CAIX in response to density (time in culture) across the three cell lines. Cell lysates were isolated from the three cell lines at appropriate days after seeding cells. Figure 4-2 shows a Western blot identifying CAIX using the M75 antibody. MCF10A cells expressed no CAIX in subconfluent cells and expression was not induced by increasing cell density. CAIX was not expressed in T47D cells and showed no response to increasing density. In MDA-MB-231 cells, CAIX expression was low in subconfluent cells and substantially increased in response to cell density. Thus, only the MDA-MB-231 cells showed both density and oxygen-dependent regulation of CAIX at protein level.

**Oligomerization State of CAIX**

To investigate the oligomerization status of CAIX in hypoxic MDA-MB-231 cells, total membranes of hypoxic MDA-MB-231 cells were analyzed by SDS-PAGE under reducing and non-reducing conditions (Figure 4-3). Under reducing conditions (in the presence of β-mercaptoethanol), CAIX migrated as a 54/58 kDa doublet which has been observed previously. Under non-reducing conditions (in the absence of β-mercaptoethanol), CAIX migrated as a single, high molecular weight band at 119 kDa which represented about 90% of the CAIX pool. These data demonstrate that the majority of CAIX in the membrane exists as dimers in MDA-MB-231 cells. Taking into consideration the activity data, which will be described in Chapter 5, we conclude that the dimeric form of CAIX represents most of the CA activity in the membrane of MDA-MB-231 cells.

**Glycosylation of CAIX and CAXII**

Glycosylation state of CAIX was detected through endoglycosidase digestion. *N*-glycosidase F (PNGF) releases the entire *N*-linked glycan attached to a protein, while

endoglycosidase H (endo H) cleaves the glycan only if the structure is high mannose or a hybrid form, but not a complex structure. Total membrane protein (50 μg) from hypoxic MDA-MB-231 cells was subjected to PNGF or endo H digestion. The 54/58 kDa doublets of CAIX were both sensitive to PNGF showing more rapid migration of these species in SDS-PAGE gels (Figure 4-4A). This indicates that the 54 kDa species is not a deglycosylated form of the 58 kDa protein. In other words, the 54 kDa species may be a truncated isoform of CAIX or the 58 kDa form may be post-translationally modified by mechanisms other than but in addition to glycosylation. To follow up on this, we investigated CAIX ubiquitination. CAIX were first immunoprecipitated using a CAIX antibody, and then ubiquitination status was analyzed by Western blotting. Our data showed that CAIX was not ubiquitinated (data not shown) indicating that the 58 kDa form is not an ubiquitinated form of 54 kDa form. As will be shown below, neither is phosphorylation and underlying cause of the slower migration of the 58kDa form.

Total membrane protein from hypoxic MDA-MB-231 cells was also digested with endo H to determine glycan structure. Figure 4-4B shows that both the 54 and 58 kDa forms of CAIX were completely sensitive to endo H. This result indicates that the attached glycans were of high mannose character.

To confirm that CAIX induced by hypoxia in MCF10A cells displays the same characteristic as that in MDA-MB-231 cells, cell lysates from MCF10A were treated with PNGF or endo H. Both bands of CAIX migrated to lower molecular weights after digestion with these two glycosidases. This provides evidence that the glycan attached to CAIX in MCF10A cells has a high mannose structure although at this point we do not know if this glycan is exactly the same as that in the MDA-MB-231 cells (Figure 4-4D).

We also investigated the glycosylation state of CAXII in T47D cells. Total membranes from T47D cells were treated with PNGF. After treatment, CAXII migration was observed as a single band, collapsing from the three bands of CAXII (Figure 4-4C). This indicates that each species of CAXII is glycosylated but has same core protein. Unlike CAIX glycosylation in MDA-MB-231 cells, the identification of three species of CAXII is due to differences in glycosylation. In other words, each species of CAXII possesses a different size oligosaccharide or more likely that there is differential glycosylation at the two potential *N*-linked glycosylation sites (*101*).

**CAIX and GLUT1 Localization in Lipid Rafts**

Lipid rafts are microdomains within the plasma membrane that serve as signaling platforms. They are enriched in specific lipids and are comprised of a select set of proteins that reside in, or transiently associate with, these domains. The goal of this set of experiments is to determine the localization of CAIX in MDA-MB-231 cells. It has been suggested that CAIX in renal carcinoma cells is translocated to lipid rafts where it forms an oligomeric structure (*37*). GLUT1, the constitutive glucose transporter, is also known to associate with lipid rafts (*76;102*). CAIX and GLUT1 are both induced by hypoxia (*103*) and have been used as markers of hypoxia tumors (*104;105*) and of poor outcome in a variety of cancer, including breast cancer (*106*). Lipid raft fractions were isolated as described in Chapter 2. The proteins in each fraction were resolved by SDS-PAGE and transferred to nitrocellulose. The response of CAIX and GLUT1 to DFO and hypoxia was measured by immunoblotting with antibodies specific for each antigen (Figure 4-5). Fractions 3 and 4 from sucrose density gradients represent membrane vesicles derived from lipid rafts. These vesicles are resistant to disruption by Triton X-100 (TX-100) because of the high cholesterol and sphingolipid content of the lipid raft membranes. The fractions that are labeled as “TX-100 Soluble” represent membrane proteins that were not

protected from detergent extraction. Thus, these proteins were not in lipid rafts to begin with and were dissolved by detergent treatment. We have used the identification of caveolin as a marker of lipid rafts and the transferrin receptor as a protein excluded from lipid rafts and thus solubilized by TX-100 exposure. Neither caveolin nor transferrin receptor expression or localization was influenced by DFO or hypoxia (Figure 4-5 A to C). The localization of GLUT1 to lipid rafts in both control and hypoxic cells represents about 25% of the total pool despite a significant 6-fold increase in expression in response to hypoxia. We interpret this to mean that hypoxia does not have a specific influence on GLUT1 localization within the plasma membrane. CAIX was not detected in lipid rafts in control cells (Figure 4-5A), perhaps a result of low total CAIX expression. Hypoxia or DFO increased the total expression of CAIX by 5-fold in this experiment with only a small increase in the amount of CAIX associated with lipid rafts, about 1.1% of the total CAIX pool. As 90% of the CAIX pool in the membrane are dimers (Figure 4-3), it is unlikely that the small shift of CAIX to lipid rafts influences dimerization of CAIX, which means that dimerization of CAIX does not require the lipid raft environment.

**Phosphorylation of EGFR, AKT and, ERK in Response to EGF Stimulation**

Recent data suggest that EGF stimulates CAIX tyrosine phosphorylation in the cytoplasmic domain in renal carcinoma cells which leads to down-stream activation of the PI3-kinase pathway (*37*). To investigate the possibility of CAIX phosphorylation in response to EGF in MDA-MB-231 cells, EGF-dependent autophosphorylation of the EGF receptor (EGFR) was first examined. MDA-MB-231 cells were serum-starved under hypoxic or normoxic conditions for 16 hours and then stimulated with EGF (16 nM) for specific times from 10 min to 40 min. Under these conditions, phosphorylation of EGFR on Tyr1173 was biphasic. There was a time-dependent increase in EGFR phosphorylation during the first 20 to 30 min but by 40 min phosphorylation was attenutated (Figure 4-6A). The extent of EGFR phosphorylation was

similar under both normoxic and hypoxic conditions. Activation of EGFR led to down-stream phosphorylation of both Akt and Erk1/2 (Figure 4-6B, C). Interestingly, Akt phosphorylation was relatively strong in hypoxic cells even in the absence of EGF suggesting that hypoxia induces Akt activation independent of EGF stimulation. Under the conditions of the experiment, EGF treatment did not influence CAIX expression (Figure 4-6D).

**Localization of CAIX in Response to EGF Stimulation**

We next determined the effect of EGF on CAIX distribution within the plasma membrane. In Figure 4-7A, we showed CAIX expression in total membranes, lipid raft fractions, and TX-100 solublized fractions from each sample. Consistent with data in Figure 4-5A, little CAIX was detected in lipid rafts from control cells. EGF, under normoxic conditions, did not cause any translocation of CAIX to lipid rafts. Hypoxia increased the amount of CAIX, again by only a small amount, while the combination of hypoxia and EGF stimulation increased the amount of CAIX by 5-fold relative to hypoxia alone. This increase was observed in at least four separate experiments even though the amount of total CAIX did not change between hypoxia and hypoxia plus EGF-treated samples. This implies that EGF induces CAIX translocation to lipid rafts but only under hypoxic conditions, although the pool associated with lipid rafts is relatively small (about 5%) compared to the total. This was re-affirmed in Figure 4-7B, which shows the expression of CAIX in total membranes and the lipid raft fractions in hypoxic cells treated with or with not EGF. EGF clearly increased CAIX association with lipid rafts in the context of hypoxia. As the association of signaling proteins with lipid rafts is important for their function, the EGF-dependent increase in CAIX associated with lipid rafts in hypoxic MDA-MB-231 cells may provide some significant cellular function, although that function is yet to be identified.

**Phosphorylation of CAIX in Response to EGF Stimulation**

To examine EGF-dependent phosphorylation of CAIX, cells were exposed to hypoxia for 16 hours and then 30 minutes with EGF. CAIX was then immunoprecipitated with a CAIX-specific polyclonal antibody and then analyzed by Western blotting using an antibody against phosphorylated tyrosine. While there appeared to be several phosphorylated proteins in the cell extracts (input) including those that were EGF-dependent, there were no phosphorylation signals in the CAIX-immunoprecipitated samples (Figure 4-8). The non-specific detection of the heavy chain IgG (arrow) should be noted. The presence of CAIX protein in the immunoprecipitates was verified by Western blot using the M75 antibody. These results indicate that CAIX is not phosphorylated on tyrosine under hypoxic conditions or in an EGF-dependent manner in MDA-MB-231 breast cancer cells.

**Antibody Specific Detection of CAIX in Breast Cancer Cells**

**Detection of CAIX by two different CAIX antibodies**

Several antibodies have been generated against CAIX. In the 1980's, Oosterwijk *et al.* created a monoclonal antibody (G250) against a cell surface protein expressed in renal carcinoma cells (*107*). Using molecular cloning, this antibody was shown to recognize CAIX (*108*). Later, Pastorekova *et al.* developed a monoclonal antibody M75 against a 54/58 kDa protein called MN expressed endogenously in a human mammary tumor cell line (*34*). This antibody was also shown to target CAIX (*42*). The specific epitope for the G250 antibody is unknown, but it has excellent specificity for CAIX in immunohistochemical analysis. The M75 (often considered the gold standard for the identification of CAIX) recognizes the extracellular proteoglycan domain and is useful for Western blotting, immunoprecipitation, and immunohistochemistry. CAIX antibodies are also now commercially available. One of the first companies to offer this product was Novus Biologicals (Littleton, CO). Their polyclonal

antibody was generated against a peptide in the C-terminus, a domain which faces the cytoplasmic compartment. R&D Systems (Minneapolis, MN) also has a number of monoclonal and polyclonal antibodies available. Santa Cruz has CAIX antibodies against different regions of CAIX.

In our initial experiments, we used anti-CAIX antibody purchased from Novus Biologicals (NB100) to detect CAIX expression in MCF10A, T47D, and MDA-MB-231 cells. Cell lysates from control, DFO, or hypoxia-treated cells were loaded on gels and analyzed by Western blotting. CAIX was apparently detected in all three breast cell lines (Figure 4-9). In the MCF10A cells, we observed three protein bands. The upper band migrated as a doublet at about 58 kDa. The bottom band appeared to be a single protein, migrating at about 54 kDa. This appeared to be consistent with the description of CAIX migration from previously published data (*42*). However, only the upper doublet appeared to be responsive to DFO and hypoxia. In the T47D cells, only two bands were observed, neither of which showed response to DFO or hypoxia. In the MDA-MB-231 cells, three bands were once again detected. Again, only the upper doublet appeared to show a response to DFO and hypoxia. After stripping, the membrane was re-probed with M75. The difference in the results was striking. In MCF10A cells, no protein was observed in controls, but three bands were detected in response to DFO and hypoxia. No protein was recognized by M75 in T47D cells, under any condition. In MDA-MB-231 cells, there was little M75-reactive protein in controls, but expression was significantly enhanced by DFO treatment or hypoxia. Because of the responsiveness to hypoxia and the high specificity of M75 for CAIX, these data suggest that the NB100 antibody might be interacting with a non-specific protein which overlaps with the migration of CAIX.

**Sub-cellular localization of the non-specific protein(s)**

CAIX is a transmembrane protein and well recognized as a hypoxia-inducible protein. We have shown that MDA-MB-231 cells express little CAIX in the subconfluent state (Figure 4-2). It is obvious that the lack of CAIX expression would be an advantage in identifying the non-specific protein(s), so we used subconfluent MDA-MB-231 cells to determine sub-cellular localization of the apparent non-specific protein(s) identified by NB100. Cytoplasmic and membrane protein from subconfluent control or MDA-MB-231 cells were separated and analyzed by Western blotting. Figure 4-10 shows a western blot of cytoplasmic and membrane proteins identified by NB100 and M75 (top and middle panels). NB100 recognized a 54 kDa cytoplasmic protein that did not respond to DFO or hypoxia. However, both the 58 kDa doublet, and a 54 kDa protein could be detected in the membrane fraction and both were induced by DFO and hypoxia. The cytoplasmic protein was not detected by the M75 antibody upon reprobing. Proteins identified in the membrane fraction by M75 were clearly similar to those identified by NB100. Taken together, these data suggest that the non-specific protein(s) are localized to the cytoplasmic fraction and migrate at the same molecular weight as does the 54 kDa form of membrane-bound CAIX.

**Isolation and identification of the non-specific protein**

To provide better resolution of the non-specific protein(s), we isolated cytoplasmic proteins from subconfluent MDA-MB-231 cells and separated them using two-dimensional gel electrophoresis (Figure 4-11A). Immunoblotting using NB100 identified an acidic protein with a pI of about 6.0 (Figure 4-11B). The corresponding protein in the Coomassie-stained gel was excised, trypsin-treated, and applied to a mass spectrometer to identify the peptide fragments. Twenty-seven unique tryptic digest fragments matched the sequence of tubulin, predominantly β -tubulin (Table 4-1).

**Confirming the identity of β -tubulin**

To confirm the identity of β-tubulin, the nitrocellulose membrane from the 2D-PAGE gel was stripped and re-probed for β-tubulin expression using an anti-β-tubulin antibody. The same spot detected by NB100 was recognized by the β-tubulin antibody (Figure 4-11B). The cytoplasmic protein detected by NB100, also tested positive when probed with the β-tubulin (Figure 4-10, bottom panel).

## Conclusions

In this chapter, we first investigated the expression of selected CA isoforms in response to DFO or hypoxia in three breast cell lines: MDA-MB-231, T47D, and MCF10A. We found that expression of these CA isoforms was cell-specific. In confluent cells, only MDA-MB-231 cells expressed CAIX, and its expression was strongly induced by DFO and hypoxia. MCF10A cells had no detectable CAIX in confluent cells, but showed enhanced CAIX expression in response to DFO and hypoxia. T47D cells expressed no CAIX either constitutively or in response to DFO or hypoxia. Yet, HIF1α was induced in each of these cells by DFO and hypoxia suggesting that the hypoxic response is intact in each line. T47D strongly expressed another membrane CA, CAXII, which was not responsive to DFO or hypoxia. However, CAXII was not expressed in the MDA-MB-231 cells. The cytosolic CA, CAII, was expressed in MCF10A and MDA-MB-231 cells, but not in T47D cells. CAIX expression was also induced by cell density in MDA-MB-231 cells, but not in MCF10A or T47D. Taken together, these data provide evidence that only MDA-MB-231 cells show both density and oxygen-dependent regulation of CAIX at the protein level. Cell density induced-hypoxia occurs frequently in tumor (*3*). Our data imply that the expression of CAIX might offer an advantage for cancer cell proliferating in the tumor microenvironment. Importantly, MDA-MB-231 cells express only one of the membrane-bound CA family members,

CAIX, which provides an advantage for analyzing specifically CAIX activity which will be documented in Chapter 5.

The oligomerization status of CAIX is unclear because of contradictory data. It was originally proposed that CAIX could form trimers (*34*). More recent characterization of CAIX reveals that CAIX can exist as a dimer. Approximately 50% of the CAIX catalytic domain constructs form dimers. In constructs containing both the proteoglycan-like domain and the catalytic domain, dimers comprised about 60% of the pool (*31*). Crystal structure of the soluble form of CAIX has confirmed that the two catalytic domains associate to form a dimer, stabilized by the formation of a single intermolecular disulfide bond (*109;110*). In the MDA-MB-231 cells, dimers comprise 90% of the CAIX pool. The equal intensity of the 54/58 kDa doublet, which we observed on reducing gels, might suggest that the doublet pair is linked by a disulfide bond in the dimer as the dimeric species that we observed migrated as a single band at about 119 kDa. While the TM domain does not appear to be required for dimerization, we believe that our data show that the extent of dimerization is affected by its presence.

CAIX migrated as a doublet of 58/54 kDa proteins. Each of these bands appeared to be glycosylated based on their individual sensitivity to the *N*-glycosidase, PNGF. These data are consistent with previously published data in HeLa cells (*35*) and reaffirms that the protein sequence differs between the 58 and 54 kDa species. Also, the oligosaccharides in CAIX were of high mannose structure because CAIX was sensitive to endoglycosidase H which only cleaves high mannose structures from the *N*-linked consensus site. It is atypical for plasma membrane proteins to retain endo H sensitivity in normal cells but not uncommon in cancer cells (*111*) and specifically in breast cancer cells as was shown recently (*112*). Like CAIX, GLUT1 has a single *N*-linked glycosylation site but migrates as a broad band suggesting heterogeneous, complex

glycosylation which is resistant to endo H digestion (*113*). Both GLUT1 and CAIX are up-regulated by hypoxia but appear to be differentially processed in the same cell. This preference for high mannose glycans may be an intrinsic feature of the CAIX structure as recombinant CAIX (constructs containing either the catalytic domain, alone, or in combination with the proteoglycan domain) expressed in a baculovirus-insect cells or in murine cells also exhibit high mannose glycan structures (*31*). Unlike CAIX, the three protein bands identified as CAXII collapsed to one band after *N*-glycosidase treatment, which suggests that the three species of CAXII contain the same core protein but are differentially glycosylated.

Previous data suggests that CAIX can translocate to lipid rafts and in that process form oligomers. In our hands, CAIX was not detected in lipid rafts isolated from normoxic MDA-MB-231 cells but hypoxia increased CAIX in lipid rafts to a measureable level (estimated as 1% of total pool). Given that the majority of CAIX (90% of the pool) exists in the membrane as is dimers, it is not likely that lipid raft localization is required for CAIX dimerization.
Dorai *et al.* demonstrated that EGF stimulates CAIX phosphorylation on tyrosine 412 in the cytoplasmic domain in a renal carcinoma cell line, SKRC-01 (*37*). However, we were unable to demonstrate EGF-dependent CAIX phosphorylation in the MDA-MB-231 cells. Clearly, the EGFR was expressed in MDA-MB-231 cells, was phosphorylated in the presence of EGF, and initiated down-stream activation of Akt and Erk (Figure 4-6). There are several reasons why we may not have observed phosphorylation of CAIX. The EGFR is known to reside in lipid rafts in both normal cells and cancer cells (*95;96*) and to mediate the activation of down-stream signaling pathways in cancer cells when recruited to lipid rafts (*97*). Dorai *et al.* indirectly demonstrated that phosphorylated CAIX was present in lipid rafts which imply that EGF stimulation causes the recruitment of CAIX to lipid rafts. We were unable to detect any CAIX in

lipid rafts in normoxic cells in the presence or absence of EGF but the overall levels of CAIX are quite low in normoxic cells. On the other hand, if EGFR is localized to lipid rafts, then the interaction between EGFR and CAIX might not occur. We did observe an EGF-dependent increase in the content of CAIX in lipid rafts under hypoxic conditions which represented about 5% of the total CAIX pool. If this particular pool was phosphorylated, admittedly, it might go undetected. Further, we must also consider the differences between MDA-MB-231 breast cancer cells and the renal cell carcinoma that were used to demonstrate CAIX phosphorylation. CAIX in renal cell carcinoma is not upregulated by the condition of hypoxia, as it is in MDA-MB-231 cells. Rather a mutation in von Hippel-Lindau tumor suppress gene (VHL) which regulate the HIF1$\alpha$ drive the CAIX expression. Thus the envionment surrounding renal carcinoma cells and breast cancer cells is quite different. Further, CAIX expression in renal carcinoma is a positive predictor of survival (*114*) while CAIX expression in breast cancer is an indicator of poor prognosis (*41*). How these differences play out with respect to EGF action is not known at this point.

There is substantial evidence that CAIX expression coincides with hypoxia and is considered a marker for hypoxia (*47;115;116*). Detection of CAIX using the M75 has been suggested as a diagnostic and prognostic marker (*60;117*) for immunohistochemistry of renal cell carcinoma, in which hypoxia is not the driver of CAIX expression. Our data suggest extreme caution be used with clinical samples. When we utilized the NB100 and M75 antibodies to examine CAIX expression in our three breast cell lines, they detected different proteins. In addition to CAIX, NB100 recognized a protein localized to the cytosol which did not respond to hypoxia. Using two-dimensional analysis, we separated this protein from other cytosolic

proteins and identified it by LC-MS/MS as β-tubulin. Thus, use of such an antibody in clinic samples could lead to false positives which could have a significant impact on patient diagnosis.

In summary, we have described the characteristics of CAIX in breast cancer cell lines, including expression, oligomerization, glycosylation, and localization. We show for the first time that the MDA-MB-231 cells, which represent the triple-negative breast cancer phenotype, show inducible expression of CAIX, while the less aggressive luminal line, T47D cells, expresses primarily CAXII. CAIX expression is induced by hypoxia in MDA-MB-231 cells. As described earlier in Chapter 3, the MDA-MB-231 cells had the highest growth rate and the highest rate of lactic acid production among the cells that were tested. In terms of glycolysis, 94% of the glucose consumed was converted to lactic acid. By comparison, the MCF10A cells converted only about 50% of the glucose to lactic acid. Thus, not only was glucose uptake increased in MDA-MB-231 cells relative to MCF10A cells but there also was a shift in metabolic flux which typifies cancer cells. Metabolic activity in T47D cells was intermediate between these cell types. Hypoxia further enhanced glucose uptake and glycolysis in MDA-MB-231 cells, but the intrinsic metabolic behavior of these cells was preestablished. Interestingly, the drop in medium pH in response to hypoxia could not be accounted for by lactic acid production alone. This lends credence to the possibility that the induction of CAIX contributes independently to acidification. The lack of constitutive or induced CAIX protein expression in T47D cells is consistent with the less aggressive phenotype of these cells *in vivo*. Thus, our data suggest that CAIX expression is associated with metabolic dysfunction in MDA-MB-231 cells. In addition, our data are important in that we show for the first time that the MDA-MB-231 cells express only one of the membrane associated CA family members, CAIX, allowing us to

demonstrate, directly, that CAIX activity changes in response to hypoxia. Data in this section provide basic work for analysis of CAIX activity which is described in next chapter.

Table 4-1. Identification of tubulin by mass spectrometry.

| Protein name | Molecular Weight kDa | Numbers of unique peptides |
|---|---|---|
| TUBB Tubulin beta chain | 50 | 27 |
| TUBA1C Tubulin alpha-1C chain | 50 | 15 |
| TUBB2C Tubulin beta-2C chain | 50 | 5 |
| KRT10 Keratin, type I cytoskeletal | 60 | 2 |
| TUBB3 Tubulin beta-3 chain1 | 50 | 8 |
| TUBB6 46 kDa protein | 46 | 6 |
| EEF1A1 Elongation factor 1-alpha | 50 | 4 |
| KRT1 Keratin, type II cytoskeletal 1 | 66 | 1 |
| HSP90AA1 heat shock protein 90kDa alpha(cytosolic) | 98 | 7 |
| TUBA4A Tubulin alpha-4A chain2 | 50 | 3 |
| RBBP7 Histone-binding protein RBBP7 | 48 | 4 |
| TUBB2A Tubulin beta-2A chain | 50 | 2 |
| TFG Protein TFG | 43 | 3 |
| ATP5B ATP synthase subunit beta, | 57 | 2 |
| HSP90AB1 85 kDa protein | 85 | 2 |
| Putative uncharacterized protein (Fragment) | 17 | 2 |
| PPM1F Protein phosphatase 1F | 50 | 2 |

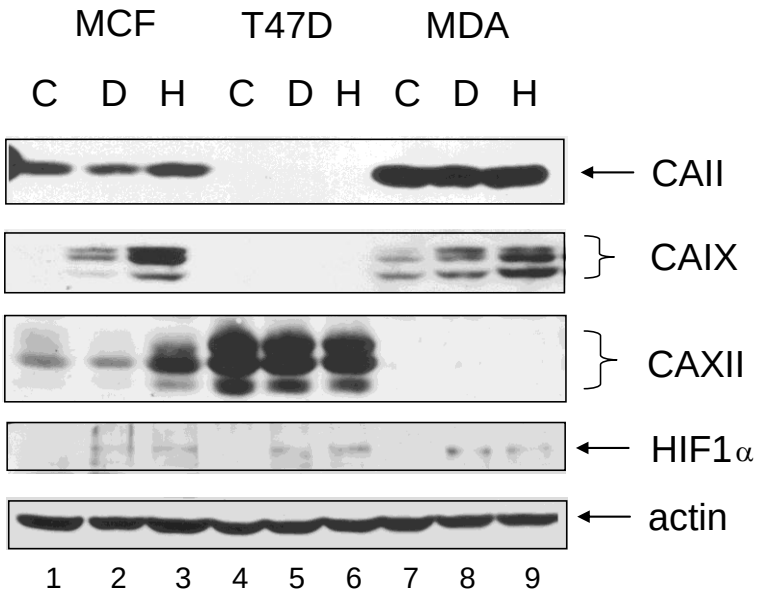


Figure 4-1. Expression of CAs in response to DFO or hypoxia in breast cancer cell lines. Cells at 75% confluence were exposed to 100 μM DFO or 1% oxygen for 16h after which they were lysed. Equal protein (100 μg) was analyzed by western blot analysis using antibodies for CAII, CAIX (M75), CAXII, and HIF1α. Identical results were obtained in two independent experiments. MCF = MCF10A cells; T47D = T47D cells; MDA = MDA-MB-231 cells; C = control, D = DFO, H = Hypoxia.

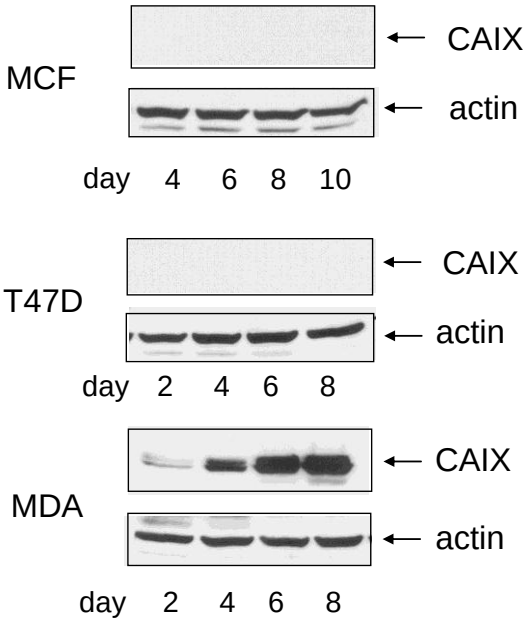


Figure 4-2. Density-dependent expression of CAIX in breast cancer cell lines. Cells were collected at specific times after plating. Cells were lysed, and equal protein was analyzed by western blot analysis using the M75 antibody. Identical results were obtained in independent duplicate experiments. MCF = MCF10A cells; T47D = T47D cells; MDA = MDA-MB-231 cells.

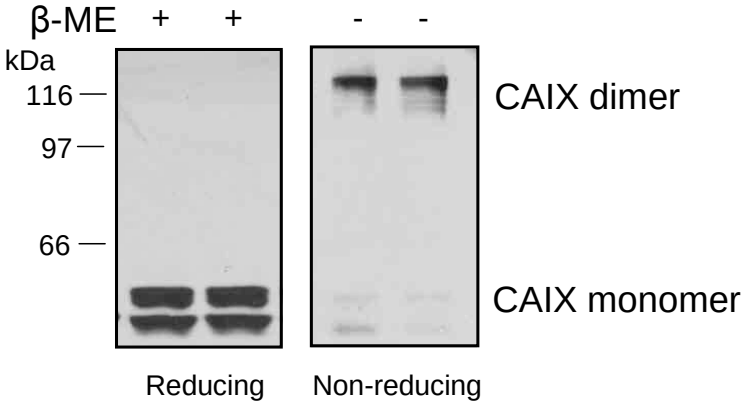


Figure 4-3. Oligomerization of CAIX. Total membranes were isolated from MDA-MB-231 cells exposed to hypoxia for 16 h. Total membrane proteins (50 µg) were separated on SDS-PAGE gel in the presence or absence of 1% β-mercaptoethanol (β-ME). CAIX expression was detected by western blotting using the M75 monoclonal antibody.

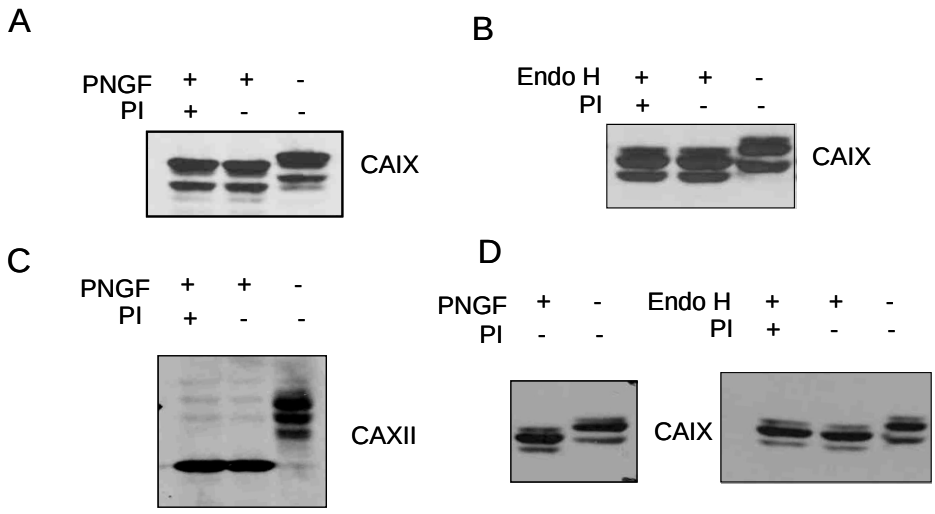


Figure 4-4. Glycosylation of CAIX and CAXII. A) Total membranes were isolated from MDA-MB-231 cells exposed to hypoxia for 16 h. Fifty µg of protein was digested with 2 µL N-glycosidase F (PNGF) in the presence or absence of protease inhibitor (PI) for 2 hours at 37ºC. B**)** Cell lysates were isolated from MDA-MB-231 cells exposed to hypoxia for 16 h. Fifty µg of protein was treated with 2 µL endoglycosidase H (endo H) in the presence or absence of protease inhibitor (PI) for 2 hours at 37ºC. CAIX expression was detected by western blotting using the M75 antibody. C) Total membranes were isolated from T47D cells. Fifty µg of protein was digested with 2 µL N-glycosidase F (PNGF) in the presence or absence of protease inhibitor (PI) for 2 hours at 37ºC. D) Cell lysates were isolated from MCF10A cells exposed to hypoxia for 16 h. Fifty µg of protein was treated with 2 µL N-glycosidase F (PNGF) or 2 µL endoglycosidase H (endo H) in the presence or absence of protease inhibitor (PI) for 2 hours at 37ºC. CAIX expression was detected by western blotting using the M75 antibody. These blots represent duplicate experiments.

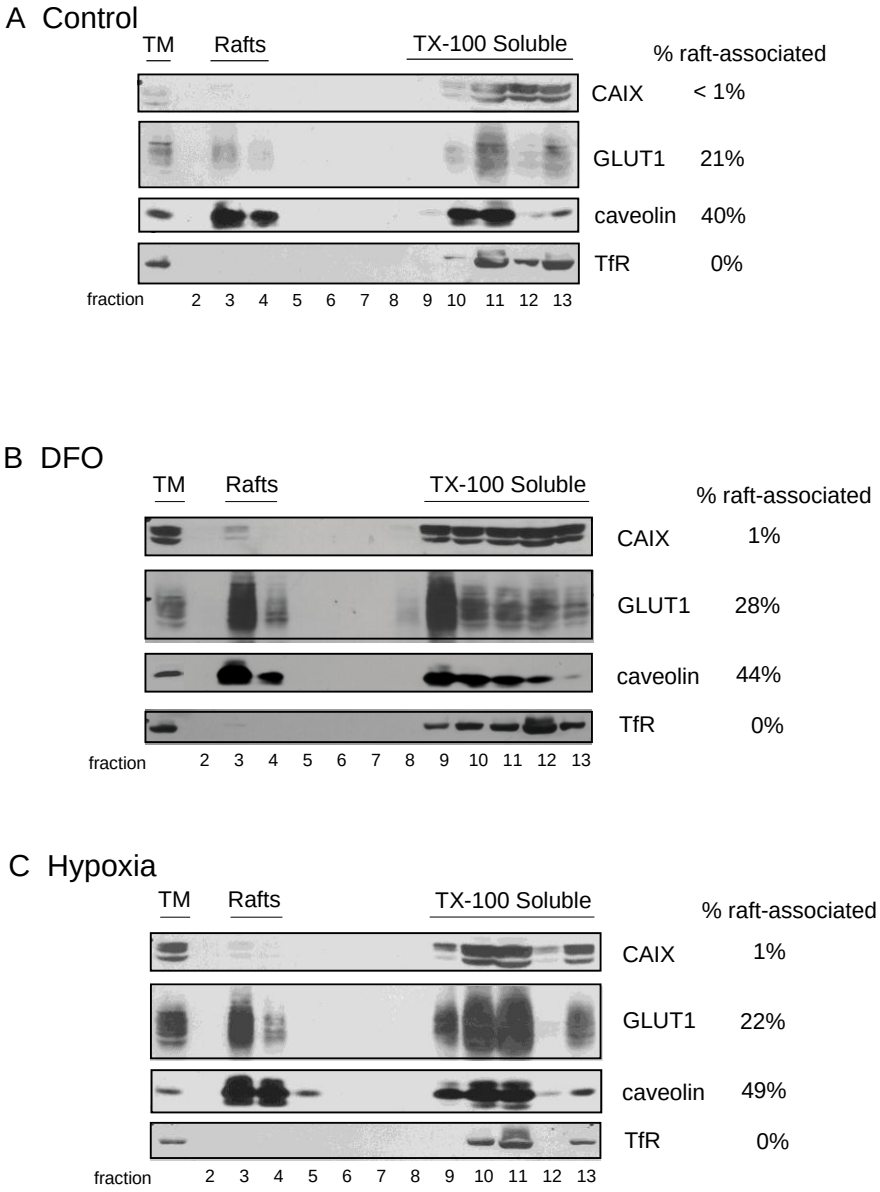


Figure 4-5. Localization of CAIX and GLUT1 in lipid rafts. Total membranes were collected from MDA-MB-231 cells after exposure to DFO or hypoxia. The Triton X-100-resistant membranes were separated from extracted protein by flotation in sucrose gradients. CAIX, GLUT1, caveolin (which is consistently found in lipid rafts) and transferrin receptor (which is excluded from lipid rafts) were detected by immunoblot analysis. These data represent three independent experiments. TM = total membranes; rafts = lipid raft-containing membranes; TX-100 Soluble = membrane proteins extracted by 1% TX-100. A) Control. B) DFO. C) Hypoxia.

A

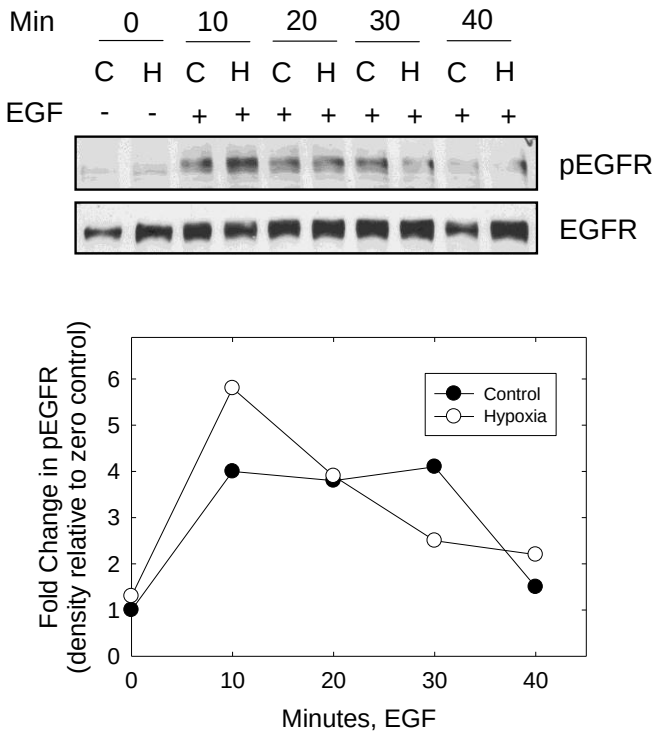


Figure 4-6. EGF-dependent activation of EGFR, Akt, and Erk. MDA-MB-231 cells were exposed to normoxic (C) or hypoxic (H) conditions for 16 h in the absence of serum and then stimulated with 16 nM EGF for specific times. Proteins (100 μg) from cell lysates were separated on SDS-PAGE gels and analyzed by western blotting. A) Total and phosphorylated pools of EGFR. B) Total and phosphorylated pools of Akt. C) Total and phosphorylated pool of Erk. D) Total pool of CAIX.

B

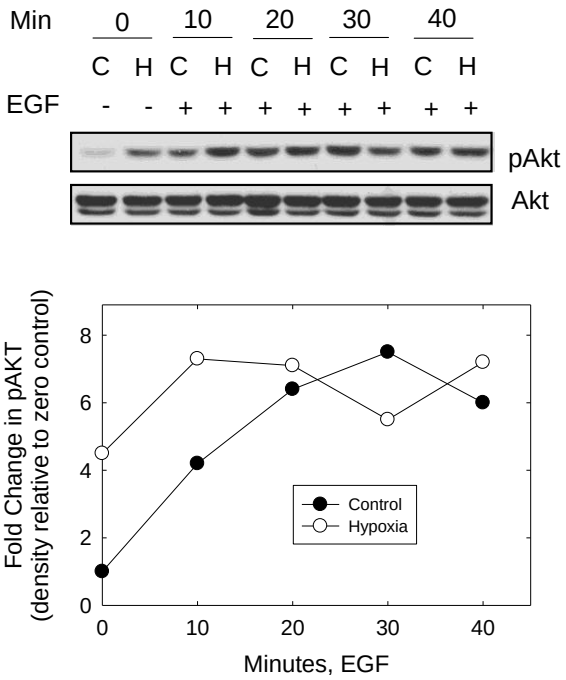


C

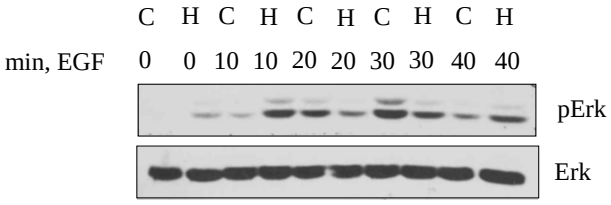


D

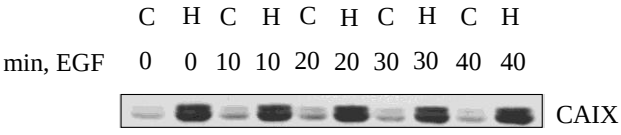


Figure 4-6 Continued

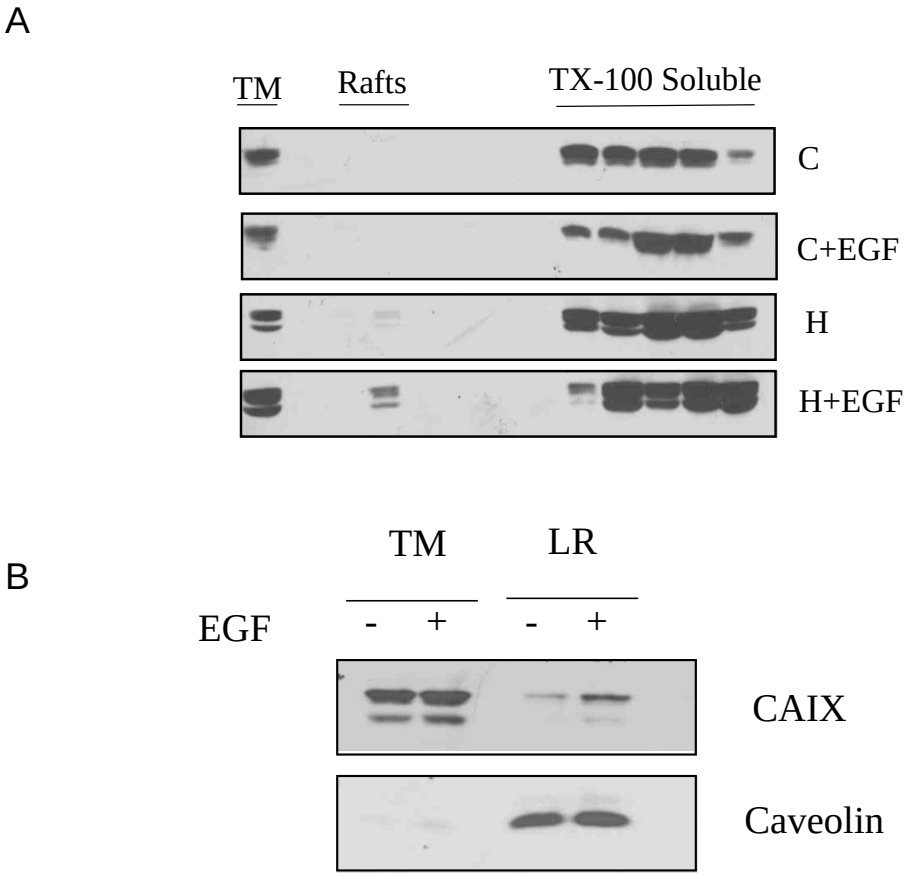


Figure 4-7. EGF-dependent localization of CAIX. MDA-MB-231 cells were serum-starved overnight under normoxic or hypoxic conditions and then stimulated with EGF (16 nM) for 30 min. Total membranes were collected and then lysed with TX-100. Detergent resistant proteins (lipid rafts) were separated from extracted proteins. A) CAIX expression in each fraction was detected by western blotting using the M75 monoclonal antibody. TM = total membrane fraction; Rafts = lipid raft-containing membranes; TX-100 Soluble = membrane proteins extracted by TX-100. C = control, C+EGF = control cells treated with EGF, H = hypoxia, H+EGF = hypoxic cells treated with EGF. B) MDA-MB-231 cells were exposed to hypoxia for 16 hours and then treated with EGF (16 nM) for 30 min. Total membranes were prepared from which lipid rafts were isolated. CAIX and caveolin expression were detected by western blotting. TM = total membrane proteins; LR = lipid raft containing membranes.

.

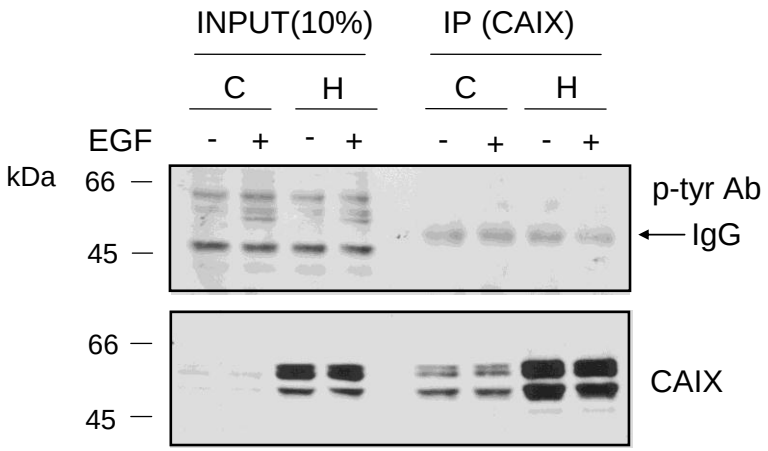


Figure 4-8. CAIX phosphorylation in response to EGF stimulation. MDA-MB-231 cells were exposed to hypoxia or not for 16 h in the absence of serum. EGF (16 nM) was added for 30 min after which total membranes were isolated. CAIX was immunoprecipitated with an antibody generated in goat (R&D Systems, # AF2188) followed by western blotting with an anti-phosphotyrosine antibody or the M75 mouse monoclonal antibody. C = control, H = hypoxia. These data represent triplicate experiments.

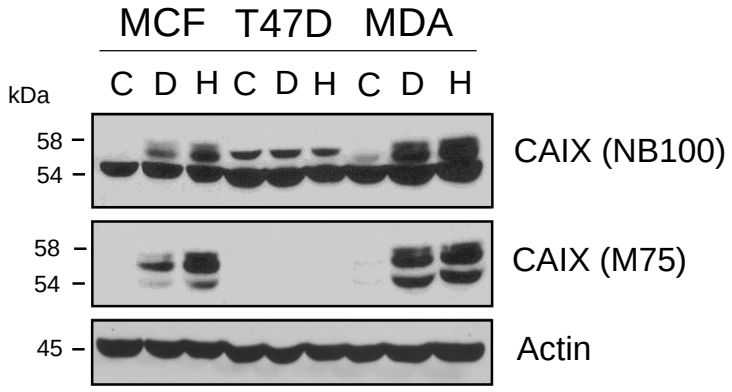


Figure: 4-9. Detection of CAIX in breast cell lines using M75 and NB100 antibodies. Subconfluent cells were lysed after exposure to DFO or hypoxia, as described in the Materials and methods. Equal protein (100 μg) was analyzed by western blot analysis using CAIX antibodies: CAIX monoclonal antibody M75 and polyclonal antibody NB100 (Novus Biologicals). Actin was used as a loading control. C = control, D = DFO, H = hypoxia. These data are representative of at least three independent experiments.

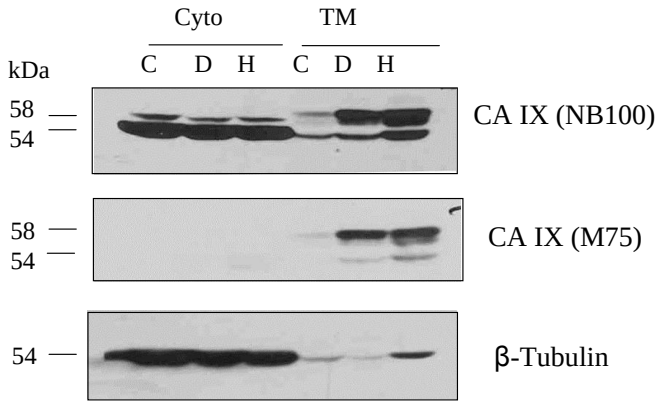


Figure 4-10. Localization of CAIX detected by NB100 and M75. Subconfluent MDA-MB-231 cells were collected and separated into a total membrane (TM) and cytoplasmic fraction (Cyto) after exposure or not to DFO and hypoxia. Equal protein (100 μg) was analyzed by western blot analysis for CAIX using M75, NB100. β-Tubulin expression was analyzed. C= Control; D= DFO; H= hypoxia. These data are representative of at least three independent experiments.

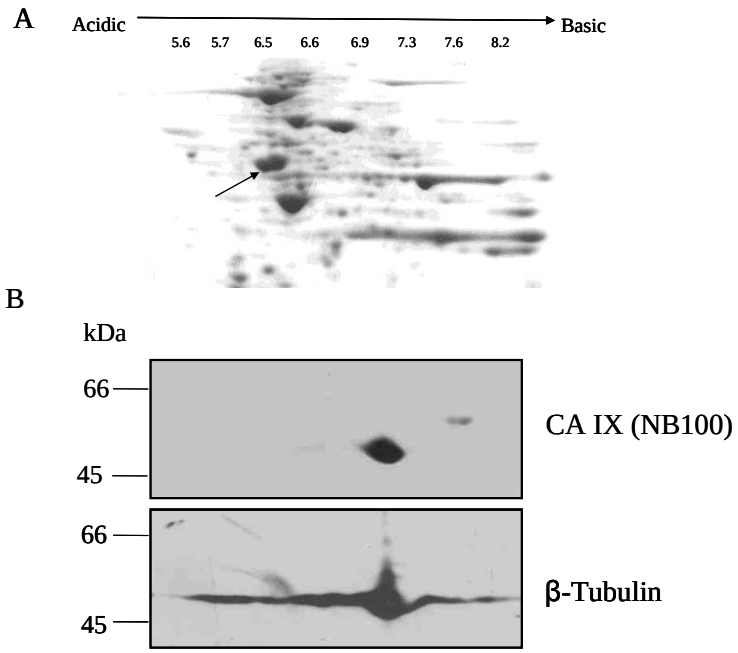


Figure 4-11. Separation of cytoplasmic proteins by two-dimensional electrophoresis. A) A cytoplasmic fraction from subconfluent MDA-MB-231 cells was separated by two dimensional electrophoresis. The gel was stained with Coomassie blue. The arrow points to the protein spot recognized by NB100. B) Proteins were transferred to nitrocellulose membranes and immunoblotted for CAIX by NB100 and β-Tubulin.

CHAPTER 5
CATALYSIS AND INHIBITION OF CAIX IN BREAST CANCER CELLS

## Introduction

Carbonic anhydrase IX (IX) expression is associated with high tumor grade, tumor necrosis and poor prognosis in breast cancer (*38;118*). CAIX contributes to the tumor progression and the poor response to traditional chemo-and radio-therapies by regulation of pH balance during tumorigenesis (*10*). CAIX is an integral plasma membrane protein with a large exofacial domain that contains the catalytic pocket. Thus, CAIX in tumor cells may be accessible to a variety of targeting tools, including CA inhibitors. In this regard, CAIX has become a potential and novel target for cancer therapy and specifically represents a new pharmacologic target for hypoxic tumors that are non-responsive to classical chemo- and radio-therapy. We have shown in previous chapters that CAIX expression is strongly induced by hypoxia and cell density in MDA-MB-231 breast cancer cells and has been linked to the basal, triple-negative phenotype (*100*), an aggressive cancer for which there are few treatment options.

Several groups have utilized soluble forms of CAIX to gain insight into catalysis. For example, the catalytic domain (CA) of CAIX was first cloned and analyzed for its kinetic properties by Wingo et al. (*30*). Their data indicate that the catalytic efficiency (Kcat/Km) for $CO_2$ hydration by CAIX, produced in a bacterial expression system, is $5.5 \times 10^7\ M^{-1}s^{-1}$. This value is similar to the catalytic efficiency of CAII ($1.0 \times 10^8\ M^{-1}s^{-1}$), which indicates that CAIX belongs to the group of CAs that have high catalytic activity (*30*). Other groups have compared the kinetic properties of the CA domain with the CA domain containing the proteoglycan (PG) extension (CA + PG) when expressed in bacterial and insect cell lines (*31*). Recombinant protein containing CA domain and the CA + PG domains shows a Kcat/ Km value of $5.5 \times 10^7\ M^{-1}s^{-1}$ and $1.5 \times 10^8\ M^{-1}s^{-1}$, respectively, the later of which is more similar to that of CAII. The pH

dependence of CAIX activity (for the $CO_2$ hydration) for the CA and the CA + PG protein fragments has also been reported (*109*). Protein constructs containing just the CA domain has a pKa of 7.01, which is similar to that observed for CAII. In contrast, the pKa for the protein fragment containing CA + PG is 6.49, which is within a typical pH range of solid and hypoxia tumors. These investigators suggested that the CA + PG domain construct acts as a better catalyst for $CO_2$ hydration at more acidic pH value. As CAIX is the only membrane-associated CA to contain a PG domain, they propose that this evolved through evolutionary adaptation to its environment providing increased buffering efficiency which makes the catalyst more efficient at pH values of 6.5, typical of the solid tumor. Earlier data, reported by Wingo et al. (*30*), contradict this notion as they reported a pKa value of 6.4 for the CA domain of CAIX. In all of these experiments, CAIX activity was determine using purified soluble protein fragments. Yet, CAIX is a membrane protein which includes the transmembrane and cytoplasmic domains, beside PG domain and CA domains. These domains and/or the transmembrane environment might affect its activity. Thus, in this chapter, we first assayed CAIX activity in intact MDA-MB-231 breast cancer cells. In addition, CAIX activity was characterized in its native state by membrane inlet mass spectrometry (MIMS).

The inhibition of CAIX by sulfonamides is well studied in term of its biochemical, physical, and medical aspects (*54;119*). To be of use in CAIX-specific inhibition in its normal cellular environment, CA inhibitors must be impermeant. Several such inhibitors have been designed and studied, and shown to be effective at umolar/nanomolar concentrations (*39;57;58*). Such low Ki values are promising for therapeutic applications. Our group has designed a pegylated sulfonamide in collaboration with Dr. Nicole Hornstein's laboratory in the Department of Chemistry at the University of Florida. This compound has a structure similar to F3500 which

was described in Chapter 1. N3500 is comprised of p-aminomethylbenzenesulfonamide chemically attached to polyethylene glycol biacetic acid resulting in PEGpAMBS (*58*). This inhibitor has a high-molecular weight (average MW 3548) and abbreviated as N3500. N3500 was determined to be membrane impermeant in red blood cells which express only CAII (*58*). Specifically the addition of 4 μM N3500 to a suspension of red blood cells for 2 hours has no effect on $^{18}O$ depletion from $CO_2$ determined by MIMS (*58*). In vitro, the binding constant (Ki) of this inhibitor for CAII was estimated at 3.4 μM. Because of the similarity of sulfonamide inhibition for CAII and CAIX (*30;31*), we assume that this value is applicable to CAIX inhibition. The impermeable feature of this inhibitor makes it attractive for targeting CAIX at the cell surface distinguishing its inhibition from that of CAII. A second inhibitor of interest is Cpd 5c. This is a fluorescent sulfonamide investigated by Svastova *et al*. in which the sulfonamide is linked to fluorescein. These investigators reported that Cpd 5c has high affinity for CAIX (Ki = 24 nM), although the value is about 9.0 nM determined by Dr. Silverman group (unpublished data). The Pasterekova group reported that this inhibitor binds only CAIX expressed MDCK epithelia cells and reduced extracellular acidity induced by CAIX expression in hypoxia but not in normoxia. (*50*). *In vivo* studies show that this inhibitor binds to tumor cells expressing CAIX in hypoxic conditions and reoxygenation of tumors significantly reduce the binding (*60;61*). These data suggest that CAIX activity is regulated not only by its expression but also by hypoxia. However, direct measurement of CAIX activity in response to changes in $O_2$ contents has not been explored.

In chapter 4, we have shown that aggressive breast cancer cells, MDA-MB-231, have both hypoxia- and density-dependent CAIX expression and that CAIX is the only membrane-associated CA expressed in the MDA-MB-231 cells. This provides an opportunity to measure

CAIX activity directly in these cells. In this chapter, CAIX activity was examined in intact cells and in the plasma membranes from control and hypoxia-induced MDA-MB-231 cells by MIMS. This method has been previously utilized to analyze purified CAII and CAIX catalytic domain activity (*30;120*). Using MIMS, we also examined inhibition of CAIX activity by a number of CA inhibitors. Moreover, we characterized CAIX activity in response to pH, $Zn^{2+}$ and $O_2$ deprivation. Finally, the effect of CAIX inhibition on cell viability, migration and invasion was assessed to determine if inhibition of CAIX affects these phenotypic features of MDA-MB-231 cells in culture.

## Results

### CA Activity in Response to Hypoxia

Using MIMS, CA activity in intact cell of MDA-MB-231 cells was directly measured. The rationale and methodology for this approach was described in Chapter 2. To better illustrate the biphasic feature of $^{18}O$ depletion and distinguish the intracellular and extracellular CA activity, the rate of loss of $^{18}O$ from $CO_2$ in red blood cell suspensions was first assayed by Dr. Chingkuang Tu in the Department of Pharmacology and shown in Figure 5-1. Red blood cells express CAII in the intracellular comparment, but do not express any extracellular carbonic anhydrase. In this experiment, red blood cells were added at time zero to a solution containing $^{13}C^{18}O_2/H^{13}C^{18}O_3^-$. The rate of change in the atom fraction of $^{18}O$ in $CO_2$ in red blood cells displayed a biphasic pattern, with a steep loss of $^{18}O$ from $CO_2$ in the initial 25 seconds (Phase 1) and followed by a phase of much slower depletion of $^{18}O$ from $CO_2$ (Phase 2) (Figure 5-1A). The initial rapid decreased in isotopic enrichment of $CO_2$ upon addition of cells is dominated by flux of $C^{18}O_2$ into the cells where it reacts with CAII to produce bicarbonate. The bicarbonate is quickly dehydrated (also by CAII) and the resulting $C^{18}O^{16}O$ and $C^{16}O_2$ (after two dehydration cycles) is released back into the extracellular medium where the loss of $^{18}O$ from $CO_2$ is detected

by the mass spectrometer. The second slower phase that is observed between 100 and 500 seconds is dominated by the depletion of $^{18}O$ from bicarbonate, which is carried by the anion exchanger across the membrane, resulting in a slower loss of $^{18}O$ from $CO_2$. Addition of acetazolamide showed little effect on either phase 1 or phase 2 of the progress curve, suggesting that acetazolamide is impermeant over the time course of the experiments. To determine the effect of extracellular CA activity on the biphasic depletion, Dr. Chingkuang Tu established a model to mimic external CA activity by adding purified human CAII (hCAII) to the reaction vessel containing red blood cells. hCAII, the soluble and wide-spread CA isozyme, does not enter the cells. Figure 5-1B demonstrates that the presence of hCA II in the extracellular solution altered the slopes in the biphasic depletion. Specifically, the slope of the second phase became greater. That is, as the concentration of extracellular hCAII increased, the pattern of $^{18}O$ depletion approached the monophasic rate observed in solutions of cell free carbonic anhydrase (*81*). These data suggest that the slope of the second phase can also provide data about external CA activity and in fact is a linear function of the concentration or activity of extracellular CA (*see insert*).

These examples with red blood cells help to understand the biphasic $^{18}O$ depletion in a suspension of MDA-MB-231 cells, the data for which is shown in Figure 5-2. We used MDA-MB-231 cells exposed or not to hypoxic conditions. The progress curve in normoxic or hypoxic cells is represented by a biphasic depletion of $^{18}O$ in from $^{13}C^{18}O_2$. Under normoxic conditions, MDA-MB-231 cells express little external CAIX but substantial intracellular CAII. As in the red blood cell system, the steep phase 1 is due to the rapid flux of $C^{18}O_2$ into cells and the subsequent loss of $^{18}O$ to $H_2O$ catalyzed by intracellular CAII. The second and slower phase is predominately due to the dehydration/hydration reaction in the extracellular solution, mediated

by CAIX. Addition of an impermeant sulfonamide (N-3500) showed a limited effect on either phase 1 or phase 2 of the progress curve. First order of rate constant of the second phase in normoxic cells is 1.1x $10^{-3}$ $s^{-1}$ and which decreased to 0.4x$10^{-3}$ $s^{-1}$ in the presence of N3500. This can be explained by the limited expression and activity of exofacial CA in normoxic MDA-MB-231 cells. Hypoxic cells showed a substantially different pattern. The rate of phase 2 was accelerated compared to normoxic cells, dominated by CAIX activity. The rate constant is 2.5 x $10^{-3}$ $s^{-1}$. Addition of N-3500 reduced the rate constant of phase 2 in hypoxic cells to 0.5x$10^{-3}$ $s^{-1}$, which is equal that of the inhibited state in normoxic cells (0.4 x$10^{-3}$ $s^{-1}$). Thus, compared with normoxic cells, the progress curve for the hypoxic MDA-MB-231 cells show little change in phase 1, while in phase 2, hypoxic cells show significant acceleration due to elevated CAIX activity. These data are unique in that they have allowed an assessment of the contribution of CAIX and CAII independently to total CA activity in MDA-MB-231 cells.

CA activity in the plasma membrane from normoxic and hypoxic MDA-MB-231 cells was also measured using MIMS. Given that CAIX is the only membrane-bound isoform in MDA-MB-231 cells, this activity reflects CAIX activity. Membranes isolated from hypoxic cells exhibited about 7-fold more CA activity than did membranes from control cells (Figure 5-2C), which is consistent with the difference its expression in normoxic and hypoxic cells (Figure 5-2B).

**Inhibition of CAIX Activity by Sulfonamides**

To analyze the inhibition of CAIX activity by sulfonamides, we tested a variety of CA inhibitors using the $^{18}O$ exchange strategy in MDA-MB-231 cells. Acetazolamide is a potent (Ki = 3-10 nM) inhibitor of CAIX and CAII (and many other isozymes of CA) with only moderate diffusability across membrane. N3500 specifically blocks exofacial activity (CAIX) because the sulfonamide is covalently attached to a polyethylene glycol moiety. Ethoxzolamide

is completely permeable and rapidly enters the cells. Consistent with earlier data, in the absence of CA inhibitors, hypoxic MDA-MB-231 cells displayed biphasic depletion of $^{18}O$ from $CO_2$ (Figure 5-3A). In the presence of ethoxzolamide, the progress curve was flat and did not display a biphasic characteristic, suggesting it rapidly enters into cells where it blocks intracellular CA along with extracellular CA activity. The progress curve after addition of acetazolamide or N3500 was more strongly biphase than in the absence of the inhibition. N3500 at 100 μM was sufficient to completely inhibit exofacial CAIX but had no effect on intracellular CA (CAII) activity. Acetazolamide displayed the same characteristic as it only blocked exofacial activity during time course of experiment. Acetazalomide, at 50 nM, completely inhibited the extracellular CA activity.

To determine the Ki of N3500 for CAIX activity, we examined dose-dependent inhibition of CAIX activity in hypoxic MDA-MB-231 cells. The phase 2 slope in the progress curves decreased with increasing of concentration of N3500 (Figure 5-3B). The apparent Ki of N3500 (for phase 2) was about 13 μM (Figure 5-3C).

Cecchi et al. have described the synthesis of a fluorescent sulfonamide (Cpd 5c) that can be used to probe CAIX expression and activity (*75*). While these authors reported similar inhibition constants for purified hCAII and the soluble catalytic domain of hCAIX (Ki = 45 and 24 nM, respectively), Cpd 5c was characterized as impermeant and thus specific for cell surface CA activity. They suggested that this inhibitor binds to CAIX only under hypoxic conditions, both *in vitro* and *in vivo* (*50;60;61*). To confirm this, we assessed the effect of Cpd 5c on CA activity in hypoxic MDA-MB-231 cells (Figure 5-4). Cpd 5c significantly affected the progress curves for the exchange of $^{18}O$ in $^{13}CO_2$. Indeed, the shape of the progress curves in the presence of Cpd 5c suggested that it was impermeant over the course of the experiment, as the biphasic

depletion was more exaggerated upon addition of the inhibitor. The apparent Ki of Cpd 5c (for phase 2) was about 85 nM.

**Estimation of CAIX Activity in MDA-MB-231 Cells**

In Figure 5-1, we have shown that the slope of phase 2 of the progress curve is a linear function of the external carbonic anhydrase activity in the red blood cell system. In order to estimate the contribution of CAIX activity in MDA-MB-231 cells suspensions, a similar experiment was performed, except that hCAII was added to suspensions of normoxic and hypoxic cells. Addition of hCAII increased the slope of second phase in both normoxic or hypoxic cells (Figure 5-5A, B). This change was observed as a linear function of the hCAII activity (Figure 5-5C). To attempt to be more quantitative, we have established the rate (value of the slope) at zero exofacial activity by treating both sets of cells with N-3500. Then, the actual values of added CAII were modified to include the exofacial activity. This was estimated by extending the lines for each data set in Figure 5-5C to the negative X-axis. That intercept was then added to the slope value for each of the concentrations of added CAII. A new plot was generated with these data (Figure 5-5D) including the slope values in the presence of N-3500 (at zero added CAII). The regressions were then used to quantify the relative values of CAIX activity in control and hypoxic cells. This scaling process revealed that the concentration of CAIX in the control cells was equivalent to approximately 2 nM hCAII and for hypoxic cells was about 8 nM hCAII. While this difference is similar to the difference in protein expression between these conditions, we are using CAII activity as a measure of CAIX activity. This is not totally accurate because the catalytic efficiency of CAII is about twice that of CAIX. Further, there is likely a difference in enzyme behavior in the environment close to the membrane versus in a soluble form.

**Regulation of CAIX Activity by pH**

Several published studies show that CAIX plays a role in regulating intracellular and extracellular pH (*26;50*). However, direct effect of pH on CAIX activity in the membrane environment has not been studied. Therefore, CAIX activity in response to pH was measured in the following experiments (Figure 5-6). To mimic changes of CAIX activity in microenvironment of normal and tumor, we measured CAIX activity at pH 6.8, the pH typical to the tumor microenvironment, pH 7.4 (more typical of normal tissue), and basic pH 7.9 (which probably has little physiological relevance) in normoxic and hypoxic cells. While control cells have low expression of CAIX, they did show sensitivity to pH (Figure 5-6A). The steep slopes of phase 1 were largely unaffected by pH. However, the slopes of phase 2 in the progress curves showed higher exofacial activity (accelerated $^{18}O$ depletion from $^{13}CO_2$) at pH values that resemble the tumor microenvironment (pH 6.8) than either physiological (pH 7.4) or even higher values (pH 7.9). Because the MIMS assay measures the synthesis of $CO_2$, this means that at low pH, CAIX activity favors $CO_2$ production. In hypoxic cells, the effect of pH was exaggerated (Figure 5-6B). Again, phase 1 was essentially unaffected by pH. While hypoxia, itself, increased the rate of $^{18}O$ depletion from $^{13}CO_2$ (phase 2) relative to normoxic cells, this was amplified by reducing pH (Figure 5-6C). The final conclusion is the same as in normoxic cells: low pH increases CAIX activity in the direction of $CO_2$ production.

We further studied this pH sensitivity in membrane ghosts, i.e., hypotonically-treated MDA-MB-231 cells. These membrane ghosts were extensively washed to remove cytosolic CA to eliminate the contribution to CA activity by CAII (Figure 5-6D). Shown in Figure 5-6E is the catalytic efficiency in the hydration versus dehydration reaction. These data confirmed that low pH significantly increases the rate of the dehydration reaction indicating that CAIX prefers to consume protons instead of generates protons at a typical tumor pH.

**Anoxia Activates CAIX**

Svastova *et al.* have suggested that hypoxia not only induces the expression of CAIX, but also activates CAIX through studying cpd5c binding to the CAIX under hypoxic re-oxegenation conditions (*50;60;61*). The MIMS assay traditionally uses buffers or media that is exposed to normal atmospheric oxygen. If hypoxia is required for maximal CAIX activity, then the exposure to oxygen both during the isolation of cells and assay for CA activity might diminish the activity that we observe. To test this, we isolated cells in medium that was flushed with nitrogen and assayed for CA activity in medium that was flushed with helium. In Figure 5-7A, we show that CAIX activity in hypoxic MDA-MB-231 cells was indeed significantly higher in the anoxic environment. However, dose response curves with cpd5c show little difference in inhibitor effectiveness (cpd 5c: Ki = 91.6 ± 35.1 vs 85.3 ± 19.8 nM, anoxic vs normoxic medium) (Figure 5-7B). This is also true for N3500 ( Ki = 13.2 ± 3.6 vs 12.6 ± 3.3 μM anoxic vs normoxic medium). This signifies that the intrinsic activity of CAIX is unchanged, suggesting that other factors have affected fluxes of $CO_2$ species and hence $^{18}O$ exchange in intact cells.

**Effect of Zinc on CAIX Activity in MDA-MB-231 Cells**

The α–carbonic anhydrase family members are zinc metalloenzymes. Zinc is found in the active site of CAIX where it coordinates with 3 histidine residues (as is true for other family members). It has been demonstrated that the catalytic activity of soluble constructs of CAIX is stimulated by low concentrations of zinc (*31*). In this study, the presence of 50 μM $ZnCl_2$ increased the catalytic efficiency of CAIX by 10-fold in fragments of the soluble catalytic domain and by 20-fold in fragments of the catalytic domain with the proteoglycan extension. Zinc also caused a 150-fold increasing in the Ki value of acetazolamide for the soluble catalytic domain with the proteoglycan extension. We sought to determine if this effect was preserved in

intact cells. When MDA-MB-231 cells were added directly to assay medium containing zinc, there was not observed effect on CAIX activity. When cells were pre-incubated with different concentration of zinc at the indicated times (Figures 5-8), zinc concentration less than 300 μM had little effect on CAIX activity (Figure 5-8 A,B). Only at 500 μM zinc (Figure 5-8C) was there a significant on CAIX activity. This insensitivity to zinc may be related to non-specific binding in the intact cell system which lowers the effective concentration seen by CAIX.

**Effect of CAIX Inhibition on Cell Viability, Migration and Invasion**

In this section, we examined the effect of CAIX inhibition on MDA-MB-231 cell viability. The MTT assay was used for this purpose and was described in Chapter 2. Figure 5-9A illustrates that the value of OD570 –OD650 in the range of 0-1.6 reflects cell number, suggesting that the method is reliable for assessing cell viability. MDA-MB-231 cells were seeded in 24-well plates in equal number, followed by inhibitor treatment for 24 hours (Figure 5-9B) or 48 hours (Figure 5-9C) under hypoxic or normoxic conditions. Hypoxia slowed cell growth. Surprisingly, Chlorzolamide was the only CA inhibitor to reduce cell viability. Chlorzolamide is a strong inhibitor for CAIX mimic designed by the McKenna group (*121*). The other three inhibitors, including acetazolamide and N3500, had no effect on cell viablity.

The migration and invasion of MDA-MB-231 cells in response to CAIX inhibitors were also performed across PMVEC monolayers using Transwell plates. Likewise, only chlorzolamide decreased the migration and invasion under hypoxic conditions (Figure 5-10).

**Effects of CAIX Inhibition on Acidification of Extracellular Environment**

The role of CAIX in regulation of pH has been evident in several studies. In MDCK epithelial cells which overexpress the human CAIX protein, the presence of CAIX is associated with a decrease in pHe in response to hypoxia, but not in normoxia (*50*). In this section, we

intended to verify CAIX-dependent regulation of pHe in breast cancer cells. We applied three CA inhibitors to the MDA-MB-231 cells under hypoxia or normoxia. Consistent with data described in Chapter 3, hypoxia led to extracellular acidification as expected. The inhibitors reduced the ability of cells to acidify the medium of hypoxic cells, but not in normoxic cells when incubated for 24 hours (Figure 5-11).

## Conclusions

In this Chapter, we have taken advantage of a unique mass spectrometer technique, specifically developed to measure CA activity, to measured directly the enhanced activity of CAIX in response to hypoxia in MDA-MB-231 breast cancer cells. MDA-MB-231 cells, in our hands, do not express other forms of membrane-bound CAs which allows us to draw a direct correlation between the increase in exofacial CA activity and the induced expression of CAIX. To better estimate the external CA activity assayed by MIMS, we first compared the $^{18}O$ depletion in $CO_2$ in red blood cells and hypoxic MDA-MB-231 cells. Red blood cells have high internal CA, CA II, expression but no external CA expression. Deletion of $^{18}O$ from $CO_2$ in these two types of cells displays different patterns although they both have biphasic features. The biphasic feature of the progress curve in hypoxic cells is not as apparent as in red blood cells. Acetazolamide had no effect on the biphasic feature of progress curve in red blood cells, which demonstrates that acetazolamide does not inhibit intracellular CA activity. However, acetazolamide makes the biphasic nature of progress curve stronger in hypoxic cells, which more closely resembles the progress curve with red blood cells. These results demonstrate that MIMS is able to detect extracellular CA activity in the intact cells and can efficiently distinguish the intracellular and extracellular CA activity. In addition, a pegylated compound, PEGpAMBS (N-3500) (*58*) which is impermeant in red blood cells and an inhibitor of CA (CAII, Ki = 3.4 ± 1 μM), blocks CA activity induced by hypoxia in MDA-MB-231 cells but has limited effect on CA

activity in normoxic MDA-MB-231 cells. We interpret this to mean that N-3500 specifically blocks exofacial CAIX.

Earlier, the Stanbridge group had suggested that CAIX may regulate the levels of protons and bicarbonate in the microenvironment by "sensing" pH (*33*). Our data provide the first evidence to support this hypothesis. At physiological extracellular pH, CAIX activity favors the hydration reaction and thus could potentially contribute to acidification. However, as the pH drops toward 6.8, the dehydration reaction is favored which utilizes protons to produce water and $CO_2$. We found this to be true whether we assayed intact hypoxic MDA-MB-231 cells or membrane ghosts made from hypoxia cells. This also supports earlier studies from the Silverman laboratory showing that CAIX catalysis (the soluble catalytic domain) is more efficient in the reaction that consumes protons at pH 6.8 than at higher values of pH (*30*). These data indicate that at acidic pH, protons are being consuming rather being produced. In the context of the tumor microenvironment, this mean CAIX is responsible for consuming protons at acidic pH which provides a more stabilized environment for the tumor. Thus, our data provide evidence that hypoxia-induced CAIX expression is a mechanism by which a specific pH value may be maintained which is advantageous to cancer cells. Together, these data suggest that CAIX contributes to the development and maintenance of the "set-point" of cancer cells in response to the proton load from intracellular metabolism.

The Supuran group has synthesized a number of sulfonamides that were designed to be impermeant (*56;59;122*). Cpd 5c, the fluorescently labeled sulfonamide also called CAI, seemed to have substantial advantages. It was shown to be a very efficient inhibitor (better than N-3500) and could be used to localize exofacial CAs while blocking activity. Indeed, we have shown that in the short term, Cd5c is impermeant which allowed us to demonstrate specific inhibition of

CAIX in MDA-MB-231 cells. The Ki for Cpd5c obtained with intact MDA-MB-231 cells is about 10 fold higher than the Ki obtained for soluble CAs. This suggests that the environment within the membrane and/or the structure of full length CAIX influences the ability of Cpd5c to bind CAIX.

Hilvo *et al*. showed that 50 μM $ZnCl_2$ increased the catalytic efficiency of the soluble CAIX catalytic domain by an order of magnitude and similarly for the construct expressing both the catalytic domain and the proteoglycan-like domain. While CAIX activity (along with other CAs) requires zinc, zinc-induced activation was unique to CAIX. In our hands, only pre-incubation with a zinc concentration that was 10 times that used by Hilvo *el al.* showed any significant effect on CAIX activity in intact MDA-MB-231 cells. While these data indicate the membrane environment might have an influence over CAIX function, it may also be true that the membrane provides many non-specific binding sites which reduces the effective concentration of free zinc.

Data published by Svastova *et al*. also suggest that hypoxia directly regulates the activity of CAIX. To follow up on this point, we have shown that maintaining an anoxic environment during the preparation and assay of the MDA-MB-231 cells does significantly increase CAIX activity. This suggested that the catalytic pocket was in some way better exposed in the anoxic environment than under normoxic conditions. These data have been supported by Dubois *et al.* who showed that hypoxic HeLa cells, but not briefly re-oxygenated hypoxic HeLa cells, were able to bind Cpd5c (*60;61*). A change in CAIX expression was eliminated as an underlying mechanism as CAIX content was essentially identical in the hypoxic and re-oxygenated cells. However, we were unable to demonstrate any difference in efficacy of CAIX inhibition in hypoxic MDA-MB-231 cells assayed under anoxic versus normoxic conditions by either N-3500

or Cpd5c. Taken together, our data would suggest that the catalytic site is functional in the presence or absence of oxygen.

Recently, CA inhibitors have been proposed as a potential new class of antitumor agents (*53;54*). Some CA inhibitors with a high affinity for the CAIX isoform have been shown to decrease tumor cell proliferation, migration and invasion (*123;124*). However, the only CA inhibitor effective in reducing viability, migration, and invasion in either normoxic or hypoxic cells is chlorzolamide. Frankly, we believe that this inhibitor is killing cells. Thus, in our hands, sulfonamides that only block CAIX activity do not have anti-growth properties.

In summary, we directly measured the activity of endogenous CAIX in cancer cells by MIMS. This is a major contribution to the field because it is the first study to determine kinetic properties of CAIX in the membrane environment of intact cells and membrane ghost. We show that the change in CAIX activity is directly correlated to the increase in protein expression which could be inhibited by an impermeant CA inhibitor which is essentially specific for CAIX. This indicates that not only is CAIX expressed, but CAIX activity at the cell surface is induced by hypoxia. We also show that sulfonamide inhibitors block CAIX activity in cancer cells. The impermeant CA inhibitor, N3500, reduces acidification induced by the hypoxia in MDA-MB-231 cells, suggesting that CAIX is involved in the regulation of pH in MDA-MB-231 cells. CAIX activity is also influenced by the $O_2$ level as we demonstrated that anoxia activates CAIX. CAIX activity is influenced by the pH and low pH substantially increases the dehydration activity. These data are important because it provides direct envidence for the hypothesis that hypoxia-induced CAIX expression senses the pH of microenviroment and maintain a specific pH which is detrimental to normal cells but advantageous to cancer cells. Together this suggests that

CAIX can contribute to the development and maintenance of the “set-point” of cancer cells in response to the proton load from intracellular metabolism.

A

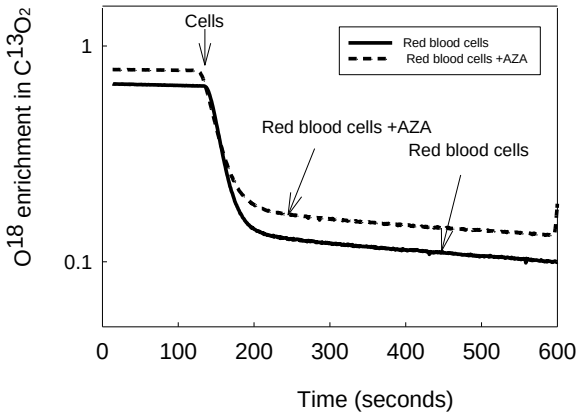


Figure 5-1. Progress curve for atom fraction of $^{18}O$ in CO2 in the suspension of human red blood cells (RBCs at $6.0x10^4$ cells/ml). Human blood was freshly obtained and red cells were washed in isotonic buffer [sodium phosphates (50 mM), sodium chloride (78 mM), and potassium chloride (2.7mM) at pH 7.4. Red blood cells were added to reaction chamber containing 2 mL of buffer in which was dissolved $^{18}O$ enriched $CO_2/HCO_3^-$ at 25 mM total $CO_2$ species. The membrane inlet was immersed in the suspension in this vessel and used to detect the atom fraction of $^{18}O$ in the extracellular $CO_2$ of the membrane-inlet mass spectrometer. A) Progress curve of red blood cells exposed or not to acetazalomide (AZA) in the mixing chamber of the membrane-inlet mass spectrometer. Solid line: RBC alone; short dashes: RBC in the presence of AZA. B) The progress curve for atom fraction of $^{18}O$ in $^{13}CO_2$ in suspensions of human red blood cells to which is added purified human CAII (hCAII). Solid line: RBCs with no extracellular hCA II; long dashes: RBC suspension containing 1.0 nM purified HCA II in the external solution; short dashes: RBC suspension containing 2.0 nM hCA II in the external solution; dotted line: RBC suspension containing 3.0 nM hCA II in the external solution. The suspending solution contained 78 mM NaCl, 50 mM sodium phosphate at pH 7.4 with initial concentrations of all species of $CO_2$ at 25 mM and 25 °C. RBCs were added at time zero. *Inset*: a plot of the catalyzed portion of the slope in the slow second phase (50 to 300 sec) versus the concentration of extracellular hCA II. The MIMS assay was performed by Dr. Chingkuang Tu.

B

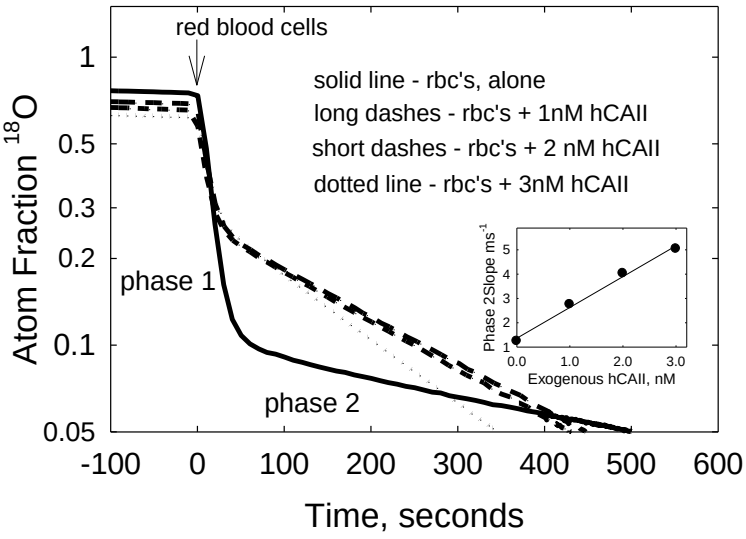


Figure 5-1. Continued.

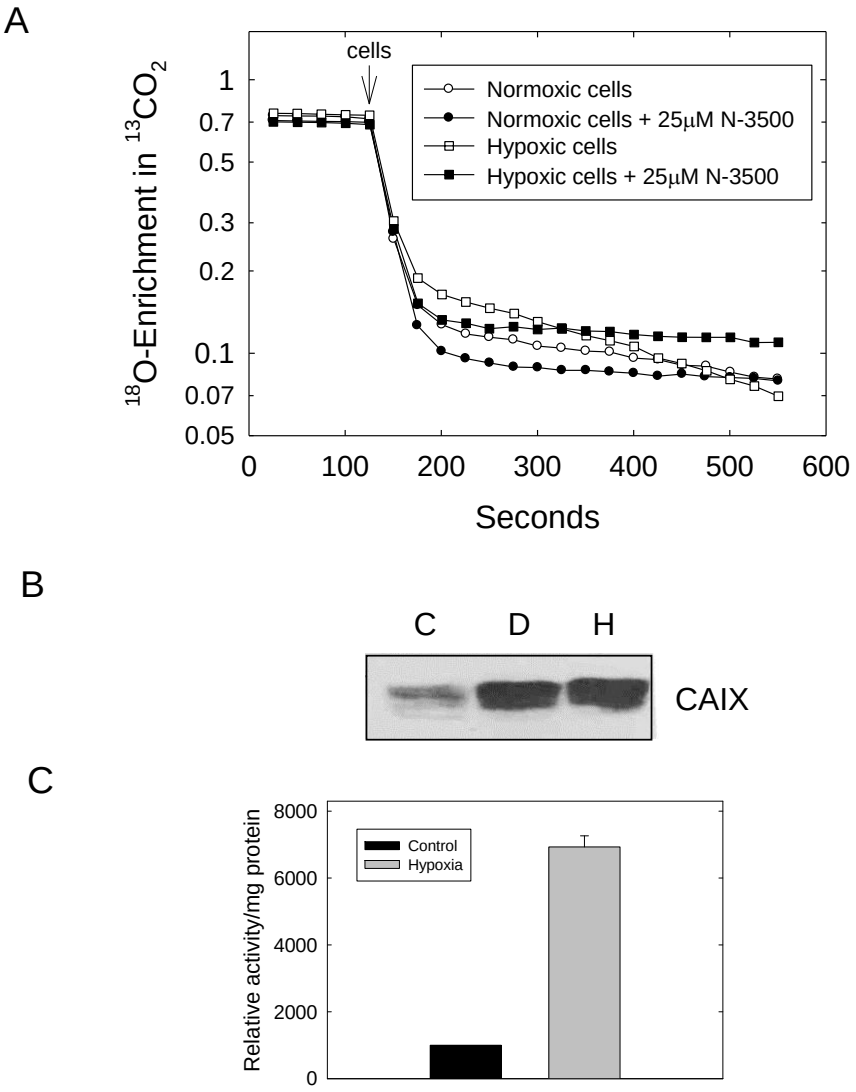


Figure 5-2. Hypoxia increases CAIX activity in plasma membranes and intact MDA-MB-231 cells. A) MDA-MB-231 cells were grown for three days at which point they were exposed to normoxic or hypoxic conditions for 16 hours. Cells were harvested and assayed for carbonic anhydrase activity using the MIMS method in the presence or absence of 25 μM N-3500. Each progress curve was generated using 1 x $10^6$ cells. While data is collected continuously, for ease of representation, only data points at 25 second intervals are shown. Data are representative of at least three independent experiments. B) Total membranes were collected from control cells or cells exposed to DFO or hypoxia for 16 hours. Western blot analysis of CAIX expression was performed using the NB100 antibody. C = Control, D = DFO, H = Hypoxia. C) Plasma membranes was isolated from control or hypoxic cells and CA activity was measured by MIMS. These data represent duplicate experiments. The plasma membrane isolation was performed by Dr. Hai Wang and the MIMS assay was performed by Dr. Chingkuang Tu.

A

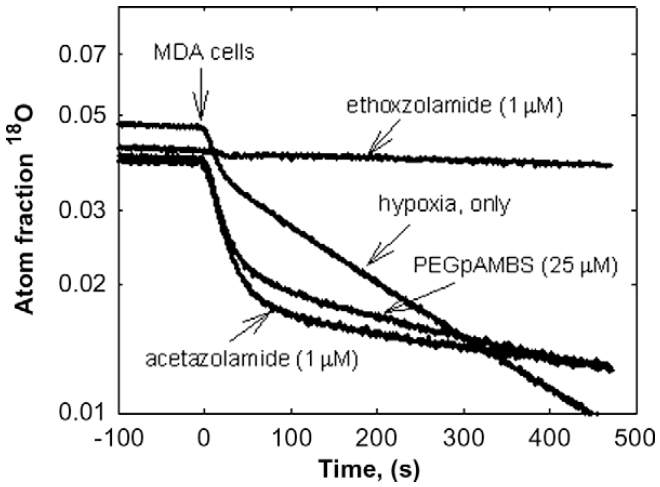


B

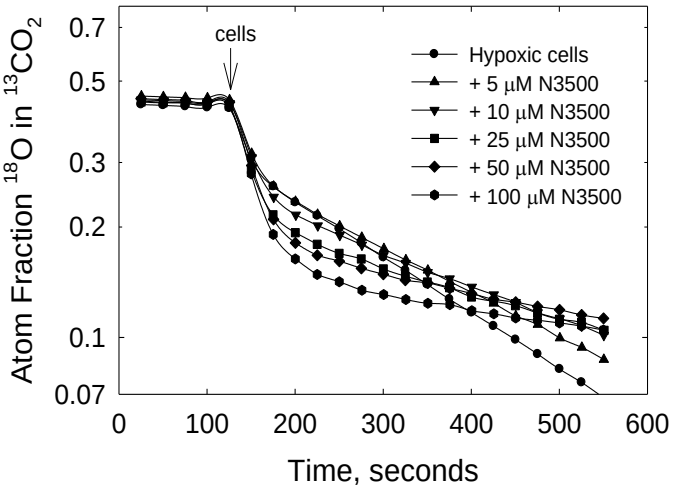


Figure 5-3. Inhibition of CAIX activity by sufonamides. A) MIMS data was collected for suspensions of hypoxic MDA-MB-231 cells (8.3 x $10^5$ cells/ml) to which were added inhibitors of carbonic anhydrase. B) CA activity was monitored by MIMS in the absence or presence of N3500 at the indicated concentrations. C) Phase 2 slopes for data in panel B are plotted against N3500 concentration to determine Ki. Other conditions were same as described in Figure 5-1. MDA-MB-231 cells were added at as indicated by the arrow. The MIMS assay was performed by Dr. Chingkuang Tu.

C

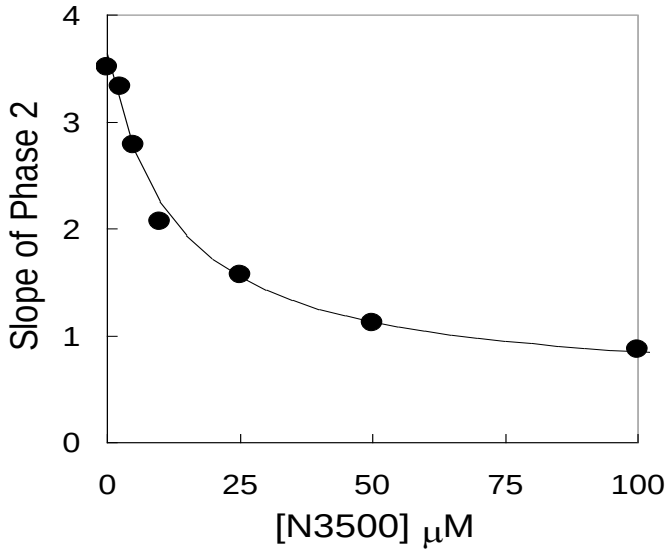


Figure 5-3. Continued.

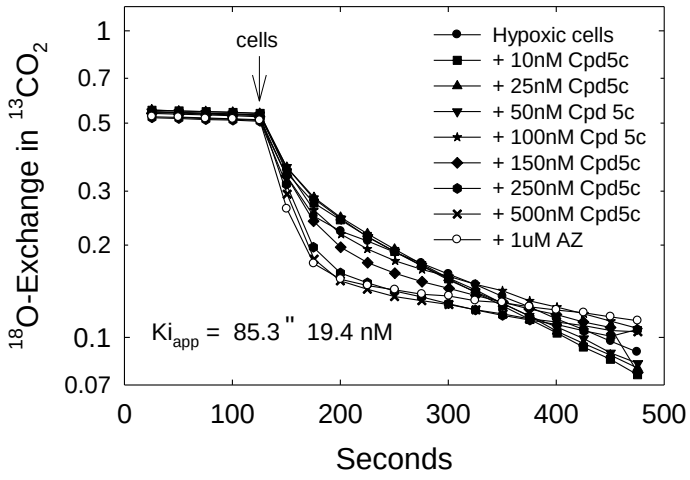


Figure 5-4. CA activity is inhibited by Cpd 5c in hypoxic MDA-MB-231 cells. Carbonic anhydrase activity was analyzed in hypoxic MDA-MB-231 cells in the presence of Cpd 5c at indicated concentration or in the presence of 1μM acetazolamide. The apparent Ki for cpd5c was 85.3 nM. The MIMS assay was performed by Dr. Chingkuang Tu who also calculated the Ki.

A

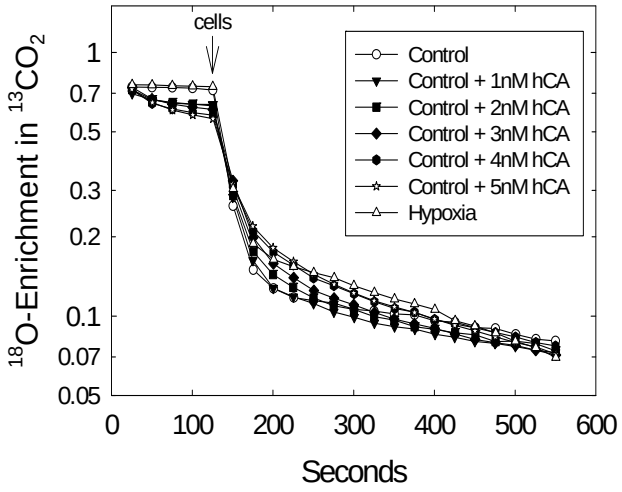


B

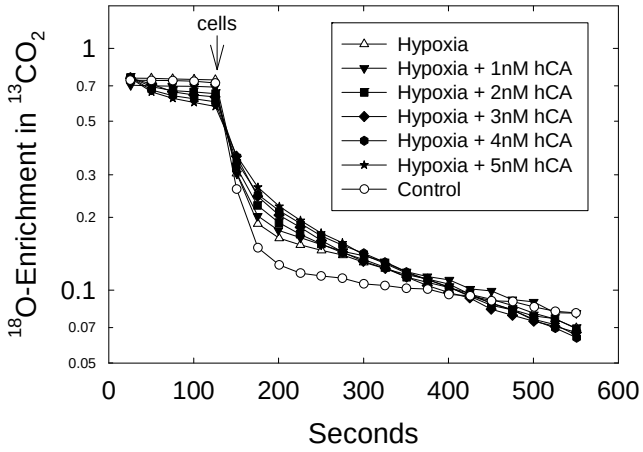


Figure 5-5. Estimation of CAIX activity in MDA-MB-231 cells by addition of hCAII. A) A progress curve for the atom fraction of $^{18}O$ in $CO_2$ in a suspension of normoxic cells was generated by the MIMS assay in the presence of increasing concentrations of hCAII. B) The enrichment of $^{18}O$ in $CO_2$ in suspensions of hypoxic cells was measured using the MIMS assay in the presence of increasing concentrations of hCAII. C) Phase 2 slopes (x $10^{-3}$ s-1) are plotted against hCAII concentrations for data from panels A and B. D) Slopes of phase 2 versus the adjusted concentration of extracellular hCAII were calculated for normoxic and hypoxic MDA-MB-231 cells. The MIMS assay was performed by Dr. Chingkuang Tu.

C

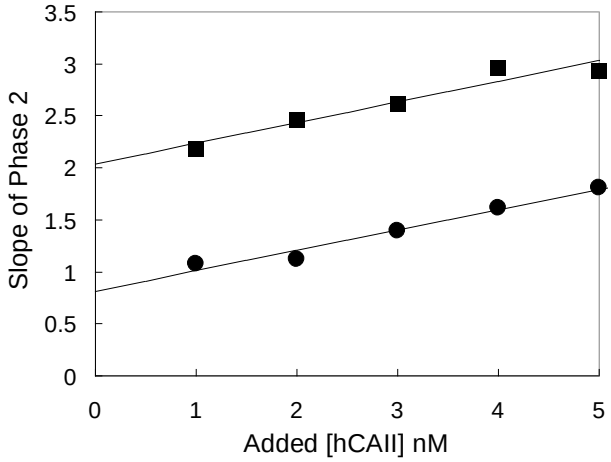


D

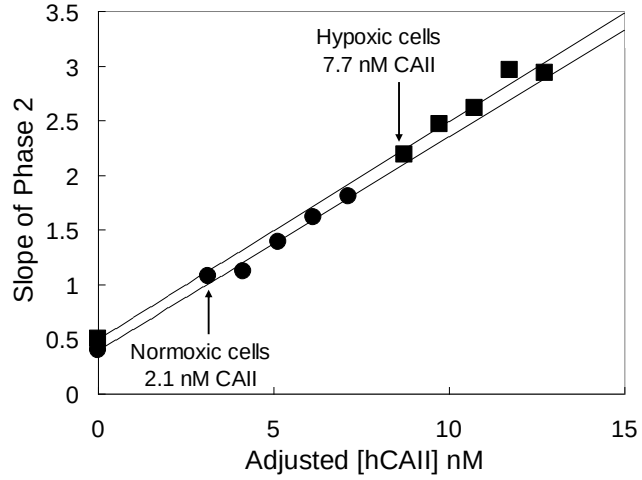


Figure 5-5. Continued.

A

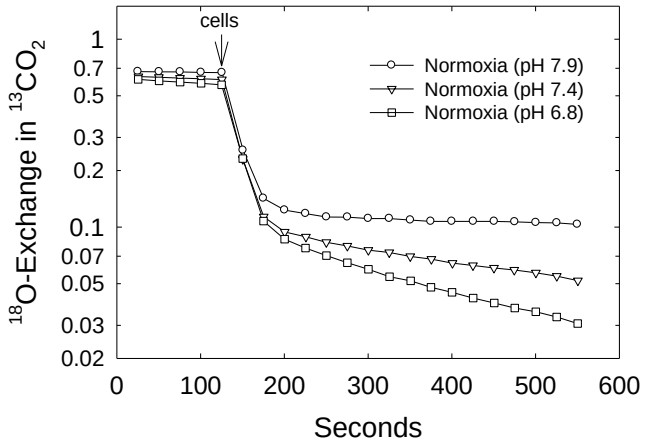


B

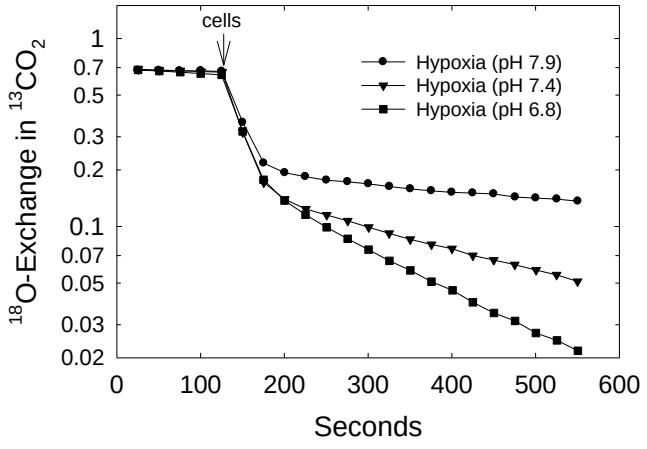


Figure 5-6. Extracellular pH influences CAIX activity. A) Normoxic MDA-MB-231 cells were assayed for CA activity at pH 6.8, 7.4, and 7.9. B) Hypoxic MDA-MB-231 cells were assayed for CA activity at pH 6.8, 7.4, and 7.9. C) Comparision of CA activity at pH 6.8 and pH 7.9. D) Membrane ghosts were analyzed by SDS-PAGE and western blotting to determine CAIX and CAII expression. C = cytosol; S = $Na_2CO_3$ (50 mM, pH 11.5)-washed membrane ghosts, P = PBS-washed membrane ghosts. E) Membrane ghosts were prepared from hypoxic MDA-MB-231 cells. Catalytic efficiency of membrane ghost was determined in both the hydration and dehydration directions of catalysis. The MIMS assay was performed by Dr. Chingkuang Tu. Dr. David Silverman performed the modeling to separate the hydration and dehydration reactions.

C

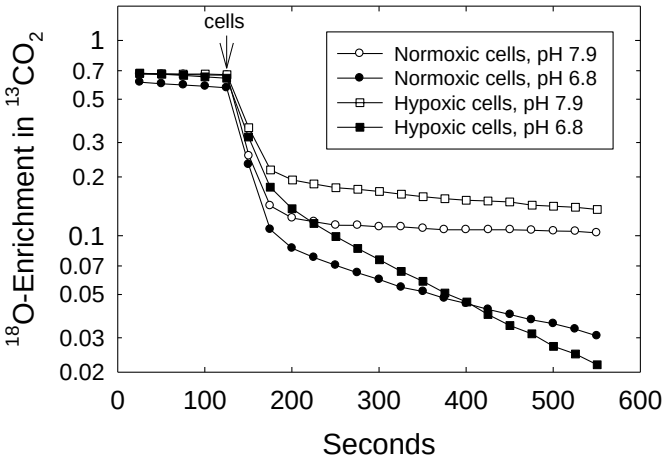


D

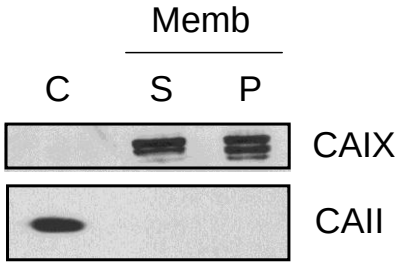


E

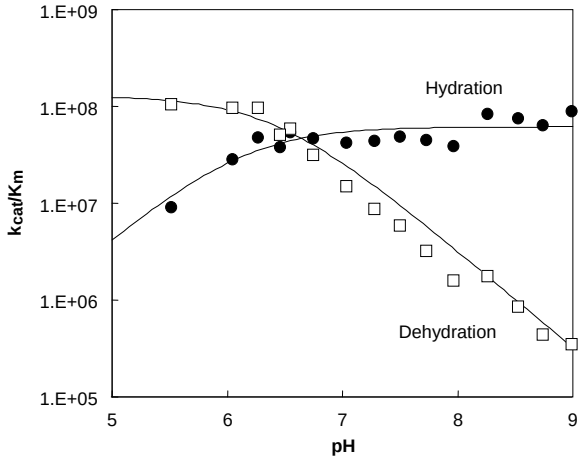


Figure 5-6. Continued.

A

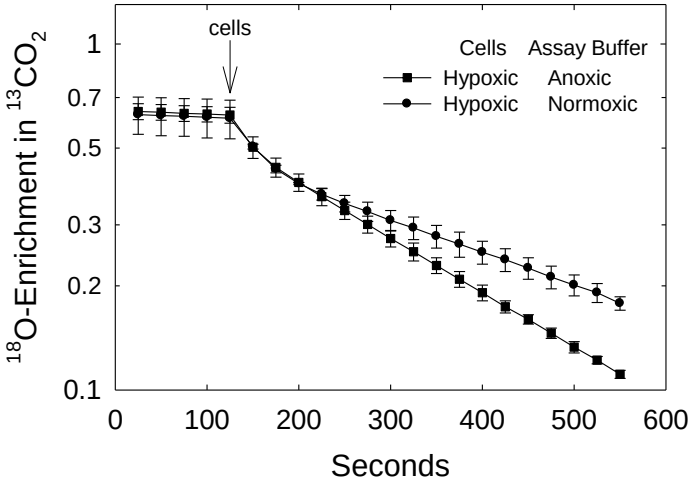


B

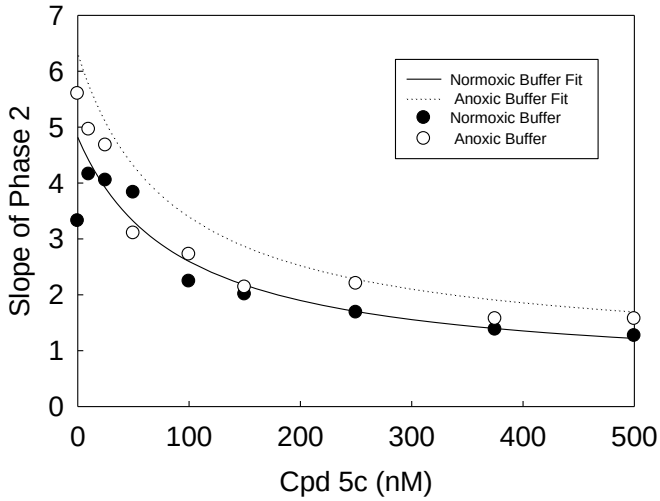


Figure 5-7. *In vitro* anoxic conditions increase CAIX activity without altering inhibitor sensitivity. A) Hypoxic MDA-MB-231 cells were prepared and assayed in normoxic or anoxic buffer. Data are the average ± SD of three independent experiments. B) Phase 2 slopes for progress cuves in the absence or presence of cpd 5c are plotted against cpd 5c concentration to determine Ki in normoxic or anoxic buffer. The MIMS assay was performed by Dr. Chingkuang Tu.

A

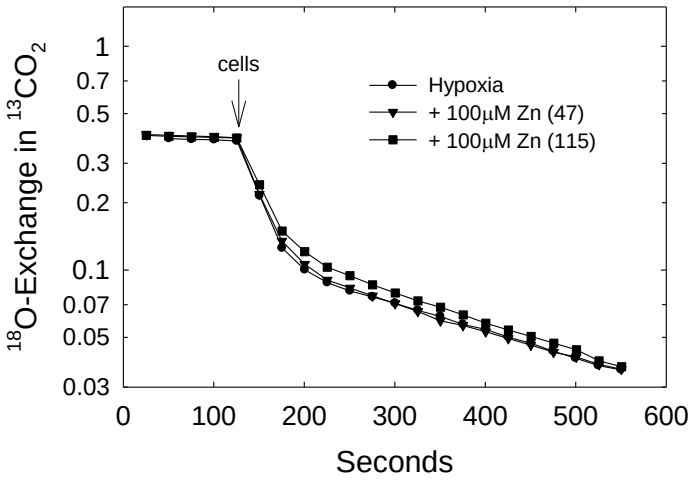


B

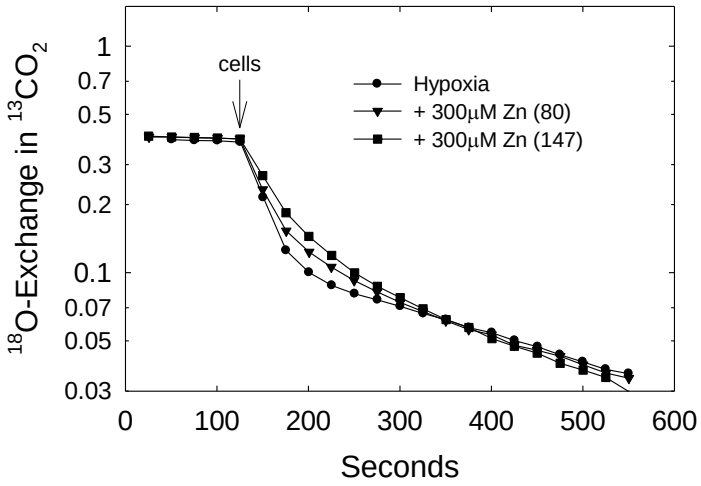


Figure 5-8. Effect of Zinc on CAIX activity in intact MDA-MB-231 cells. Hypoxic MDA-MB-231 cells were incubated with specific concentrations of zinc for the times indicated in parentheses. CA activity was then measured using the MIMS assay. A) Cells were preincubated with 100 μM zinc. B) Cells were pre-incubated with 300 μM zinc. C) Cells were pre-incubated with 500 μM zinc. The MIMS assays were performed by Dr. Chingkuang Tu.

C

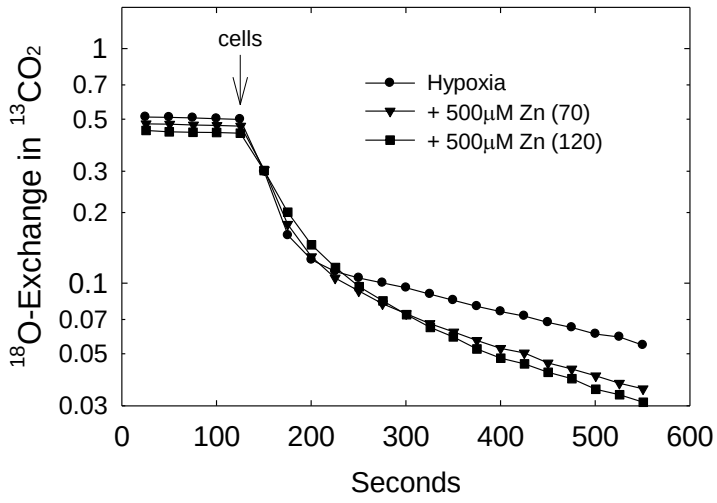


Figure 5-8. Continued.

A

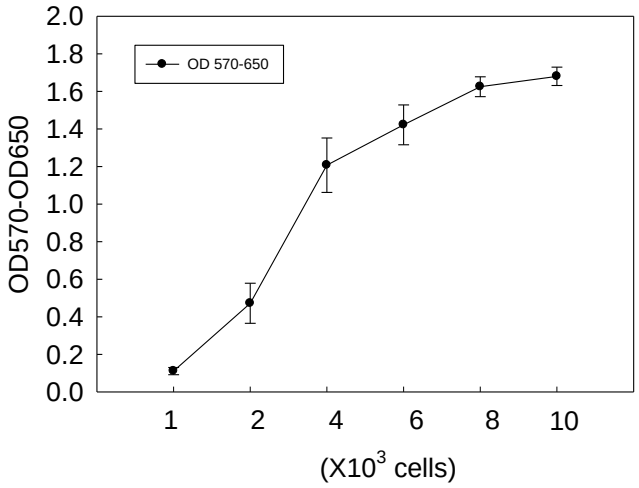


B

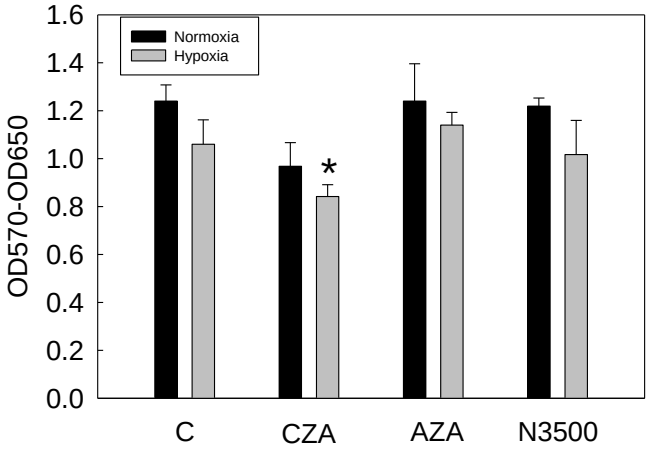


Figure 5-9. Effect of CA inhibitors on cell growth and viability in MDA-MB-231 cells. A) MDA-MB-231 cells were seeded in each well at the indicated density in 24 well plates. Cells were incubated in 37°C for 24 hours to allow the cells to attach to the wells. Fifty μL of the MTT reagent (5 mg/ml) was added to each well and incubated in $CO_2$ incubator held at 5% $CO_2$ at 37°C for 2 hours. Optical density was read at 570 nm from which the background OD at 650 nm was subtracted. B) MDA-MB-231 cells were seeded in 24 well at density of 2,000 /per well in 24 well plates. Cells were incubated in 37°C for 24 hours to allow the cells to attach to the wells. Then medium was replaced with 500 μL of the medium containing 100 μM of CA inhibitors: acetazolamide, chlorzolamide, and N3500. Cells were either incubated under normoxic (5% $CO_2$, 20% $O_2$) or hypoxic (1% $O_2$) conditions for 24 hours (B) or 48 hours (C). Data represent the mean ± S.D. of 3 independent experiments, each of which evaluated duplicate samples. (* $P < 0.05$, vs normoxic control or hypoxic control).

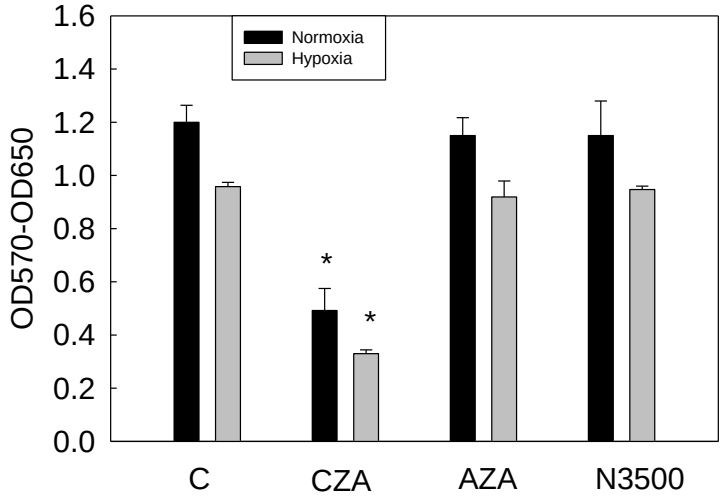


Figure 5-9. Continued.

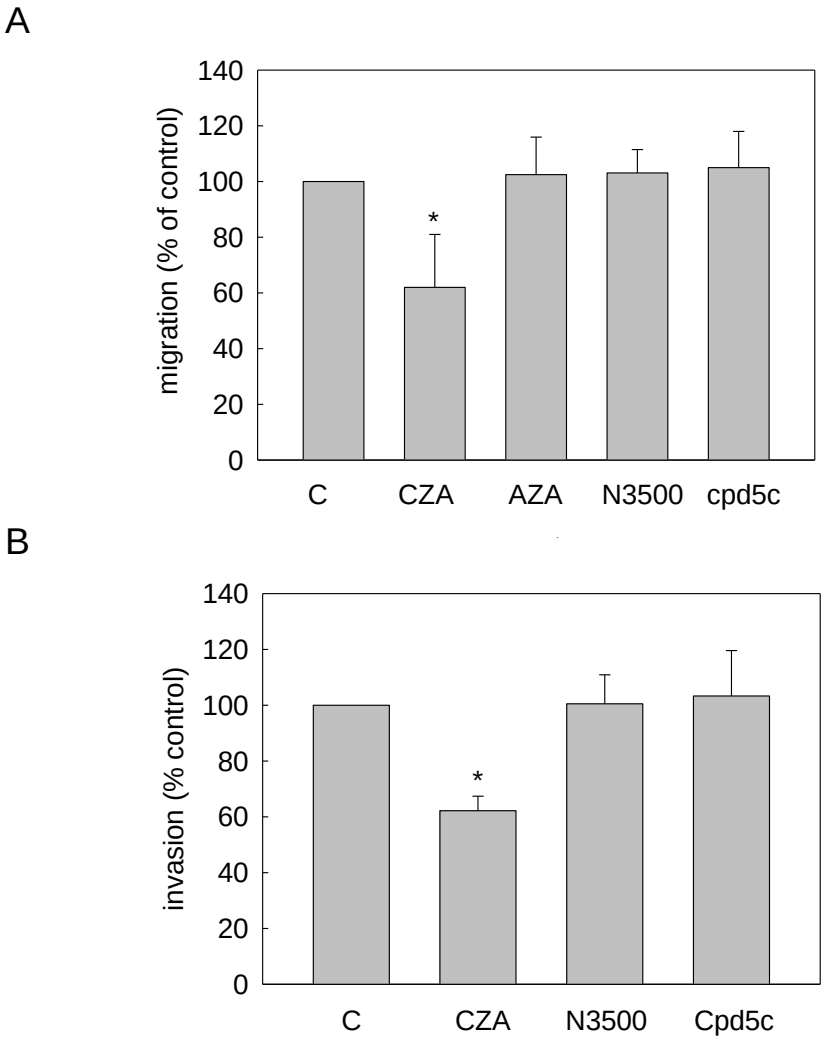


Figure 5-10. Effect of CA inhibitors on the cell migration and invasion in MDA-MB-231 cells. A) MDA-MB-231 cells (1 x $10^5$) in FBS-free DMEM containing 100 μM CA inhibitor was plated onto Millipore 12 μm cell culture inserts. DMEM containing 10% FBS was placed in the lower chamber. Cells were exposed to hypoxia for 24 hours. Migration was measured after 24 hours using MTT staining. B) Cell culture inserts were first covered with Matrigel and overlayed with $1\times10^5$ cells in FBS-free DMEM containing 100 μM CA inhibitors. Cells were then exposed to hypoxia for 24 hours. Migration was measured after 24h using MTT staining. The experiments were repeated twice, each in duplicate. Data represented mean ± S.D. with that of control being 100%. (* $P < 0.05$ vs control).

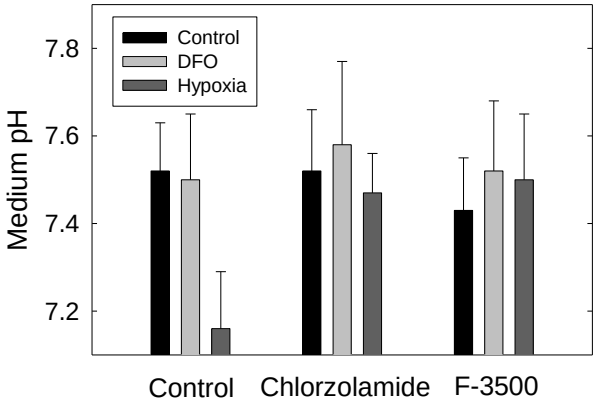


Figure 5-11. Effect of CA inhibitors on medium pH in MDA-MB-231 cells. MDA-MB-231 cells were cultured in 35 mm plates. At 75% confluence, CA inhibitors were added to the medium at a final concentration 100 μM. Cells were then exposed to DFO or hypoxia for 24 hours. Medium pH was measured immediately after removing the plates from the incubator with a portable pH meter. Data represent the mean ± S.D. of 3 independent experiments where each experimental point was conducted in triplicate.

# CHAPTER 6
# THE PHYSICAL AND FUNCTIONAL COUPLING OF CAIX AND BICARBONATE TRANSPORTER

## Introduction

Bicarbonate transporters are widely expressed and involved in the regulation of intracellular pH, cell volume, and transepithelial acid/base and $Cl^-$ secretion (*63;65*). The anion exchange (AE) family of proteins is comprised of AE1, AE2, and AE3. AE1 is expressed abundantly in erythrocytes and a trucated form is also present in the kidney and heart. AE1 transports anions over a broad pH range (pH 5-11) (*125*). AE2 is almost ubiquitous and is most abundant in the stomach. AE2 is thought to be responsible for basolateral uptake of $Cl^-$ in parietal cells destined for HCl secretion and the extrusion of $HCO_3^-$ generated for intracellular acid secretion AE2, on the other hand, is negatively regulated by acidic pH, consistent with its role in cellular acidification (*126*). In HEK 293 cells, AE2 was active at pH 7.3 and activity was reduced to 37% of maximum at pH 6.0. AE3 expression is restricted to the brain, heart, and retina. Its activity is insensitive to change of intracellular pH (*125*).

Gastric parietal cells are one cell type where there is a functional link between CAs and bicarbonate transport proteins in faciliating transepithelial bicarbonate transort, in some cases through direct interaction. Several lines of evidence have demonstrated an interaction between cytosolic CAII and AE1, AE2, and AE3. Bicarbonate transport proteins are closely associated with CA and together they eliminate metabolic waste, $CO_2$, from the body. For example, CAII has been shown not only to bind to the AE family of $Cl^-$/ $HCO_3^-$ anion exchang proteins, but also to potentiate their transport activity by formation of a transport metabolon (*62;68;127*). A metabolon is a complex of interacting proteins involved in a metabolic pathway. Formation of a metabolon allows metabolites to move rapidly from one active site to the next. Association of CAII with AE localizes $HCO_3^-$ to the transport site accelerating bicarbonate flux. The basic N-

terminal region of CAII has been shown to interact with the acidic LDADD motif of AE1 and increase CAII activity upon its interaction with the binding site on AE (*62*). In addition, it has been demonstrated that CAIV, which is anchored to the extracellular surface, interacts with extracellular loop four of AE1 (*68*). Localization of CAs immediately adjacent to a bicarbonate transporter in the metablon may maximize the transmembrane bicarbonate concentration gradient in the immediate locale of the transport polypeptide thus increasing the bicarbonate transport rate. A recent study provides evidence that another membrane CA, CAIX, when coexpressed with different AE family members in HEK 293 cells, increased AE2 transport activity, and also activated the transport mediated by AE1 and AE3. Under these circumstances, CAIX is coimmunoprecipitated with the coexpressed AE. GST pull-down assay with a series of domain deletions of CAIX revealed that catalytic domain mediates the interaction with AE2 (*128*).

However, evidence against direct interaction of CAII and C-terminal domain of bicarbonate transporters has recently been presented (*129*). In this study, investigators examined the interaction of CAII and a C-terminal domain of AE1. When expressed as GST fusion proteins, GST-AE1 C-terminal domain binds to CAII better than does pure GST. However, the pure AE peptides do not bind to GST-CAII. Moreover, the investigators were not able to detect binding of CAII to the immobilized pure AE1 C-terminal domain. Also, they found that more CAII binds to GST than to GST-AE fusion proteins. Importantly, using surface plasmon resonance, they detected no binding of CAII to immobilized AE1 C-terminal or vice versa. In an earlier study, Lu *et al.* argued that it was unlikely that the catalytic activity of CAII would substantially enhance the activity of an $HCO_3^-$ transporter (*130*). Because of these contradictory data, our question was to ask whether CAIX and/or CAII interact with one of the AE transporters under physiological conditions creating a metabolon? Thus, in this chapter we

attempt to investigate whether CAIX and/or CAII physically and functionally interacted with AE to influence bicarbonate transport, further influenced by the intracellular pH in hypoxic MDA-MB-231 cells. Which AE isoform is expressed in breast tumors even in breast cancer cells is unknown. So we first attempted the detection of individual AE family members in MDA-MB-231 cells. Next, we investigated the possibility for physical and functional interactions between AE and CAIX.

## Results

### Expression of AE in MDA-MB-231 cells

While we have shown that hypoxia stimulates the expression of CAIX in MDA-MB-231 cells and that CAII has high expression in this cell line, the endogenous expression of AE in breast cancer cells has not yet been reported. Thus, we first sought to identify the expression pattern of AE family members, AE1, AE2 and AE3 in MDA-MB-231 cells at the mRNA and protein level. Detecting AE expression in MDA-MB-231 cells is obviously a prerequisite for detecting interactions between AE, CAIX, and CAII.

Using semiquatitative RT-PCR, the expression of the three AE family members in MDA-MB-231 cells was examined (data not shown). AE1 was not expressed, whereas AE2 was constitutively expressed and not affected by exposure to DFO or hypoxia. On the other hand, AE3 expression was induced by both DFO and hypoxia. To verify these data at the protein level, AE2 expression was evaluated by Western blotting using an AE2 specific antibody recognizing the N-terminal region. Consistent with RT-PCR data, AE2 was present in MDA-MB-231 cells, and unaffected by DFO or hypoxia (Figure 6-1). AE3 expression was examined using the commercially available antibody against AE2 which was raised against a rat AE3 peptide. We hoped that the 95% sequence similarity between the rat and human AE3 peptide would be sufficient for detection of AE3 in MDA-MB-231 cells. However, AE3 protein expression was

not detected in MDA-MB-231 cells. While AE3 may be the most interesting of the AE family members because of its hypoxic regulation, we pursued the interaction of AE2 and CAIX for lack of a suitable AE3 antibody.

**Detection of Physical Interaction of AE2 and CAIX**

To investigate the physical interaction between AE2 and CAIX, immunoprecipitation of CAIX using a CAIX-specific antibody was performed. MDA-MB-231 cells were exposed to hypoxia for 16 hours to induce CAIX expression. Extracts of cells were prepared using RIPA buffer and IPB buffer containing 1% detergent Igapel. The M75, CAIX antibody was used for immunoprecipitation. Immuno-complexes were collected and then run on the 10% SDS-PAGE gels. The proteins were transferred to nitrocellulose membranes and probed for CAIX by the rabbit polyclonal CAIX antibody NB100. Figure 6-2 shows that we were able to detect CAIX but not AE2 in the immuno-complex. While these data would suggest that CAIX is not interacting with AE2 under our experimental conditions, little AE2 detected in the lysates. Thus, it is possible that the AE2 antibody was not of sufficient titer to detect AE2 in the cell lysates resulting in the negative result.

AE2 and CAIX are both membrane proteins and AE2 expression was detectable in a total membrane fraction from MDA-MB-231 cells (Figure 6-1). To enrich for AE2, total membrane extracts were used for imunoprecipitation experiments. Total membrane were extracted in the buffer containg detergent 1% Igepal and immunocomplexes were washed with a series of wash buffers which contained reduced amount of detergent Igepal, making the washing process a more gentle process than that with the lysis buffer alone. AE2 was detected in the total membrane extracts but not in immunocomplexes with CAIX. Interestingly, a small amount of CAII was associated with total membrane extracts in both control and hypoxic MDA-MB-231 cells. However, there was no CAII associated with CAIX (Figure 6-3A). To confirm this result,

AE2 was immunoprecipated using AE2 antibody from membrane extracts. The AE2 antibody was able to pull down AE2. However, there was no CAIX found in AE2 antibody immunoprecipitates, confirming the lack of interaction between CAIX and AE2 (Figure 6-3B). Again, these data provide evidence that CAIX does not form a stable complex with either AE2 or CAII under our experimental conditions. This suggests that there is no physical interaction between CAIX, CAII with AE2 in hypoxic MDA-MB-231 cells.

While our data suggest that AE2 does not interact with CAIX, it is possibile that the interaction is transient and thus difficult to detect. To capture or freeze these momentary contacts, we used cross-linking reagents to create covalent bonds between proteins that are in close proximity. The rapid reactivity of the common functional groups in crosslinkers allow even transient interactions to be "frozen" in place or weakly interacting molecule to be seized in a complex stable enough for isolation and characterization. We chose a membrane permeant crosslinker, dithiobis (succinimidyl propionate) (DSP), which allows conjugation of both intracellular and intramembrane interactions. The spacer arm for DSP is 12.0 Å (8 atoms). After crosslinking the protein, immunoprecipitation of CAIX using the M75 antibody was performed. AE2 was not detected in the crosslinked complex (Figure 6-4A). While CAIX monomer disappeared after crosslinking, crosslinked structure differed from CAIX dimer which suggests that an unidentified protein may interact with CAIX (Figure 6-4B).

**Detection of Functional Interactions of AEs and CAs**

The preceding experiments show that there is no physical interaction between AE2 and CAIX. Thus, we sought to determine if there was a functional interaction between these two proteins. That is, we thought that by inhibiting the function of one of the presumed partners, we might affect the function of the other. In Chapter 5, we demonstrated that $^{18}O$ exchange technique allowed us to evaluate CAIX activity in MDA-MB-231 cells. To take advantage of

this technique, we utilized the anion exchange inhibitors, SITs (4-acetamido-4'-isothiocyanostilbene-2, 2'-disulfonic acid) and DIDs (4, 4'-diisothiocyanostilbene-2, 2'-disulfonic acid) to block AE activity. Our goal was to compare CAIX activity in the presence or absence of these inhibitors. In the red blood cell system, the IC50 of DIDs for AE1 is between 80 nM and 2 μM. For overexpressed AE2 and AE3, the IC50's of DIDs varies (142 μM and 430 μM, respectively) perhaps indicating structural differences in the ectodomains of AE2 and AE3. The IC50 values for SITs range from 20 μM–80 μM. Most investigators use 500 μM for SITs and 100 μM for DIDs. Using MIMS assay, CA activity was measured in the presence or absence of DIDs or SITs in MDA-MB-231 cells (Figure 6-5). Figure 6-5A shows that SITs at 100 μM inhibited CAIX activity as observed by a decrease in the phase 2 slope of the progress curve when compared to the absence of SITs. This was also true for DIDs at 1 mM (Figure 6-5B), while 100 μM DIDs increased slope of phase 2 (data not shown). AE inhibitors had no effect on the phase 2 progress curves in the presence of acetazolamide, which blocks exofacial CA during the time frame of the experiment (Figure 6-5). To distinguish between inhibitory effects of AE inhibitors on AE transporters versus CAIX, Dr. Chingkuang Tu tested the effect of SITs and DIDs on the activity of purified hCAII activity using MIMS. Figure 6-6 shows a plot of CAII activity relative to the concentration of DIDs or SITs. With increasing of concentration of DIDs, CAII activity was reduced. The Ki value of DIDs for purified CAII was 180 μM (Figure 6-6A). A similar value was determined for SITS (Ki = 160 μM) (Figure 6-6B). By inference, this suggests that AE inhibitors have a direct effect on CAIX activity at elevated concentrations.

To reduce the possibility of direct inhibition of CAIX activity, we repeated the above experiment at concentrations of SITs and DIDs (50 μM) at which only 20% of purified CAII activity is blocked. Under these conditions, neither DIDs, SITs, nor DNDs (4, 4'-dinitrostilbene-

2, 2'-disulfonfonic acid) had an effect on CAIX activity (Figure 6-7). These results indicate that AE inhibitors, at high concentrations, directly inhibit CAIX activity, while at low concentrations they have no effect on CAIX activity. This suggests that the AE bicarbonate transporters play only a small role in $CO_2$ transport in hypoxic MDA-MB-231 cells.

## Conclusions

In this chapter, we investigated the physical and functional interaction between CAIX, CAII and the bicarbonate transporters in MDA-MB-231 cells. Several studies have reported that the C-terminal domain of AEs may directly associate with carbonic anhydrases. In a recent study using overexpression of AE and CAIX in HEK 293 cells, it was shown that CAIX interacted with AEs suggesting that these two partners functionally and physically interact with each other (*69*). We were interested in the interaction of these partners under physiological conditions. Thus, we used hypoxic MDA-MB-231 cells as our model to study the interaction of AEs and CAIX, as we have demonstrated that CAIX is induced by hypoxia in these cells. Because it is unclear which AE isoforms are expressed in MDA-MB-231 cells, we first determined the expression pattern of AE1, AE2, and AE3 in these cells. Immunoblotting and RT-PCR showed that AE2 was expressed in MDA-MB-231 cells, but did not respond to hypoxia. RT-PCR showed that AE1 was not expressed in MDA-MB-231 cells. AE3 showed hypoxia-dependent expression by RT-PCR, but no suitable antibody was available to assess protein expression. Therefore, we focused on the interaction of AE2 and CAIX. Yet, immunoprecipitation using antibodies against either CAIX or AE2 were unsuccessful at pulling down their potential partner. Thus, we were unable to detect a physical interaction between AE2 and CAIX. In addition, interaction was not observed even after proteins in the presumed complex were chemically cross-linked. Given that CAIX-AE2 interaction might be sensitive to the detergent in RIPA buffer, we used different detergents in the immunoprecipitation assay,

such as NP40 or Igapel. However, with neither detergent did we detect any interaction between CAIX and AE2. We can not rule out the possibility, however, that interactions between AE2 and CAIX were not detected because of low efficiency (titer) of the AE2 antibody.

In the absence of a physical interaction, it is possible that there is a functional relationship between CAIX and AE2. The MIMS assay, however, provided evidence that bicarbonate transporters play only a small role in CAIX function. Also revealed by our studies is the direct inhibition of CAII (and presumably CAIX) by bicarbonate transport inhibitors. Some sulfonamide CA inhibitors also inhibit $Cl^-/HCO_3^-$ exchange. Interestingly, in a study of 26 sulfonomide CA inhibitors, acetazolamide is the only sulfonamide that did not inhibit $Cl^-/HCO3^-$ exchange directly (*131*). Therefore, acetazolamide is particularly useful in the $^{18}O$ exchange assay as used in this and previous Chapters (the impermeant sulfonamides have not been tested). While 1 mM DIDs partially inhibited CAIX activity, acetazolamide proved to be a very effective inhibitor with complete inhibition of CAIX with 0.5 μM acetozolamide which is consistent with our early studies (Figure 5-3A). In the presence of acetazolamide, DIDs did not alter the phase 2 progress curves. Similar phenomena were observed in CA activity assay by SITs. SITs at 0.1 mM, partially block CAIX activity. There are two interpretations for these data. DIDs and SITs affect CAIX activity through inhibition of bicarbonate transport across the cell membrane. If this is true, these data will prove that our hypothesis that CAIX and AE functionally interact with each other. It is also possible that DIDs and SITs directly bind to CAs and inhibit its activity. To test this possibility, purified CAII was used in the $^{18}O$ exchange assay since the catalytic domain is conserved in CA family members and Kcat/Km of CAIX is very close to that of CAII as was described in Chapter 1. Our results show that purifed CAII activity is inhibited by DIDs and SITs with Ki 160 μM and 180 μM, respectively. Inhibitors of bicarbonate transporter, such

as DIDs and SITs also inhibit CAII activity directly. We presume that AEs inhibitors also inhibit CAIX activity. Thus it is not feasible to use these inhibitors at high concentration to assess CAIX function. At low concentrations of the AE inhibitors, there was essentially no effect on either intracellular or extracellular CA

In this chapter, we have examined the physical and functional relationship between CAIX, and AE2 in the breast cancer cells under conditions in which both proteins are endogenously expressed/induced. In other words, we have studied these proteins in a physiologically relevant manner. On the basis of our results, we conclude that there is no physical interaction that occurs between CAIX and AE2 in hypoxic MDA-MB-231 cells. It would not be unusual for only a small pool of either CAIX or AE2 to interact. Thus, we can not exclude the possibility that the AE2 antibody has a sufficient titer to AE2 under conditions where a limited number of interactions are likely. DIDs and SITs can not be used in the detection of the functional interaction of CAs and AE2 due to direct inhibition of CA activity. This result might represent an interesting topic for further study.

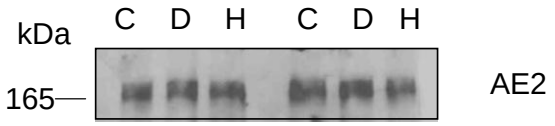


Figure 6-1 Expression of AE2 in response to hypoxia in MDA-MB-231 cells. MDA-MB-231 cells were exposed to 100 μM DFO or to 1% oxygen for 16 hours. Total membranes were isolated and proteins (100 μg) were separated by SDS-PAGE. Shown is a western blot using an antibody specific for human AE2. These represent two separate (but identical) experiments. C = control; D = DFO; H= hypoxia.

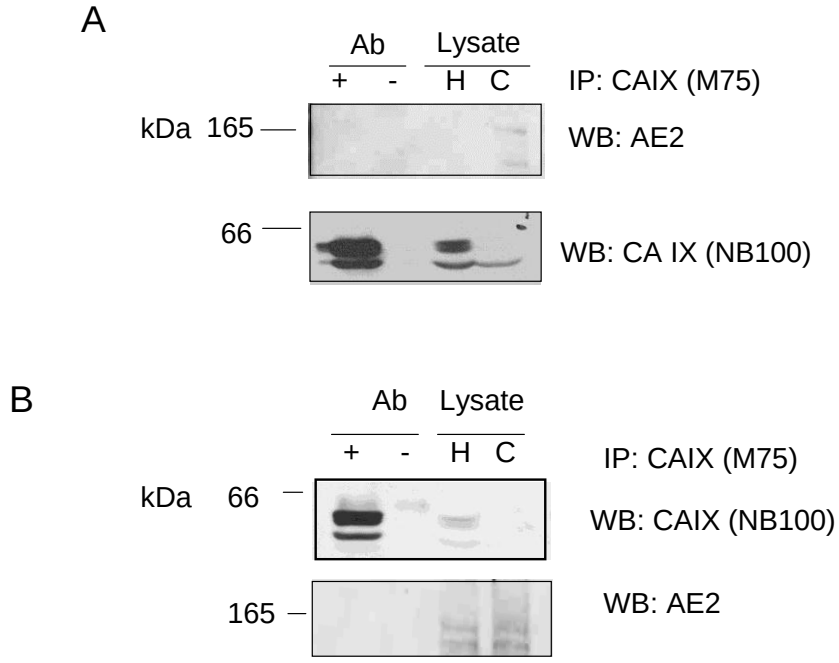


Figure 6-2. Detection of interactions between AE2 and CAIX by co-immunoprecipitation. MDA-MB-231 cells were exposed to hypoxia for 16 hours. Cells were lysed by either RIPA buffer (A) or IPB buffer (B). Cell lysates were immunoprecipitated (IP) with anti-CAIX (M75), resolved by SDS/PAGE, blotted and probed with anti-AE2 antibodies. Samples of the lysate (Input Lysate) from control or hypoxic cells were probed to show the relative amount of CAIX and AE2 in each sample. The amount of material loaded from lysate samples is 10% that for the immunoprecipitated samples.

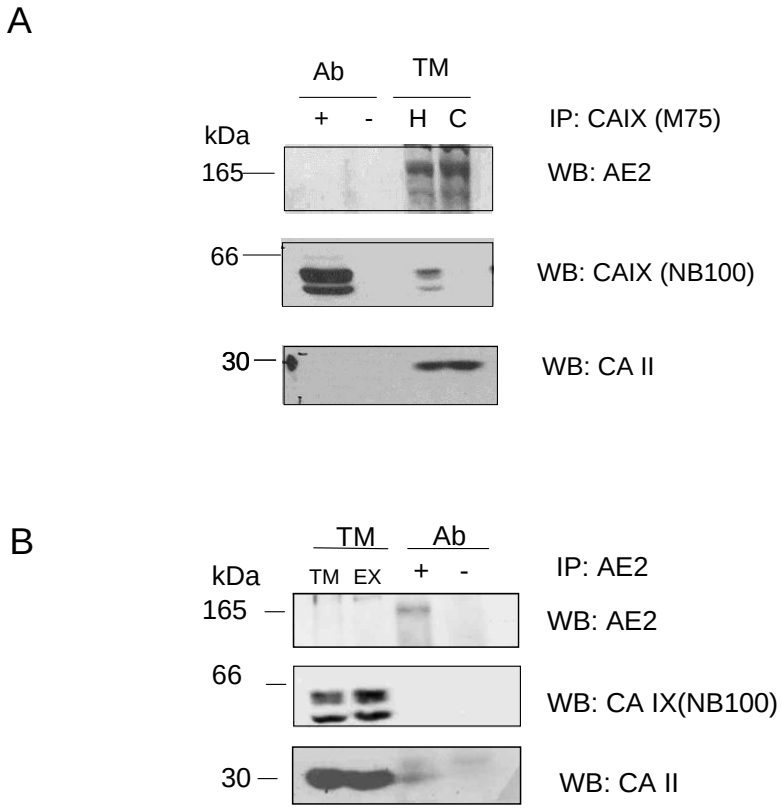


Figure 6-3. Detection of interaction between AE2 and CAIX from membrane lysates by co-immunoprecipitation. MDA-MB-231 cells were exposed to hypoxia or not for 16 hours. Total membranes were isolated from cells and lysed by IPB buffer. A) Membrane lysates were immunoprecipitated (IP) with anti-CAIX (M75), resolved by SDS/PAGE, blotted and probed with an anti-AE antibody and anti-CAII antibodies. Total membrane from control or hypoxic cells were probed to indicate the relative amount of input CAIX, AE2 and CAII in each sample. B) Membrane extracts were immunoprecipitated with anti-AE2 antibody and probed for CAIX and CAII by Western blotting. Membrane lysate (EX) and total membrane (TM) from hypoxic cells were probed to indicate the relative amount of AE2, CAIX, and CAII in each sample.

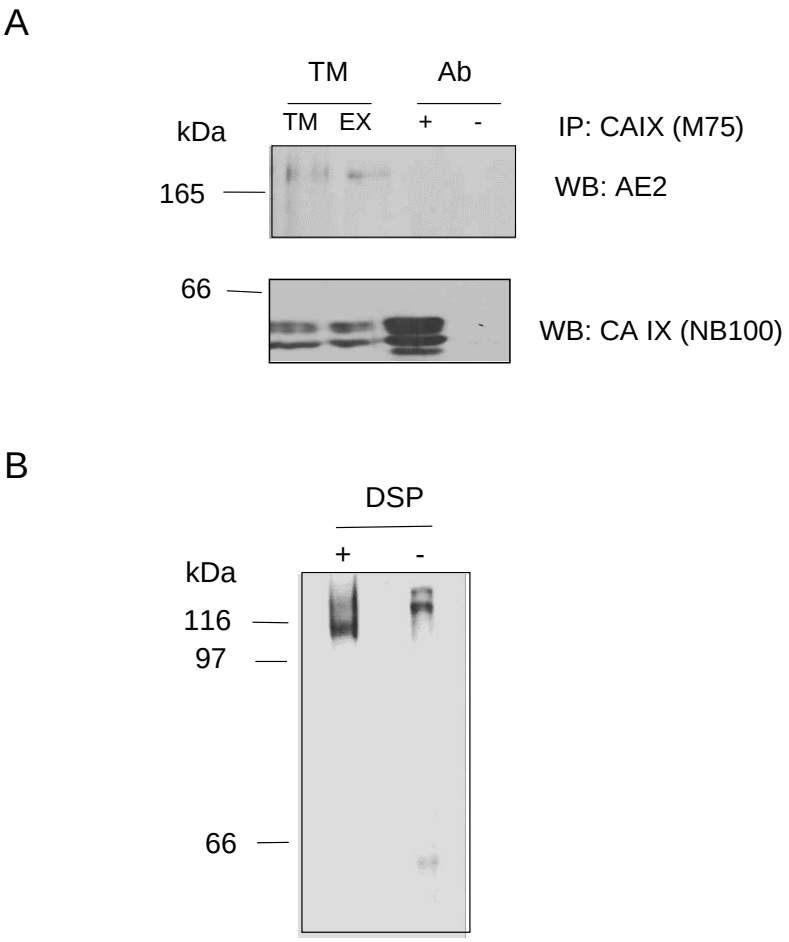


Figure 6-4. Detection of interaction between AE2 and CAIX by immunoprecipitation after chemical crosslinking. A) Hypoxic MDA-MB-231 cells were treated with DSP. Total membrane was isolated from cells and lysed by IPB buffer. Membrane extracts from hypoxic cells were used for immunoprecipitation (IP) with the anti-CAIX antibody M75, and blotted and probed with AE2 antibody and CAIX antibody NB-100. Membrane lysate (EX) and total membrane(TM) from hypoxic cells were probed to indicate the relative amount of AE2 and CAIX in each sample. B) Hypoxic MDA-MB-231 cells were treated with DSP or not. Total membrane proteins were resolved by non reducing PAGE, blotted and probed with anti-CAIX antibody M75.

A

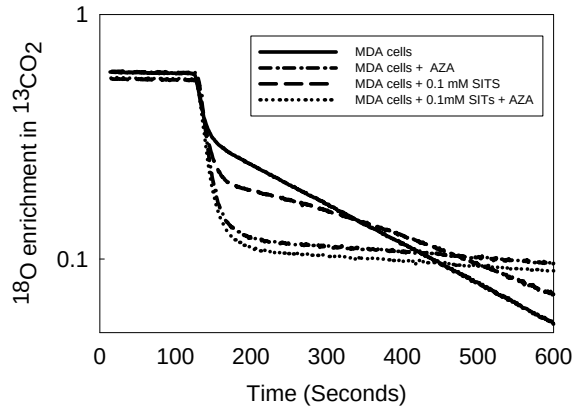


B

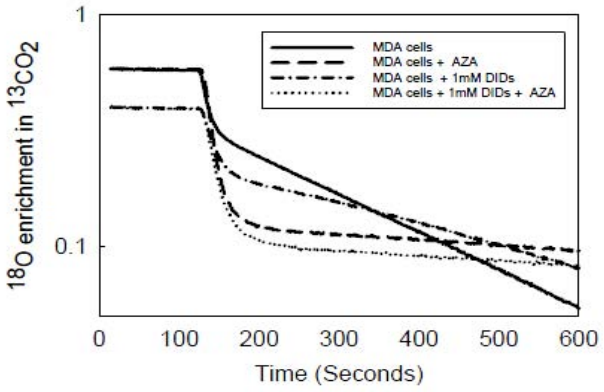


Figure 6-5. DIDs and SITs reduce CAIX activity in MDA-MB-231 cells. Cells were exposed to hypoxia for 16 h and released from plates by cell dissociation buffer. Cells (5.9 x $10^5$/mL) were added to the mixing chamber. Carbonic anyhydrase activity was then measured using the MIMS assay in the presence or absence of SITs (A) or DIDs (B) at 0.1mM and 1 mM respectively. The MIMS assay was performed by Dr. Chingkuang Tu.

A

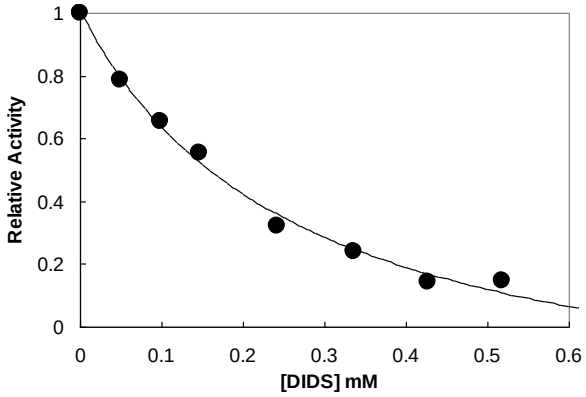


B

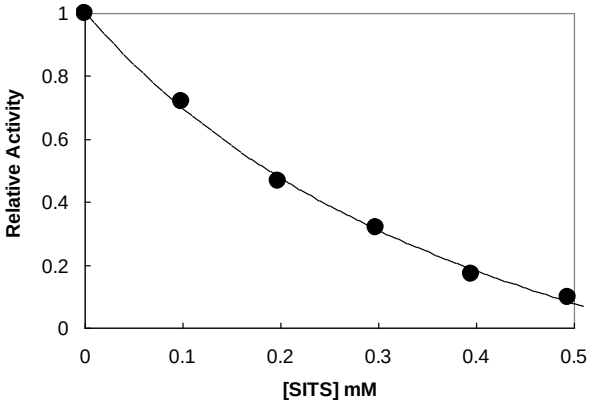


Figure 6-6. DIDs and SITs inhibit purified hCAII activity. Purified hCAII activity was assayed by MIMS for activity in the presence of DIDs or SITs at the indicated concentration. (A) CAII activity was plotted against concentrations of DIDs. (B) CAII activity was plotted against concentrations of SITs. The MIMS assay was performed by Dr. Chingkuang Tu who also determined the Ki value for each inhibitor.

A

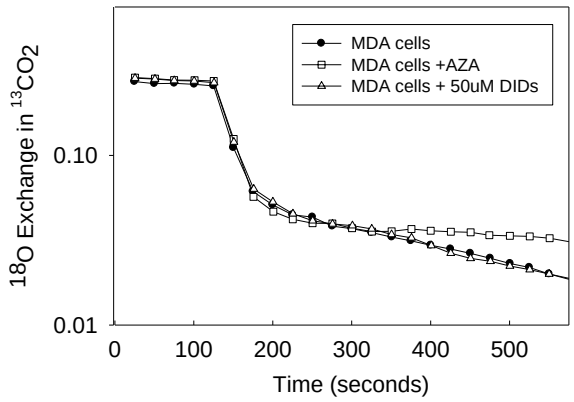


B

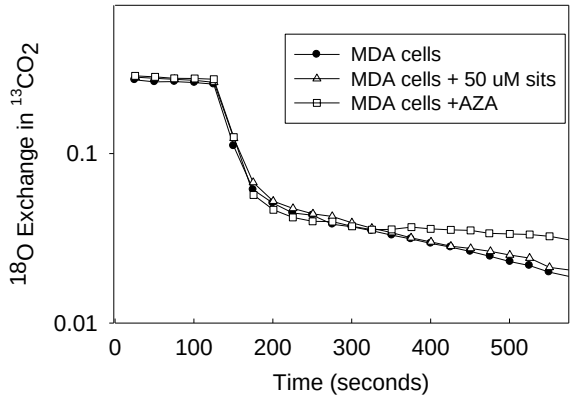


C

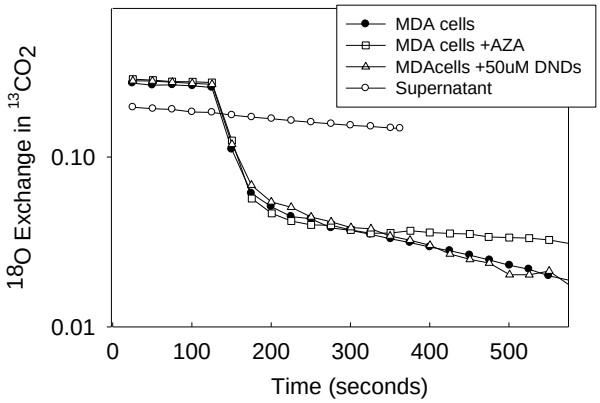


Figure 6-7 AE inhibitors at concentrations with limited CAII inhibitory activity have no effect on CAIX activity. MDA-MB-231 cells were exposed to hypoxia for 16 h and released from plates by cell dissociation buffer. Cells ($1x10^6$) were added to the mixing chamber in the presence or absence of 50 μM of DIDs (A), SITs (B) and DNDs (C). Carbonic anyhydrase activity was then measured using the MIMS assay. The MIMS assay was performed by Dr. Chingkuang Tu.

# CHAPTER 7
# CONCLUSIONS AND FUTURE DIRECTIONS

## Conclusions

This work examines the role of carbonic anhydrase IX (CAIX) in the development and maintenance of the glycolytic phenotype in breast cancer cells. CAIX expression is observed in many tumors including breast cancer. Compared to normal tissue, solid tumors have high glycolytic activity and create an acidic environment, which favors tumor cell growth and apoptosis of normal cells. This glycolytic phenotype (creating an acidic microenvironment through elevated glucose metabolism) contributes to the metastatic potential of tumors cells. To study the role of CAIX in breast cancer, we used breast cancer cell lines as the model. Many breast cancer cell lines reflect the feature of cancers from which they derived from. We focused on three cell lines, the MCF10A, T47D and MDA-MB-231 which represent normal breast cells, non-invasive breast cancer cells and highly invasive breast cancers cells, respectively. We have demonstrated that the MDA-MB-231 cells grow faster than MCF10A and T47D cells in culture, which is consistent with their invasive phenotype. Comparision of glucose uptake and production of lactic acid in these three cell lines proved that at confluence, MDA-MB-231 cells consume significantly more glucose and secrete significantly more lactic acid than do the T47D and MCF10A cells. These data provide evidence that tumor cells upregulate glycolysis to provide the energy and metabolic acid and invasive tumor cells have greater glycolytic capatity than do normal or non-invasive cancer cells. Because abnormal vascular system and rapid tumor growth lead to insufficient $O_2$ in the tumors, we cultured cells in low oxygen to mimic the tumor microenviroment. Under hypoxic conditions, each of these three cell lines exhibits a more acidic medium (lower pH) than under normoxic conditions. While this observation is not new for

cancer cells, the comparison across these lines in a single study is unique and established the conditions for subsequent experiments.

In evaluating the expression of several membrane-associated carbonic anhydrase family members in these three breast cell lines in response to hypoxia and density, we have demonstrated the CAIX expression is induced by hypoxia and density only in MDA-MB-231 cells. In fact, CAIX is only membrane-associated CA expressed in the MDA-MB-231 cell line, in our hands. T47D cells do not express CAIX but instead express CAXII whose expression is also associated with tumors. Surprisingly, CAIX expression in MCF10A cells is also induced by hypoxic conditions but not in response to higher densities in cell culture, as is the case in the MDA-MB-231 cells. Given that there is evidence that the MCF10A cells arise from a basal B cell progenitor, this observation is perhaps not that unexpected. Yet, the MCF10A cells do not form tumors when injected into nude mice nor do they have a robust glycolytic signature in cell culture. With this in mind, we have focused much of our attention on the MDA-MB-231 cells to understand the role of CAIX in controlling the microenvironment.

The tools by which we examine CAIX expression are critical and we found at the outset that the commercially available CAIX antibody (NB-100, Novus Biologicals) recognized a cytoplasmic protein that co-migrated with cellular lysates of CAIX. This protein was not detected by the M75 antibody which is considered the gold standard for detection of CAIX. Using 2-dimensional SDS-PAGE gel, we isolated this protein and subjected it to mass spectrometry. The protein was identified as beta-tubulin. Therefore, the NB-100 antibody recognizes at least one protein in addition to CAIX. CAIX is a marker for hypoxic tumors and is being used in the clinic as an indicator of poor prognosis. Clearly, this cross-reactivity could lead to false-positives for CAIX expression in samples where cytosolic proteins are present.

This non-specific interaction with β-tubulin had not been shown before which is of concern as NB-100 antibody has been touted for use in the clinical setting. Thus, this simple observation provides a cautionary note to the use of the NB-100 antibody as a diagnostic tool.

We also have investigated several physical features of CAIX in the MDA-MB-231 cells. In our hands, CAIX migrated as a 54/58 kDa doublet in agreement with previous work (*34*). We have provided evidence that both forms of CAIX are *N*-glycosylated and contain high mannose glycans by sensitivity to two diagnostic glycosidases: *N*-glycosidase F and endoglycosidase (endo H) H. The former enzyme specifically removes the entire *N*-linked glycan in the protein, while endo H removes the glycan only if it is of high mannose structure. We also established that majority CAIX (90%) in the membrane exists as a dimer. While there is a single study that provides indirect evidence that CAIX localizes to lipid rafts (*37*), we saw very little distribution of CAIX to this compartment in the MDA-MB-231 cells. In fact, it has been proposed that CAIX monomers translocate to lipid rafts where they form dimers (*37*). Our data provide evidence against this proposal as the 90% of CAIX pool exists in dimeric form while only a small amount of CAIX (1% or less) resides in lipid rafts. Thus it is unlikely that lipid rafts play a major role in the regulation of CAIX dimerization or activity. It has also been shown that EGF mediates CAIX phosphorylation on tyrosine 412, which contributes to activation of Akt via the PI3 kinase pathway in renal carcinoma cells. Although we observed EGF-dependent activation of EGFR and downstream activation of molecular targets like Akt and Erk, CAIX phosphorylation on tyrosine was not detected in immunoprecipitation assays. Interestingly, hypoxia activated Akt independent of EGF exposure. In MDA-MB-231 cells, neither hypoxia nor EGF increased the lipid raft content of CAIX. However, the combination of EGF and hypoxia increased the amount of CAIX recruited to lipid raft by about 5-fold.

With some understanding of the physical characteristics of CAIX in breast cancer cells, our next focus was on the analysis of CAIX function. The general role of carbonic anhydrase is in regulation of acid and base balances. In tumor cells, CAIX is proposed to reduce extracellular pH, maintain the intracellular pH at about 7.2, and adapt tumor cells to hypoxic conditions. Our strategy was to use some general CA inhibitors and CAIX specific inhibitors to assess CAIX activity in the MDA-MB-231 cells. A mass spectrometric method was used to assess and quantitate CAIX activity based on the biphasic depletion of $^{18}O$ from $CO_2$ measured by membrane inlet mass spectrometry (MIMS) in collaboration with Dr. David Silverman and Dr. Chingkuang Tu. We found that CAIX activity is increased by hypoxia either in intact cells or in membrane preparations isolated from MDA-MB-231 cells. Activity correlated well with its expression. Sulfonamides are well studied CA inhibitors (*54*). In our work, CAIX inhibition by a number of sulfonamides in the MDA-MB-231 cells was determined. Ethoxzolamide, which rapidly diffuses into cells, blocks intracellular CA (CAII) and exofacial CA (CAIX) activity simultaneously. N3500, an impermeant inhibitor, inhibits only CAIX activity. Acetazolamide, the classical CA inhibitor, is selective for CAIX since it only slowly diffuses into cells. The fluorescent CA inhibitor, Cpd 5c, also inhibits CAIX activity at nanomolar concentrations. It has been suggested that this inhibitor only binds to hypoxia-activated CAIX (*50*) although our data does not support this hypothesis. Using $^{18}O$ exchange measured by MIMS, we quantified the catalytic activity of CAIX in membrane ghosts and intact cells. Data from membrane ghosts showed that the the catalytic efficiency of CAIX in the membrane environment is 62 $\mu M^{-1}s^{-1}$, which is very similar to that measured for the purified, recombinant, truncated form (55 $\mu M^{-1}s^{-1}$) (*30*). Hence, activity of CAIX is not affected by the proteoglycan extension or membrane environment.

In addition to the induction of expression and activity by hypoxia, CAIX activity is also regulated by the other factors. In this study, we also investigated effect of $O_2$, pH and Zn ion on the CAIX activity in MDA cells. Using MIMS, we provide the first direct evidence that catalytic activity is regulated by oxygen availability which is in agreement with earlier studies (*60;61*). However, the efficacy for inhibitors does not change which is interpreted to mean that the intrinsic activity of CAIX is not altered. Further, we have shown that the dehydration activity of CAIX increases as pH is decreased from pH 7.9, reaching a maximum at approximately pH 6.5. The typical tumor pH (pH 6.8) increases CAIX dehydration activity, indicating that CAIX prefers to consume protons at the pH maintained in the tumor microenvironment. This suggests that CAIX plays a role in the maintenance of the tumor microenvironment to the advantage of cancer cells, but to the detriment to surrounding of normal cells. Last, CAIX activity in response to zinc was investigated. Previous work showed that recombinant proteins containing the CAIX CA domain or the CA domain with the proteoglycan extension, were activated by 50 μM Zn ion (*31*). However, we demonstrated that native CAIX in the context of the cell membrane is unaffected by Zn ion concentrations lower than 500 μM. It is perhaps likely, that non-specific Zn binding sites lowers the effective concentration of free Zn which limits its ability to stimulate CAIX.

After confirming that sulfonamide inhibitors block exofacial CAIX activity in MDA-MB-231 cells, we further explored effects of CAIX inhibition on the acidification of medium induced by hypoxia. Hypoxic conditions reduce medium pH in MDA-MB-231 cells in culture and incubation with CA inhibitors partially abrogated this acidification. These data suggest that CAIX is involved in the acidification of the tumor microenviroment. Recent published data indicates that the selective inhibition of CAIX decreases cell proliferation and induces apoptosis

in CAIX-positive cells but not in CAIX-negative cells (*132*). We demonstrated that among the CAIX inhibitors tested; only Chlorzolamide significantly reduced MDA-MB-231 cell growth. Likewise, only chlorzolamide decreased cell migration under hypoxic conditions. Although acetazolamide, N3500, and Cpd 5c blocked acidification of medium pH, they had no impact on the cell growth, migration, or invasion in MDA-MB-231 cells in culture. One possible explanation for this latter result is the time course (20 hours) over which the experiment was conducted. Decreasing the acidification through blocking CAIX may be insufficient to affect the cellular phenotype during this time frame. Thus, we can not rule out that CAIX activity alters this specific behavior in MDA-MB-231 cells. Further studies are necessary in this regard, which are discussed in the next section.

Last, we have examined the physical and functional relationship between CAIX and AE2 in the breast cancer cells under physiological condition. On the basis of our results, we believe that there is no physical interaction between CAIX and AE2 in hypoxic MDA-MB-231 cells. Indeed, we have little evidence that there is a functional relationship between CAIX and the bicarbonate transporters because it appears that there are only minor contributions to CAIX activity from bicarbonate pools. However, we are mindful of the fact the bicarbonate transport inhibitors are of limited use because they appear to inhibit CA activity, directly. Thus this area requires further study, as well, which will be discussed in future directions.

## Future Directions

This research is primarily focused on the characterization of CAIX in breast cancer cells and demonstration of its role in the development of the glycolytic phenotype. Among the breast cells we studied, aggressive breast cancer cell line MDA-MB-231 cells display high glucose uptake and more acidic medium pH even in normoxic condition. Corresponding to its glycolytic phenotype, MDA-MB-231 cells have hypoxia-and density-induced CAIX expression. Also, we

have established CAIX activity is induced by hypoxia and its activity can be blocked by some inhibitors. Inhibition of CAIX activity partially blocks the acidification of extracellular environment.

Both our inhibition studies and pH dependency provide evidence that CAIX is involved in the development of the glycolytic phenotype, additional evidence could be provided by CAIX gene silencing studies. So, establishing a CAIX knockdown in MDA-MB-231 cells is an important future direction for this work. CAIX ablation can be established using transient or stable transfection of RNAi or shRNAs. We would like to approach this by using shRNA technology taking advantage of retroviral expression systems. We have designed three shRNAs targetting different sequences of CAIX using shRNA tool developed in Hannon laboratory in Cold Spring Harbor (Table 7-1). The Phoenix retroviral expression system is a highly efficient system for delivery of genes into cells. After establishing stable ablation of CAIX in MDA-MB-231 cells, CAIX activity can be monitored in control and knockdown cells. This selective knockdown in MDA-MB-231 cells is advantageous in that all hypoxia-induced mechanisms remain intact, other than CAIX. Thus changes that we observe will be directly related to CAIX ablation. In other systems that investigators have explored, CAIX is overexpressed or not in systems that do not necessarily have the additional components that contribute to the glycolytic phenotype, like the proton transporters that are upregulated by hypoxia. Thus, we will be able to provide specific information regarding the function of CAIX (or lack of function) in a system that replicates the true hypoxic environment.

Next, the fluorophore carboxy-SNARR-1 could be utilized to assay intracellular pH in these cells. This method would be more accurate and sensitive than method we used in this study by measurement of the benzoic acid uptake which is discussed in Appendix B. Apart from

the determination of the phenotype in CAIX knock down cell lines, mechanisms by which the CAIX interference phenotype (if any) will be important. Regulation of p38 MAPK, Erk, and Akt signaling pathways in the CAIX knockdown cell line could also be determined. Understanding changes in these pathways will help to define CAIX signaling properties, if they exist, and how these pathways affect cellular phenotype.

In addition to *in vitro* studies, we could test the effect of CAIX knockdown in *in vivo* studies. This would allow us to determine if CAIX ablation affects tumor growth and metatasis. CAIX knockdown cells or parental MDA-MB-231 cells will be inoculated into the mammary fat pad of nude mice. Tumor size can be monitored by a GFP signal since transected tumor cells will have GFP expression. Metastasis could be analyzed by sacrificing mice and counting the number of lung metastases. Ultimately, this set of experiments will allow us to understand the role of CAIX in the maintainence of the tumor microenvironment, *in vivo.* With that understanding, we can envision that CAIX inhibitors might provide useful tools for modifying that environment.

With respect to our proposed mechanism for CAIX and AEs metabolon theory in cancer cells, we were unable to detect interactions between AE2 and CAIX perhaps due to low expression of AE2 or inefficient commercially-available AE2 antibodies. To avoid this question, we could transfect AE2 tagged with HA into MDA-MB-231 cells and then use and antibody recognizing HA to detect AE2 expression to better understand possible interactions between CAIX and AE2.

In summary, several important facets of CAIX expression and activity required for development of glycolytic phenotype elaborated in this work. Further analysis of the CAIX

knockdown cell line will enhance our understanding in the role of CAIX in the development of glycolytic phenotype in breast cancer cells.

Table 7-1. shRNA targetting sequence in CAIX

| shRNA | shRNA targetting sequence | Position in CAIX |
|---|---|---|
| shRNA1 | TACACACCGTGTGCTGGGACAC | 5-27 |
| shRNA2 | GACAGTGATGCTGAGTGCTAAG | 1082-1104 |
| shRNA3 | TGCTGAGCCAGTCCAGCTGAAT | 1241-1263 |

# APPENDIX A
# CAIX EXPRESSION AND PHOSPHORYLATION IN SKRC-01 CELLS

In the chapter 4, we have investigated CAIX phosphorylation in response to EGF stimulation in MDA-MB-231 cells. Our data showed that CAIX was not phosphorylated in response EGF stimulation in MDA-MB-231 cells. This result was different from a previous study by Dorai and his co-workers. In this studiy, they examined CAIX phosphorylation in SKRC-01 cells, a renal carcinoma cell line. They found phosphorylation of CAIX in response to EGF stimulation (*37*). Therefore, we utilized same cell line to verify this data. SKRC-01 cells were obtained from Dr. Gerd Ritter at the Ludwig Institute, Sloan Kettering. To be consistent with conditions used in the Dorai paper, SKRC-01 cells were grown in Minimal Essential Medium (MEM) supplemented with 10% FBS and 1% non-essential amino acids (NEAA) to 50 % confluence in 10 cm plates. The cells were then serum starved by growing in MEM supplemented with 0.1 % FBS and 1% NEAA overnight and in serum-free medium for a further 2 hours. Serum-starved cells were stimulated with 50 ng/mL (8 nM) or 100 ng/ml (16 nM) EGF for 30 minutes. RIPA buffer extracts were made from these cells. CAIX was then immunoprecipitated with CAIX-specific polyclonal antibody (R&D system) and then analyzed by Western blotting using an antibody against phosphorylated tyrosine (pY-20). CAIX phosphorylation was not observed in cells treated with EGF or without EGF (Figure A-1). Interestingly, CAIX expression in the input was very low in this cell line. Note that the strong band detected by the NB-100 antibody is likely beta tubulin. To confirm CAIX expression in this celll line, cell lysates from subconfluent, confluent and overconfluent SKRC-01 cells were run on PAGE gels and blotted for CAIX expression using M75. CAIX expression level was very low in SKRC-01 cells compared to hypoxic MDA-MB-231 cells (Figure A-2). As CAIX expression in these cells was incredibly low in our hands, it was not surprisly that we did not

observed CAIX phosphorylation in this "positive" cell line. However, Dorai and colleagues showed that SKRC-01 cells have strong endogenous CAIX expression. So the question arises as to how the same cell line shows different expression for specific proteins. It is appreciated that cancer arises from a stepwise accumulation of genetic changes that afford an incipient cancer cell the properties of unlimited, self-sufficient growth and resistance to normal homeostatic regulatory mechanisms(*133*). This genetic instability is considered to play a key role in the generation of genetic and phenotypic heterogeneity in cancer cells. Recently, Masramon et al. have demonstrated genetic drift in clonal lines originating from isolated (colon) cancer cells(*134*). This indicates that genetic instability is not lost in cultured cells and can continue to contribute to genetic and phenotypic differences. It is logical to assume that this genetic drift is responsible for the protein expression differences in the SKRC-01 cells used in our studies and those used by Dorai *et al.* Another example for this genetic drift is the MDA-MB-231 used in our study and same cell lines used by Heish *et al* (*135*). In their study, the expression of CAXII appeared to be significantly higher than CAIX. Further, the authors showed that knocking down expression of CAXII decreased the invasion and migration capability of the cells. However, in our hand, CAIX is the only membrane CA isoform expressed in MDA-MB-231 cells. There is no CAXII expression in these cells. The different CAIX and CAXII expression pattern in MDA-MB-231 cells could also be attributed to genetic drift.

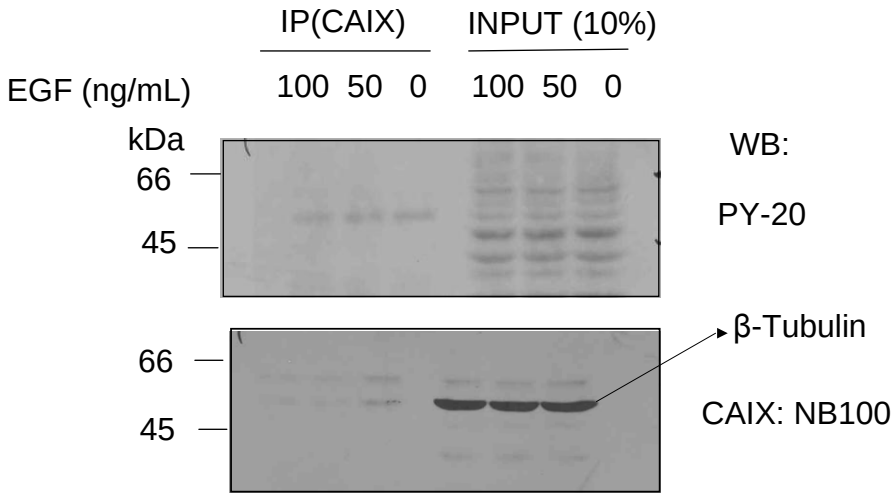


Figure A-1. CAIX phosphorylation in response to EGF stimulation in SKRC-01 cells. SKRC-01 cells were serum starved overnight and exposed to EGF (50 ng/mL or 100 ng/mL) for 30 min. RIPA extracts were made from these cells. CAIX was immunoprecipitated with an antibody generated in goat (R&D Systems, # AF2188) followed by western blotting with an anti-phosphotyrosine antibody (PY20) or the polyclonal CAIX antibody NB100 antibody.

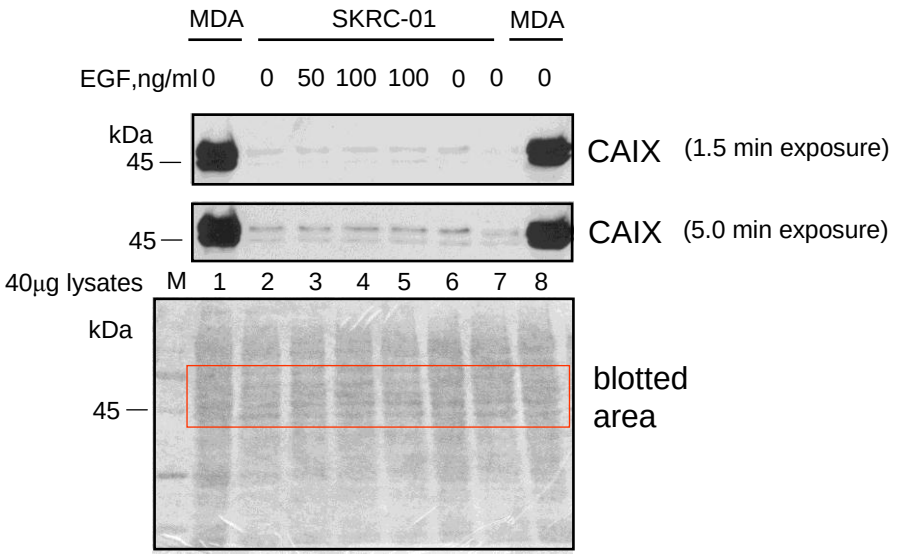


Figure A-2. CAIX expression in SKRC-01 cells and hypoxic MDA-MB-231 cells. SKRC-01 cells were serum starved overnight and exposed to EGF for 30 min from which RIPA extracts were made. Forty μg proteins were loaded on 10% SDS-PAGE gels and followed by Western blotting with the M75 antibody. Top panel: The same Western blot was exposed for 1.5 minutes or 5 minutes. Bottom panel: This represents the amido black staining of the nitrocellulose membrane to indicate equal protein loading. M: molecular weight marker lane. Lane: 1: hypoxic MDA-MB-231 cells. 2: 50% confluent SKRC-01 cells, no EGF. 3: 50% confluent SKRC-01 cells, 50 ng/mL EGF, 30'. 4: 50% confluent SKRC-01 cells, 100 ng/mL EGF, 30'. 5: 50% confluent SKRC-01 cells, 100 ng/mL EGF, 30', washed out 30'. 6: 100% confluent SKRC-01 cells, no EGF. 7: Overconfluent SKRC-01cells, no EGF. 8: hypoxic MDA-MB-231 cells.

# APPENDIX B
# INTRACELLULAR PH IN MDA-MB-231 CELLS

CAIX has been proposed to contribute the regulation of cytoplasmic pH and to maintain it at 7.2, similar to normal cells. Chiche *et al.* found that CAIX expression affected pHi in isolated cells only when cells were exposed to bicarbonate-free buffer in an acidic milieu (*51*). The goal of this set of experiments was to examine if hypoxia-induced CAIX expression is responsible for maintaining intracellular pH (pHi) in acidic environment in MDA-MB-231 cells. The pHi was measured using the distribution of the weak acid [7-$^{14}$C] benzoic acid as described in in Chapter 2. The pHi of hypoxic MDA-MB-231 cells was more alkaline compared with that of control MDA-MB-231 cells when incubated in $HCO_3^-$ /$CO_2$ free solution set at a pHe of 6.6 and 7.4 (Figure B-1). Hypoxic cells have higher pHi in buffer without bicarbonate, either in an extracellular environment of pH 6.6 or 7.4. There was a difference of 0.15 units in either case, but the difference was not significant. In the presence of 25 mM bicarbonate-containing buffer, there was no difference in pHi between hypoxic MDA-MB-231 cells and control cells. These data suggest that CAIX expression might be associated with intracellular alkalinization in the bicarbonate-free solution, which requires further studies using more accurate methods to measure pHi as discussed in future directions.

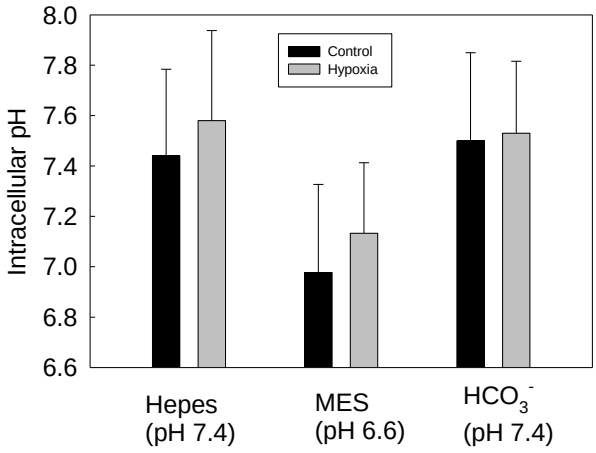


Figure B-1. CAIX expression increases pHi. The pHi was determined in control and hypoxic MDA-MB-231 cells with [$^{14}$C] benzoic acid. MDA-MB-231 cells at 75 % confluence were exposed to hypoxia for 16 hours. Normoxic or hypoxic cells were equilibrated for 15 min in a 25 mmol/L $HCO_3^-$ solution (7.4), a $HCO_3^-$ free MES, or Hepes-buffered solution adjusted to 6.6 or 7.4, respectively. Cells were then shifted for 15 min to the same solution containing [$^{14}$C] benzoic acid at a specific activity of 1 μCi/mL. pHi was calculated as described under Materials and Methods. Data are for duplicate assays and are the average of three independent experiments ± S.D.

LIST OF REFERENCES


1. Gatenby, R. A. and Gillies, R. J. (2004) Why Do Cancers Have High Aerobic Glycolysis? *Nat. Rev. Cancer 4*, 891-899.

2. Gillies, R. J. and Gatenby, R. A. (2007) Adaptive Landscapes and Emergent Phenotypes: Why Do Cancers Have High Glycolysis?, *J. Bioenerg. Biomembr. 39*, 251-257.

3. Vaupel, P., Kallinowski, F., and Okunieff, P. (1989) Blood Flow, Oxygen and Nutrient Supply, and Metabolic Microenvironment of Human Tumors: A Review, *Cancer Res. 49*, 6449-6465.

4. Vaupel, P., Schlenger, K., Knoop, C., and Hockel, M. (1991) Oxygenation of Human Tumors: Evaluation of Tissue Oxygen Distribution in Breast Cancers by Computerized $O_2$ Tension Measurements., *Cancer Res. 51*, 3316-3322.

5. Bauer, D. E., Harris, M. H., Plas, D. R., Lum, J. J., Hammerman, P. S., Rathmell, J. C., Riley, J. L., and Thompson, C. B. (2004) Cytokine Stimulation of Aerobic Glycolysis in Hematopoietic Cells Exceeds Proliferative Demand, *FASEB J. 10.1096/fj.03-1001fje*.

6. Gillies, R. J., Robey, I., and Gatenby, R. A. (2008) Causes and Consequences of Increased Glucose Metabolism of Cancers, *Journal of Nuclear Medicine 49*, 24S-42S.

7. Yamagata, M., Hasuda, K., Stamato, T., and Tannock, I. F. (1998) The Contribution of Lactic Acid to Acidification of Tumours: Studies of Variant Cells Lacking Lactate Dehydrogenase, *Br. J. Cancer 77*, 1726-1731.

8. Fantin, V. R., St-Pierre, J., and Leder, P. (2006) Attenuation of LDA-A Expression Uncovers a Link Between Glycolysis, Mitochondrial Physiology, and Tumor Maintenance, *Cancer Cell 9*, 425-434.

9. Dang, C. V. and Semenza, G. L. (1999) Oncogenic Alterations of Metabolism, *Trends Biochem. Sci. 24*, 68-69.

10. Cairns, R., Papandreou, I., and Denko, N. (2006) Overcoming Physiologic Barriers to Cancer Treatment by Molecularly Targeting the Tumor Microenvironment, *Mol. Cancer Res. 4*, 61-70.

11. Brahimi-Horn, M. C. and Pouyssegur, J. (2009) HIF at a Glance, *J. Cell Sci 122*, 1055-1057.

12. Greijer, A. E., van der Groep, P., Kemming, D., Shvarts, A., Semenza, G. L., Meijer, G. A., van de Wiel, M. A., Belien, J. A. M., van Diest, P. J., and van der Wall, E. (2005) Up-regulation of Gene Expression by Hypoxia is Mediated Predominantly by Hypoxia-inducible Factor 1 (HIF1), *J. Pathol. 206*, 291-304.

13. Brown, R. and Wahl, R. (1993) Overexpression of Glut-1 Glucose Transporter in Human Breast Cancer. An Immunohistochemical Study, *Cancer 72*, 2979-2985.

14. Koukourakis, M. I., Giatromanolaki, A., Harris, A. L., and Sivridis, E. (2006) Comparison of Metabolic Pathways in Cancer Cells and Stromal Cells in Colorectal Cancer: a Metabolic Survival Role for Tumor-associated Stroma, *Cancer Res. 66*, 623-627.

15. Giatromanolaki, A., Koukourakis, M. I., Sivridis, E., Pastorek, J., Wykoff, C. C., Gatter, K. C., and Harris, A. L. (2001) Expression of Hypoxia-inducible Carbonic Anhydrase-9 Relates to Angiogenic Pathways and Independently to Poor Outcome in Non-Small Cell Lung Cancer, *Cancer Res. 61*, 7992-7998.

16. Gillies, R. J., Liu, Z., and Bhujwalla, Z. (1994) $^{31}$P-MRS Measurements of Extracellular pH of Tumors Using 3-Aminopropylphosphonate, *Am. J. Physiol. 267*, 195-203.

17. McLean, L. A., Roscoe, J., Jorgensen, N. K., Gorin, F. A., and Cala, P. M. (2000) Malignant Gliomas Display Altered pH Regulation by NHE1 Compared to Nontransformed Astrocytes, *Am. J. Physiol. 278*, C676-C688.

18. Halestrap, A. P. and Meredith, D. (2004) The *SLC16* Gene Family - From Monocarboxylate Transporters (MCTs) to Aromatic Amino Acid Transporters and Beyond, *Pflugers Arch. 447*, 619-628.

19. Sennoune, S. R., Luo, D., and Martinez-Zaguilan, R. (2004) Plasmalemmal Vacuolar-Type $H^+$-ATPase in Cancer Biology, *Cell Biochem. Biophys. 40*, 185-205.

20. Gottlieb, R. A., Giesing, H. A., Zhu, J. Y., Engler, R. L., and Babior, B. M. (1995) Cell Acidification in Apoptosis: Granulocyte Cology-stimulating Factor Delays Programed Cell Death in Neutrophils by Up-regulating the Vaculolar $H^+$-ATPase, *Proc. Natl. Acad. Sci. USA 92*, 5965-5968.

21. Stubbs, M., McSheehy, P. M. J., Griffiths, J. R., and Bashford, C. L. (2000) Causes and Consequences of Tumour Acidity and Implications for Treatment, *Molec. Med. Today 6*, 15-19.

22. Gatenby, R. A., Smallbone, K., Maini, P. K., Rose, F., Averill, J., Nagle, R. B., Worrall, L., and Gillies, R. J. (2007) Cellular Adaptations to Hypoxia and Acidosis During Somatic Evolution of Breast Cancer, *Br. J. Cancer 97*, 646-653.

23. Newell, K., Franchi, A., Pouyssegur, J., and Tannock, I. (1993) Studies with Glycolysis-deficient Cells Suggest that Production of Lactic Acid is not the Only Cause of Tumor Acidity, *Proc. Natl. Acad. Sci. USA 90*, 1127-1131.

24. Swietach, P., Wigfield, S., Cobden, P., Supuran, C. T., Harris, A. L., and Vaughan-Jones, R. D. (2008) Tumor-Associated Carbonic Anhydrase 9 Spatially Coordinates Intracellular pH in Three-Dimensional Multicellular Growths, *J. Biol. Chem. 283*, 20473-20483.

25. Griffiths, J. R., McIntyre, D. J., Howe, F. A., and Stubbs, M. (2001) Why Are Cancers Acidic? A Carrier Mediated Diffusion Model for $H^+$ Transport in the Interstitial Fluid, *Novartis Found. Symp. 240*, 46-62.

26. Swietach, P., Patiar, S., Supuran, C. T., Harris, A. L., and Vaughan-Jones, R. D. (2009) The Role of Carbonic Anhydrase 9 in Regulating Extracellular and Intracellular pH in 3-D Tumor-Cell Growths, *J. Biol. Chem. 284*, 20299-20310.

27. Parkkila, S. (2000) An Overview of the Distribution and Function of Carbonic Anhydrases in Mammals, in *The Carbonic Anhydrases: New Horizons* (Chegwidden, W. R., Carter, N., and Edwards, Y., Eds.) pp 76-93, Birkhauser Verlag, Basel, Switzerland.

28. Pastorekova, S. and Pastorek, J. (2004) Cancer-related Carbonic Anhydrase Isozymes and Their Inhibition, in *Carbonic Anhydrase: Its Inhibitors and Activators* (Supuran, C. T., Scozzafava, A., and Conway, J., Eds.) pp 255-281, CRC Press, Bocal Raton.

29. Supuran, C. T. (2008) Carbonic Anhydrase: Novel Therapeutic Applications for Inhibitors and Activators, *Nature Reviews 7*, 168-181.

30. Wingo, T., Tu, C., Laipis, P. J., and Silverman, D. N. (2001) The Catalytic Properties of Human Carbonic Anhydrase IX, *Biochem. Biophys. Res. Comm. 288*, 666-669.

31. Hilvo, M., Baranauskiene, L., Salzano, A. M., Scaloni, A., Matulis, D., Innocenti, A., Scozzafava, A., Monti, S. M., Di Flore, A., De Simone, G., Lindfors, M., Janis, J., Valjakka, J., Pastorekova, S., Pastorek, J., Kulomaa, M. S., Mordlund, H. R., Supuran, C. T., and Parkkila, S. (2008) Biochemical Characterization of CA IX, One of the Most Active Carbonic Anhydrase Isozymes, *J. Biol. Chem. 283*, 27799-27809.

32. Potter, C. P. S. and Harris, A. L. (2003) Diagnostic, Prognostic and Therapeutic Implications of Carbonic Anhydrases in Cancer, *Br. J. Cancer 89*, 2-7.

33. Ivanov, S., Liao, S.-Y., Ivanova, A., Danilkovitch-Miagkova, A., Tarasova, N., Weirich, G., Merrill, M. J., Proescholdt, M. A., Oldfield, E. H., Lee, J., Zavada, J., Waheed, A., Sly, W., Lerman, M. I., and Stanbridge, E. J. (2001) Expression of Hypoxia-inducible Cell-surface Transmembrane Carbonic Anhydrases in Human Cancer, *Am. J. Pathol. 158*, 905-919.

34. Pastorekova, S., Zavadova, Z., Kostal, M., Babusikova, O., and Zavada, J. (1992) A Novel Quasi-viral Agent, MaTu, is a Two-Component System, *Virology 187*, 620-626.

35. Pastorek, J., Pastoreková, S., Callebaut, I., Mornon, J. P., Zelník, V., Opavsky, R., Zat'ovicová, M., Liao, S., Portetelle, D., Stanbridge, E. J., Závada, J., Burny, A., and Kettmann, R. (1994) Cloning and Characterization of MN, a Human Tumor-associated Protein with a Domain Homologous to Carbonic Anhydrase and a Putative Helix-Loop-Helix DNA Binding Segment, *Oncogene 9*, 2877-2888.

36. Svastova, E., Zilka, N., Zatovicova, M., Gibadulinova, A., Ciampor, F., Pastorek, J., and Pastorekova, S. (2003) Carbonic Anhydrase IX Reduces E-Cadherin-mediated Adhesion of MDCK Cells via Interaction with β-Catenin, *Exp. Cell Res. 290*, 332-345.

37. Dorai, T., Sawczuk, I. S., Pastorek, J., Wiernik, P. H., and Dutcher, J. P. (2005) The Role of Carbonic Anhydrase IX Overexpression in Kidney Cancer, *Eur. J. Can. 41*, 2935-2947.

38. Span, P. M., Bussink, J., Manders, P., Beex, L. V. A. M., and Sweep, C. G. J. (2003) Carbonic Anhydrase-9 Expression Levels and Prognosis in Human Breast Cancer: Association with Treatment Outcome, *Br. J. Cancer 89*, 271-276.

39. Thiry, A., Dogne, J.-M., Masereel, B., and Supuran, C. T. (2006) Targeting Tumor-associated Carbonic Anhydrase IX in Cancer Therapy, *Trends in Pharmacological Sciences 27*, 566-573.

40. Potter, C. and Harris, A. L. (2004) Hypoxia Inducible Carbonic Anhydrase IX, Marker of Tumor Hypoxia, Survival Pathway and Therapy Target, *Cell Cycle 3*, 164-167.

41. Hussain, S. A., Ganesan, R., Reynolds, G., Gross, L., Stevens, A., Pastorek, J., Murray, P. G., Perunovic, B., Anwar, M. S., Billingham, L., James, N. D., Spooner, D., Poole, C. J., Rea, D. W., and Palmer, D. H. (2007) Hypoxia-regulated Carbonic Anhydrase IX Expression Is Associated with Poor Survival in Patients with Invasive Breast Cancer, *Br. J. Cancer 96*, 104-109.

42. Pastorekova, S., Parkkila, S., Parkkila, A., Opavsky, R., Zelnik, V., Saarnio, J., and Pastorek, J. (1997) Carbonic Anhydrase IX, MN/CAIX: Analysis of Stomach Complementary DNA Sequence and Expression in Human and Rat Alimentary Tracts, *Gastroenterology 112*, 398-408.

43. Saarnio, J., Parkkila, S., Parkkila, A.-K., Waheed, A., Casey, M. C., Zhou, X. Y., Pastoreková, S., Pastorek, J., Karttunen, T., Haukipuro, K., Kairaluoma, M. I., and Sly, W. S. (1998) Immunohistochemistry of Carbonic Anhydrase Isozyme IX (MN/CA IX) in Human Gut Reveals Polarized Expression in Epithelial Cells with the Highest Proliferative Capacity, *J. Histochem. Cytochem. 46*, 497-504.

44. Helmlinger, G., Yuan, F., Dellian, M., and Jain, R. K. (1997) Interstitial pH and $pO_2$ Gradients in Solid Tumors *In Vivo*: High-resolution Measurements Reveal Lack of Correlation, *Nat. Med. 3*, 177-182.

45. Shannon, A. M., Bouchier-Hayes, D. J., Condron, C. M., and Toomey, D. (2003) Tumor Hypoxia, Chemotherapeutic Resistance and Hypoxia-related Therapies, *Cancer Treatment Reviews 29*, 297-307.

46. Hockel, M., Schlenger, K., Mitze, M., Schaffer, U., and Vaupel, P. (1996) Hypoxia and Radiation Response in Human Tumors, *Semin. Radiat. Oncol. 6*, 3-9.

47. Loncaster, J. A., Harris, A. L., Davidson, S. E., Logue, J. P., Hunter, R. D., Wykoff, C. C., Pastorek, J., Ratcliffe, P. J., Stratford, I. J., and West, C. M. L. (2001) Carbonic Anhydrase (CAIX) Expression, a Potential New Intrinsic Marker of Hypoxia: Correlations with Tumor Oxygen Measurements and Prognosis in Locally Advanced Carcinoma of the Cervix, *Cancer Res. 61*, 6394-6399.

48. Kaluz, S., Kaluzová, M., Chrastina, A., Olive, P. L., Pastoreková, S., Pastorek, J., Lerman, M. I., and Stanbridge, E. J. (2002) Lowered Oxygen Tension Induces Expression of the Hypoxia Marker MN/Carbonic Anhydrase IX in the Absence of Hypoxia-inducible Factor 1α Stabilization: A Role for Phosphatidylinositol 3'-Kinase, *Cancer Res. 62*, 4469-4477.

49. Wykoff, C. C., Beasley, N. J. P., Watson, P. H., Turner, K. J., Pastorek, J., Sibtain, A., Wilson, G. D., Turley, H., Talks, K. L., Maxwell, P. H., Pugh, C. W., Ratcliffe, P. J., and Harris, A. L. (2000) Hypoxia-inducible Expression of Tumor-associated Carbonic Anhydrase, *Cancer Res. 60*, 7075-7083.

50. Svastova, E., Hulikova, A., Rafajova, M., Zatovicova, M., Gibadulinova, A., Casini, A., Cecchi, A., Scozzafava, A., Supuran, C. T., Pastorek, J., and Pastorekova, S. (2004) Hypoxia Activates the Capacity of Tumor-associated Carbonic Anhydrase IX to Acidify Extracellular pH, *FEBS Lett. 577*, 439-445.

51. Chiche, J., Ilc, K., Laferriere, J., Trottier, E., Dayan, F., Mazure, N. M., Brahimi-Horn, M. C., and Pouyssegur, J. (2009) Hypoxia-Inducible Carbonic Anhydrase IX and XII Promote Tumor Cell Growth by Counteracting Acidosis through the Regulation of the Intracellular pH, *Cancer Res. 69*, 358-368.

52. Chia, S. K., Wykoff, C. C., Watson, P. H., Han, C., Leek, R. D., Pastorek, J., Gatter, K. C., Ratcliffe, P., and Harris, A. L. (2005) Prognostic Significance of a Novel Hypoxia-Regulated Marker, Carbonic Anhydrase IX, in Invasive Breast Cancer, *J. Clin. Oncol. 19*, 3660-3668.

53. Supuran, C. T. (2008)
Carbonic Anhydrase: Novel Therapeutic Applications for Inhibitors and Activators, *Nature Reviews 7*, 168-181.

54. Supuran, C. T., Briganti, F., Tilli, S., Chegwidden, W. R., and Scozzafava, A. (2001) Carbonic Anhydrase Inhibitors: Sulfonamides as Antitumor Agents?, *Bioorg. Med. Chem. 9*, 703-714.

55. Vullo, D., Innocenti, A., Nishimori, I., Pastorek, J., Scozzafava, A., Pastorekova, S., and Supuran, C. T. (2005) Carbonic Anhydrase Inhibitors: Inhibition of the Transmembrane Isozyme XII with Sulfonamides - a New Target for the Design of Antitumor and Antiglaucoma Drugs, *Bioorganic and Medicinal Chemistry Letters 15*, 963-969.

56. Alterio, V., Vitale, R. M., Monti, S. M., Pedone, C., Scozzafava, A., Cecchi, A., De Simone, G., and Supuran, C. T. (2006) Carbonic Anhydrase Inhibitors: X-ray and Molecular Modeling Study for the Interaction of a Fluorescent Antitumor Sulfonamide with Isozyme II and IX, *Journal of American Chemical Society 128*, 8329-8335.

57. Conroy, C. W., Wynns, G. C., and Maren, T. H. (1996) Synthesis and Properties of Two New Membrane-impermeant High-molecular-weight Carbonic Anhydrase Inhibitors, *Bioorganic Chemistry 24*, 262-272.

58. Delacruz, J., Mikulski, R., Tu, C., Li, Y., Wang, H., Shiverick, K. T., Frost, S. C., Horenstein, N. A., and Silverman, D. N. (2010) Detecting Extracellular Carbonic Anhydrase Activity Using Membrane Inlet Mass Spectrometry, *Anal. Biochem. 403*, 74-78.

59. Scozzafava, A., Briganti, F., Ilies, M. A., and Supuran, C. T. (2000) Carbonic Anhydrase Inhibitors: Synthesis of Membrane-impermeant Low Molecular Weight Sulfonamides Possessing in Vivo Selectivity for the Membrane-bound Versus Cytosolic Isozymes, *J. Med. Chem. 43*, 292-300.

60. Dubois, L., Douma, K., Supuran, C. T., Chiu, R. K., vanZandvoort, M. A. M. J., Pastorekova, S., Scozzafava, A., Wouters, B. G., and Lambin, P. (2007) Imaging the Hypoxia Surrogate Marker CAIX Requires Expression and Catalytic Activity for Binding Fluorescent Sulfonamide Inhibitors, *Radiotherapy and Oncology 83*, 367-373.

61. Dubois, L., Lieuwes, N. G., Maresca, A., Thiry, A., Supuran, C. T., Scozzafava, A., Wouters, B. G., and Lambin, P. (2009) Imaging of CA IX with Fluorescent Labelled Sulfonamides Distinguishes Hypoxic and (re)-Oxygenated Cells in a Xenograft Tumour Model, *Radiother. Oncol. 92*, 423-428.

62. Sterling, D., Reithmeier, R. A. F., and Casey, J. R. (2001) A Transport Metabolon: Functional Interaction of Carbonic Anhydrase II and Chloride/Cicarbonate Exchangers, *J. Biol. Chem. 276*, 47886-47894.

63. Sterling, D. and Casey, J. R. (2002) Bicarbonate Transport Proteins, *Biochem. Cell Biol. 80*, 483-497.

64. Pushkin, A. and Kurtz, I. (2006) SLC4 Base ($HCO^{-3}$, $CO^{2-3}$) Transporters: Classification, Function, Structure, Genetic Diseases, and Knockout Models, *Am. J. Physiol. 290*, F580-F599.

65. Alper, S. L. (2007) Molecular Physiology of SLC4 Anion Exchangers, *Exp. Physiol. 91*, 153-161.

66. Vince, J. W. and Reithmeier, R. A. F. (1998) Carbonic Anhydrase II Binds to the Carboxyl-Terminus of Human Band 3, the Erythrocyte $Cl^-/HCO_3^-$ Exchanger, *J. Biol. Chem. 273*, 28430-28437.

67. Vince, J. W., Carlsson, U., and Reithmeier, R. A. F. (2002) Localization of the Cl-/HCO3- Anion Exchanger Binding Site to the Amino-Terminal Region of Carbonic Anhydrase II, *Biochem. 39*, 13344-13349.

68. Sterling, D., Alvarez, B. V., and Casey, J. R. (2002) The Extracellular Component of a Transport Metabolon: Extracellular Loop 4 of the Human AE1 $Cl^-/HCO_{3-}$ Exchanger Binds Carbonic Anhydrase IV, *J. Biol. Chem. 277*, 25239-25246.

69. Morgan, P. E., Pastorekova, S., Stuart-Tilley, A. K., Alper, S. L., and Casey, J. R. (2007) Interactions of Transmembrane Carbonic Anhydrase, CAIX, with Bicarbonate Transporters, *Am. J. Physiol. 293*, C738-C748.

70. Swietach, P., Vaughan-Jones, R. D., and Harris, A. L. (2007) Regulation of Tumor pH and the Role of Carbonic Anhydrase 9, *Cancer Metastasis Rev. 26*, 299-310.

71. Lacroix, M. and Leclercq, G. (2004) Relevance of Breast Cancer Cell Lines as Models for Breast Tumours: An Update, *Breast Cancer Res. Treat. 83*, 249-289.

72. Neve, R. M., Chin, K., Fridlyand, J., Yeh, J., Baehner, F. L., Fevr, T., Clark, L., Bayani, N., Coppe, J., Tong, F., Speed, T., Spellman, P. T., DeVries, S., Lapuk, A., Wang, N. J., Kuo, W., Stilwell, J. L., Pinkel, D., Albertson, D. G., Waldman, F. M., McCormick, F., Dickson, R. B., Johnson, M. D., Lippman, M., Ethier, S., Gazdar, A., and Gray, J. W. (2006) A Collection of Breast Cancer Cell Lines for the Study of Functionally Distinct Cancer Subtypes, *Cancer Cell 10*, 515-527.

73. Engel, L. W. and Young, N. A. (1978) Human Breast Carcinoma Cells in Continuous Culture: A Review, *Cancer Res. 38*, 4327-4339.

74. Kitzman, H. H., Jr., McMahon, R. J., Williams, M. G., and Frost, S. C. (1993) Effect of Glucose Deprivation on GLUT1 Expression in 3T3-L1 Adipocytes, *J. Biol. Chem. 268*, 1320-1325.

75. Cecchi, A., Hulikova, A., Pastorek, J., Pastorekova, S., Scozzafava, A., Winum, J.-Y., Montero, J.-L., and Supuran, C. T. (2005) Carbonic Anhydrase Inhibitors: Design of Fluorescent Sulfonamides as Probes of Tumor-Associated Carbonic Anhydrase IX That Inhibit Isozyme IX-Mediated Acidification of Hypoxic Tumors, *J. Med. Chem. 48*, 4841.

76. Kumar, A., Xiao, Y.-P., Laipis, P. J., Fletcher, B. S., and Frost, S. C. (2004) Glucose Deprivation Enhances Targeting of GLUT1 to Lipid Rafts in 3T3-L1 Adipocytes, *Am. J. Physiol. 286*, E568-E576.

77. L'Allemain, G., Paris, S., and Pouyssegur, J. (1984) Growth Factor Action and Intracellular pH Regulation in Fibroblasts: Evidence for a major Role of the $Na^+/H^+$ Antiporter, *J. Biol. Chem. 259*, 5809-5815.

78. Markwell, M. A. K., Haas, S. M., Lieber, L. L., and Tolbert, N. E. (1978) A Modification of the Lowry Procedure to Simplify Protein Determination in Membrane and Lipoprotein Samples, *Anal. Biochem. 87*, 206-210.

79. Laemmli, U. K. (1970) Cleavage of Structural Proteins During the Assembly of the Head of Bacteriophage T4, *Nature 227*, 680-685.

80. Semple-Rowland, S. L., Adamus, G., Cohen, R. J., and Ulshafer, R. J. (1991) A Reliable Two-dimensional Gel Electrophoresis Procedure for Separating Neural Proteins, *Electrophoresis 12*, 307-312.

81. Silverman, D. N. (1982) Carbonic Anhydrase: Oxygen-18 Exchange Catalyzed by an Enzyme with Rate-contributing Proton-transfer Steps, *Meth. Enzymol. 87*, 732-752.

82. Tu, C., Wynns, G. C., McMurray, R. E., and Silverman, D. N. (1978) $CO_2$ Kinetics in Red Cell Suspensions Measured by $^{18}O$ Exchange, *J. Biol. Chem. 253*, 8178-8184.

83. Sennoune, S. R., Bakunts, K., Martinez, G. M., Chua-Tuan, J. L., Kebir, Y., Attaya, M. N., and Martinez-Zaguilan, R. (2004) Vacuolar $H^+$-ATPase in Human Breast Cancer Cells with Distinct Metastatic Potential: Distribution and Functional Activity, *Am. J. Physiol. 286*, C1443-C1452.

84. Warburg, O. (1930) The Metabolism of Tumours, *London: Onstable*.

85. Airley, R., Loncaster, J., Davidson, S., Bromley, M., Roberts, S., Patterson, A., Hunter, R., Stratford, I., and West, C. (2001) Glucose Transporter Glut-1 Expression Correlates with Tumor Hypoxia and Predicts Metastasis-free Survival in Advanced Carcinoma of the Cervix, *Clin. Cancer Res. 7*, 928-934.

86. Younes, M., Brown, R. W., Mody, D. R., Fernandez, L., and Laucirica, R. (1995) GLUT1 Expression in Human Breast Carcinoma: Correlation with Known Prognostic Markers, *Anticancer Res. 15*, 2895-2898.

87. Semenza, G. L., Roth, P. H., Fang, H.-M., and Wang, G. L. (1994) Transcriptional Regulation of Genes Encoding Glycolytic Enzymes by Hypoxia-inducible Factor 1, *J. Biol. Chem. 269*, 23757-23763.

88. Reshkin, S. J., Bellizzi, A., Albarini, V., Guerra, L., Tommasino, M., Paradiso, A., and Casavola, V. (2000) Phosphoinositide 3-kinase Is Involved in the Tumor-specific Activation of Human Breast Cancer Cell $Na^+/H^+$ Exchange, Motility, and Invasion Induced by Serum Deprivation, *J. Biol. Chem. 275*, 5361-5369.

89. Reitzer, L. J., Wice, B. M., and Kennell, D. (1980) The Pentose Cycle: Control and Essential Function in HeLa Cell Nuclei Acid Synthesis, *J. Biol. Chem. 255*, 5616-5626.

90. Zavada, J., Zavadova, Z., Zatovicova, M., Hyrsi, L., and Kawaciuk, I. (2003) Soluble Form of Carbonic Anhydrase IX (CAIX) in the Serum and Urine of Renal Carcinoma Patients, *Br. J. Cancer 89*, 1067-1071.

91. Brennan, D. J., Jirstrom, K., Kronblad, A., Millikan, R. C., Landberg, G., Duffy, M. J., Ryden, L., Gallagher, W. M., and O'Brien, S. L. (2006) CA IX is an Independent Prognostic Marker in Premenopausal Breast Cancer Patients with One to Three Positive Lymph Nodes and a Putative Marker of Radiation Resistance, *Clin. Cancer Res 12*, 6421-6431.

92. Wykoff, C. C., Beasley, N., Watson, P. H., Campo, L., Chia, S. K., English, R., Pastorek, J., Sly, W. S., Ratcliffe, P., and Harris, A. L. (2001) Expression of Hypoxia-Inducible and Tumor-Associated Carbonic Anhydrases in Ductal Carcinoma *in Situ* of the Breast, *Am. J. Pathol. 158*, 1011-1019.

93. Jarvela, S., Parkkila, S., Bragge, H., Kahkonen, M., Parkkila, A.-K., Soini, Y., Pastorekova, S., Pastorek, J., and Haapasalo, H. (2008) Carbonic Anhydrase IX in Oligodendroglial Brain Tumors, *BMC Cancer 8*, 1.

94. Linda, J. P. (2004) Lipid Rafts: Heterogeneity on the High Seas, *Biochem. J. 378*, 281-292.

95. Smart, E. J., Ying, Y., Mineo, C., and Anderson, R. G. W. (1995) A Detergent-free Method for Purifying Caveolae Membrane from Tissue Culture Cells, *Proc. Natl. Acad. Sci. USA 92*, 10104-10108.

96. Sun, J., Nanjundan, M., Pike, L. J., Wiedmer, T., and Sims, P. J. (2002) Plasma Membrane Phospholiid Scramblase 1 is Enriched in Lipid Rafts and Interacts with the Epidermal Growth Factor Receptor, *Biochem. 41*, 6338-6345.

97. Nanjundan, M., Sun, J., Zhao, J., Zhou, Q., Sims, P. J., and Weidmer, T. (2008) Plasma Membrane Phospholipid Scramblase I Promotes EGF-dependent Activation of c-Src through the Epidermal Growth Factor Receptor, *J. Biol. Chem. 278*, 37413-37418.

98. Chen, X. and Resh, M. D. (2002) Cholesterol Depletion from the Plasma Membrane Triggers Ligand-independent Activation of the Epidermal Growth Factor Receptor, *J. Biol. Chem. 277*, 49631-49637.

99. Ringerike, T., Blystad, F. D., Lvey, F. O., Madshus, I. H., and Stang, E. (2002) Cholesterol is Important in control of EGF Receptor Kinase Activity but EGF Receptors are Not Concentrated in Caveolae, *J. Cell Sci. 115*, 1331-1340.

100. Li, Y., Wang, H., Oosterwijk, E., Tu, C., Shiverick, K. T., Silverman, D. N., and Frost, S. C. (2009) Expression and Activity of Carbonic Anhydrase IX Is Associated with Metabolic Dysfunction in MDA-MB-231 Breast Cancer Cells, *Cancer Investigation 27*, 613-623.

101. Whittington, D. A., Waheed, A., Ulmasov, B., Shah, G. N., Grubb, J. H., Sly, W. S., and Christianson, D. W. (2001) Crystal Structure of the Dimeric Extracellular Domain of Human Carbonic Anhydrase XII, a Bitopic Membrane Protein Overexpressed in Certain Cancer Tumor Cells, *Proc. Natl. Acad. Sci. USA 98*, 9545-9550.

102. Foster, L. J., deHoog, C. L., and Mann, M. (2003) Unbiased Quantitative Proteomics of Lipid Rafts Reveals High Specificity for Signaling Factors, *Proc. Natl. Acad. Sci. USA 100*, 5813-5818.

103. Chen, C.-L., Chu, J.-S., Su, W.-C., Huang, S.-C., and Lee, W.-Y. (2010) Hypoxia and Metabolic Phenotypes druing Breast Cancer Carcinogenesis: Expression of HIF1α, GLUT1, and CAIX, *Virchows Archiv 457*, 53-61.

104. Hoskin, P. J., Sibtain, A., Daley, F. M., and Wilson, G. D. (2003) GLUT1 and CAIX as Intrinsic Markers of Hypoxia in Bladder Cancer: Relationship with Vascularity and Proliferation as Predictors of Outcome of ARCON, *Br. J. Cancer 89*, 1290-1297.

105. de Schutter, H., Landuyt, W., Verbeken, E., Goethals, L., Hermans, R., and Nuyts, S. (2005) The Prognostic Value of the Hypoxic Markers CA IX and GLUT1and the Cytokine VEGF and IL6 in Head and Neck Squamous Cell CarcinomaTreated by Radiotherapy +/- Chemotherapy, *BMC Cancer doi:10.1186/1471-2407-5-42*.

106. Younes, M., Lechago, L. V., Somoano, J. R., Mosharaf, M., and Lechago, J. (1996) Wide Expression of the Human Erythrocyte Glucose Transporter GLUT1 in Human Cancers, *Cancer Res. 56*, 1164-1167.

107. Oosterwijk, E., Ruiter, D. J., Hoedemaeker, Ph. J., Pauwels, E. K. J., Jonas, U., Zwartendijk, I., and Warnaar, S. O. (1986) Monclonal Antibody G 250 Recognizes a Determinant Present in Renal-Cell Carcinoma and Absent from Normal Kidney, *Int. J. Cancer 38*, 489-494.

108. Grabmaier, K., Vissers, J. L. M., de Weijert, M. C. A., Oosterwijk-Wakka, J. C., Bokhoven, A. V., Brakenhoff, R. H., Noessner, E., Mulders, P. A., Merkx, G., Figdor, C. G., Adema, G. J., and Oosterwijk, E. (2000) Molecular Cloning and Immunogenicity of Renal Cell Carcinoma-Associated Antigen G250, *Int. J. Cancer 85*, 865-870.

109. Alterio, V., Hilvo, M., Di Fiore, A., Supuran, C. T., Pan, P., Parkkila, S., Scaloni, A., Pastorek, J., Pastorekova, S., Pedone, C., Scozzafava, A., Monti, S. M., and De Simone, G. (2009) Crystal Structure of the Catalytic Domain of the Tumor-associated Human Carbonic Anhydrase IX, *Proc. Natl. Acad. Sci. USA 106*, 16233-16238.

110. De Simone, G. and Supuran, C. T. (2010) Carbonic Anhycrase IX: Biochemical and Crystallographic Characterization of a Novel Antitumor Target, *Biochim. Biophys. Acta 1804*, 494-409.

111. Wong, N. K., Easton, R. L., Panico, M., Sutton-Smith, M., Morrison, J. C., Lattanzio, F. A., Morris, H. R., Clark, G. F., Dell, A., and Patankar, M. S. (2003) Characterization of the Oligosaccharides Associated with the Human Ovarian Tumor Marker CA125, *J. Biol. Chem. 278*, 28619-28634.

112. Goetz, J. A., Mechref, Y., Kang, P., Jeng, M., and Hovotny, M. V. (2009) Glycomics Profiling of Invasive and Non-invasive Breast Cancer Cells, *Glycoconj. J. 26*, 117-131.

113. McMahon, R. J. and Frost, S. C. (1995) Nutrient Control of GLUT1 Processing and Turnover in 3T3-L1 Adipocytes, *J. Biol. Chem. 270*, 12094-12099.

114. Bui, M. H. T., Seligson, D., Han, K. R., Pantuck, A. J., Dorey, F. J., Huang, Y., Horvath, S., Leibovich, B. C., Chopra, S., Liao, S.-Y., Stanbridge, E., Lerman, M. I., Palotie, A., Figlin, R. A., and Belldegrun, A. S. (2003) Carbonic Anhydrase IX is an Independent Predictor of Survival in Advanced Renal Clear Cell Carcinoma: Implication fro Prognosis and Therapy, *Clin. Cancer Res 9*, 802-811.

115. Olive, P. L., Aquino-Parsons, C., MacPhail, S. H., Liao, S.-Y., Raleigh, J. A., Lerman, M. I., and Stanbridge, E. J. (2001) Carbonic Anhydrase 9 as an Endogenous Marker for Hypoxic Cells in Cervical Cancer, *Cancer Res. 61*, 8924-8929.

116. Ebbesen, P., Pettersen, E. O., Gorr, T. A., Jobst, G., Williams, K., Kieninger, J., Wenger, R. H., Pastorekova, S., Dubois, L., Lambin, P., Wouters, B. G., van den Beucken, T., Supuran, C. T., Poellinger, L., Ratcliffe, P., Kanopka, A., Gorlach, A., Grasmann, M., Harris, A. L., Maxwell, P., and Scozzafava, A. (2009) Taking Advantage of Tumor Cell Adaptations to Hypoxia for Developing New Tumor Markers and Treatment Strategies, *Journal of Enzyme Inhibition and Medicinal Chemistry 24*, 1-39.

117. Pastorekova, S. and Zavada, J. (2004) Carbonic Anhydrase IX (CA IX) as a Potential Target for Cancer Therapy, *Cancer Therapy 2*, 245-262.

118. Generali, D., Fox, S. B., Berruti, A., Brizzi, M. P., Campo, L., Bonardi, S., Wigfield, S. M., Bruzzi, P., Bersiga, A., Allevi, G., Milani, M., Aguggini, S., Dogliotti, L., Bottini, A., and Harris, A. L. (2006) Role of Carbonic Anhydrase IX Expression in Prediction of the Efficacy and Outcome of Primary Epirubicin/Tamoxifen Therapy for Breast Cancer, *Endocrine-Related Cancer 13*, 921-930.

119. (2000) The Carbonic Anhydrases, (Chegwidden, W. R., Carter, N. D., and Edwards, Y. H., Eds.) 90 ed., Birkhauser Verlag, Basil.

120. Silverman, D. N., Tu, C. K., and Roessler, N. (1981) Diffusion-limited Exchange of $^{18}O$ between $CO_2$ and Water in Red Cell Suspensions, *Respir. Physiol. 44*, 285-298.

121. Genis, C., Sippel, K. H., Case, N., Cao, W., Avvaru, B. S., Tartaglia, L. J., Govindasamy, L., Tu, C., Agbandje-McKenna, M., Silverman, D. N., Rosser, C. J., and McKenna, R. (2009) Design of A Carbonic Anhydrase IX Active-Site Mimic to Screen Inhibitors for Possible Anticancer Properties, *Biochem. 48*, 1322-1331.

122. Vullo, D., Steffansen, B., Brodin, B., Supuran, C. T., Scozzafava, A., and Nielson, C. U. (2006) Carbonic Anhydrase Inhibitors: Transepithelial Transport of Thioureido Sulfonamide Inhibitors of the Cancer-associated Isozyme IX is Dependent on Efflux Transporters, *Bioorg. Med. Chem. 10.1016/j.bmc.2005.11.019*, 1-10.

123. Parkkila, S., Rajaniemi, H., Parkkila, A., Kivela, J., Waheed, A., Pastorekova, S., Pastorek, J., and Sly, W. S. (2000) Carbonic Anhydrase Inhibitor Suppresses Invasion of Renal Cancer Cells *In Vitro*, *Proc. Natl. Acad. Sci. USA 97*, 2220-2224.

124. Chiche, J., Ilc, K., Brahimi-Horn, M. C., and Pouyssegur, J. (2010) Membrane-bound Carbonic Anhydrases are Key pH Regulators controlling Tumor Growth and Cell Migration, *Adv. Enz. Regulat. 50*, 20-33.

125. Sterling, D. and Casey, J. R. (1999) Transport Activity of AE3 Chloride/Bicarbonate Anion-Exchange Proteins and Their Regulation by Intracellular pH, *Biochem. J. 344*, 221-229.

126. Stewart, A. K., Chernova, N. N., Kunes, Y. Z., and Alper, S. L. (2001) Regulation of AE2 Anion Exchanger by Intracellular pH: Critical Regions of the $NH_2$-terminal Cytoplasmic Domain, *Am. J. Physiol. 281*, C1344-C1354.

127. Sterling, D., Brown, N. J. D., Supuran, C. T., and Casey, J. R. (2002) The Functional and Physical Relationship between the DRA Bicarbonate Transporter and Carbonic Anhydrase II, *Am. J. Physiol. 283*, C1522-C1529.

128. Jacobs, M. S., McFarland, W. L., and Morgane, P. J. (1979) *The Anatomy of the brain of the bottlenose dolphin (Tursiops truncatus):rhinic lobe (rhinencephalon), the archicortex* Ankho International, Fayetteville, N.Y.

129. Piermarini, P. M., Kim, E. Y., and Boron, W. F. (2007) Evidence Against a Direct Interaction between Intracellullar Carbonic Anhydrase II and Pure C-Terminal Domains of SLC4 Bicarbonate Transporters, *J. Biol. Chem. 282*, 1409-1421.

130. Lu, J., Daly, C. M., Parker, M. D., Gill, H. S., Piermarini, P. M., Pelletier, M. F., and Boron, W. F. (2006) Effect of Human Carbonic Anhydrase II on the Activity of the Human Electrogenic $Na/HCO_3$ Cotransporter NBCel-A in Xenopus Oocytes, *J. Biol. Chem. 281*, 19241-19250.

131. Cousin, J. L., Motais, R., and Sola, F. (1975) Transmembrane Exchange of Chloride with Bicarbonate Ion in Mammalian Red Blood Cells: Evidence for a Sulphonamide-sensitive 'Carrier', *J. Physiol. 253*, 385-399.

132. Cianchi, F., Vinci, M. C., Supuran, C. T., Peruzzi, B., De Guili, P., Fasolis, G., Perigli, G., Pastorekova, S., Papucci, L., Pini, A., Masini, E., and Puccetti, L. (2010) Selective Inhibition of Carbonic Anhydrase IX Decreases Cell Proliferation and Induces Ceramide-mediated Apoptosis in Human Cancer Cells, *J. Pharmacol. Exper. Therap. 334*, 710-719.

133. Hanahan, D. and Weinberg, R. A. (2000) Hallmarks of Cancer, *Cell 100*, 57-70.

134. Masramon, L., Vendrell, E., Tarafa, G., Capella, G., Miro, R., Ribas, M., and Peinado, M. A. (2006) Genetic Instability and Divergence of Clonal Populations in Colon Cancer Cells *in Vitro*, *J. Cell Sci. 119*, 1477-1482.

135. Hsieh, M.-J., Chen, K.-S., Chiou, H.-L., and Hsieh, Y.-S. (2010) Carbonic Anhydrase XII Promotes Invasion and Migration Ability of MDA-MB-231 Breast Cancer Cells through the p38 MAPK Signaling Pathway, *Eur. J. Cell Biol. 89*, 598-606.

# BIOGRAPHICAL SKETCH

Born and raised in China, Ying Li began her undergraduate degree at Innermongolia University in the fall of 1987. She graduated in 1991, receiving a Bachelor of Science in botany. After graduation, she joined the Agricultural Institute of Innermongolia and worked on plant crossbreeding and plant pathology for 3 years. She entered the graduate program at Innermogolia University to pursue a master's in biology, specializing in molecular virology. She earned master's degree in the summer of 1997. Right after graduation, she received offer from the Department of Biotechnology at the Innermongolia Agricultural University and worked there for 5 years. In 2003, Ying came to the United States with her husband and son. She enrolled in Interdicipline Program (IDP) in College of Medicine at the University of Florida in 2005. Ying will be granted a Doctor of Philosophy in medical science through the College of Medicine, in fall of 2010.